NYO-2706

FUEL ELEMENT DEVELOPMENT PROGRAM

for the

PEBBLE BED REACTOR

PROGRESS REPORT - Phase I

May 1, 1959 to Oct. 31, 1959

November 30, 1959

Work performed under Contract No. AT(30-1)-2378

SANDERSON & PORTER

NEW YORK, N. Y.

DISCLAIMER

TABLE OF CONTENTS

PBR Fuel Element Development Program
Phase I Progress Report
May 1, 1959 to October 31, 1959

Abstract

Numerous types of high temperature ceramic fuel elements for the Pebble Bed Reactor are being evaluated. Specimens are 1-1/2 in diameter uranium graphite spheres with external coatings such as silicon carbide or pyrolytically deposited high density graphite and fuel particle coatings such as alumina. Low fission product leakage rates at high temperatures have been observed for some of these coatings. High level irradiation has given no visible evidence of radiation damage to either the silicon carbide coating or the coating-graphite bond.

1.0 Introduction

This report summarizes the progress during the first six month period of a two-year program to establish the feasibility of utilizing spherical uranium-graphite fuel elements in a large scale Pebble Bed Reactor power plant. 150 fuel element specimens encompassing 25 types of PBR fuel elements have been obtained from 10 manufacturers. A uniform and consistent procedure for evaluating these specimens both in pre-irradiation, irradiation, and post-irradiation tests has been established. This report describes the requirements for PBR fuel elements, the various types of fuel elements incorporated in the program, the methods of testing, and results obtained to date.

2.0 Objectives

The objectives for Pebble Bed Reactor fuel elements are based on the design study of a 125 eMW Pebble Bed Reactor Steam Power Plant described in NYO 2373. This reactor is a high-temperature, all-ceramic, helium-cooled breeder reactor producing 1450 psi 1000°F steam. The basic requirements for the fuel elements for this reactor can be summarized as follows:

1. The fuel element shall be suitable for operation in the maximum temperature range of 2000°F to 2500°F while in a helium atmosphere.
2. The fuel element shall be spherical in shape to facilitate loading and unloading by pouring operations.
3. The fuel element shall be capable of being mass-produced in an economical manner.
4. The fuel element shall retain sufficient fission products to permit economical operation of a large power reactor.

In setting the objectives of the test program, the operating requirements of the 125 eMW PBR have been used. For this design, a 1-1/2 in diameter spherical element was selected as the optimum size, based on heat transfer, pumping power, and economic considerations. Consequently, the 1-1/2 in diameter sphere has been adopted as the standard type of specimen throughout the test program. A description of the reference fuel element and its operating conditions is given in Table 2-1.

In order to facilitate the test program and enhance radiation damage effects, the U233 and Th of the reference element have been replaced by U235-U238 in the test specimens. Normal enrichment uranium is used for pre-irradiation tests and certain low level fission product diffusion tests, while highly enriched uranium is used for high level capsule irradiations.

TABLE 2-1

Fuel Element Performance Characteristics for the 125 eMW-PBR

Shape	Spherical
Diameter, in	1-1/2
U233 content, gms	.396
Th content, gms	4.31

Table 2-1 continued

Min carbon content, gms	48.5
Power Level, KW/ball	
Max.	3.0
Avg.	1.37
Max. Temperature °F	
Surface	1800°F
Center	2100°F
Burnup, KWH/ball	
Max.	8900
Avg.	5500

In addition to the general requirements listed in Table 2-1, there are certain specific objectives in the development of Pebble Bed Reactor fuel elements, some of which are unique to PBR fuels.

Fission Product Retention: The maximum feasible fission product release rate into the primary loop depends on several factors. These include the ultimate location of the radioactive isotopes (i.e. in the gas stream or on the surfaces), the efficiency of various types of concentrating and trapping systems in reducing activity level, and the ease of decontaminating the surfaces. These factors are being investigated by Sanderson & Porter under Contract AT(30-1)-2207. Pending developments in this work, the emphasis under the present Fuel Cycle Program is on maximum retention of fission products through the use of ceramic coatings and low permeability graphite. An indication of the retention factors which would be of interest is given in NYO 2373. It is shown in this report that the total activity due to volatile fission products and their daughters is about 1 curie per watt of reactor power. Thus, if all this activity escaped from the fuel elements of the 125 eMW PBR, the activity level would be 3.5×10^8 curies. If a retention factor of 10^6 could be achieved, then a first approximation of the activity level would be 350 curies, an easily manageable activity level in a large plant. Obviously, if this reduction factor were achieved, all isotopes would not be reduced by the same amount due to difference in decay rates during diffusion. Nonetheless, a leakage factor (i.e. rate of leakage/rate of production) of 10^{-6} has been established as an objective pending further clarification of the effect of decay rate and diffusion rate for different isotopes and species.

Impact Loads: Present PBR designs envisage a maximum free fall of the fuel elements during loading of 20 ft. The resultant impact load acts

on both the fresh fuel element and the partially irradiated fuel elements at the top of the core.

Compressive Load: The compressive load on the bottom row of fuel elements due to the dead weight of the fuel elements and the dynamic head loss of the helium coolant is 10 lbs. However, an objective of 500 lbs has been set to allow for compressive loads which may arise due to differential thermal expansion of the ball bed and its container wall.

Self-Welding: In order to prevent an obstruction to gravity unloading of the core, it is imperative that adjacent fuel elements not stick together due to any reaction between the coating, graphite, or fuel materials.

Internal Pressure: If all the gaseous fission products are released from the fuel particles and graphite grains, an internal pressure of about 300 psi would build up inside a 1.65 density graphite sphere. This pressure would be achieved in a surface coated sphere at the end of the desired burnup. Surface coatings should be sufficiently well bonded to the graphite in order to contain this pressure without rupture.

The objectives outlined in this section have been used as the basis for establishing the fuel element evaluation work described in Sections 6, 7 and 8, of this report.

3.0 Design Considerations

There are several variables among the types of Pebble Bed Reactor fuel elements described in Sections 4.0 and 5.0 that can affect the overall design of the reactor. The important variables include an unfueled shell whose thickness can vary between the limits of a uniform dispersion of fissile material throughout the element (no shell) and a lumped pellet of fissile material (maximum shell thickness). Also, the use of non-carbonaceous coatings will cause the graphite moderator to be displaced and will introduce further barriers for heat flow. The effect of these variables on internal temperature gradients in the fuel element, on thermal stress and on carbon/uranium ratio is described in this section.

3.1 Fueled Spheres

The basic equation for the temperature gradient within a sphere in which heat is being generated can readily be derived from

$$\frac{d}{dr}\left(r^2 \frac{dT}{dr}\right) = \frac{-qr^2}{K} \qquad (3\text{-}1)$$

On the assumption that heat is generated uniformly in the sphere (i.e. q = const = Q/V), eq. 3-1 readily reduces to:

$$T_{center} - T_{surface} = \frac{Q}{8\pi K r_o} \qquad (3\text{-}2)$$

As discussed in Section 2.0, previous design studies have set the sphere diameter at 1-1/2 in and the maximum heat generation rate of 3 KW per sphere (Q = 10,240 BTU/hr). Thermal conductivity, k, of the graphite depends on the type of graphite and the extent of irradiation damage to the graphite, and can range from values of k = 80 to k = 15 BTU/hr-ft-°F. The effect of various heat generation rates and thermal conductivities on the internal temperature gradients in a 1-1/2 in sphere is shown in Figure 3-1.

The assumption of uniform heat generation in the fueled region is valid for the reference fuel element which is highly loaded with fertile material. However, in the test specimens loaded entirely with fissile material, flux depression factors of about 80% (i.e. effective flux/incident flux) have been experimentally determined for uniformly loaded spheres. It was of interest to determine whether there would be a significant

reduction in central temperature due to the higher heat generation rates near the surface of the sphere. This was done by approximating the variable heat generation in the form of $q = ar^2 + b$ and substituting into eq. 3-1. This results in:

$$\Delta T = \frac{ar_o^4}{20K} - \frac{br_o^2}{6K} \qquad (3\text{-}3)$$

Utilizing dosimetry data for both 1 in and 1-1/2 in unfueled spheres, the following results were found.

TABLE 3-1

Effect of Non-Uniform Heat Generation of Internal Temperature Gradient

	1" sphere	1-1/2" sphere
Q_{total}, KW/sphere	2	2
q_{avg}, BTU/hr-in^3	13,000	3860
q_{max}, BTU/hr-in^3	18,750	4325
Power depression factor	.694	.892
$\Delta T_{non\text{-}uniform}/\Delta T_{uniform}$	.910	.868

These temperature factors are sufficiently small so that the assumption of uniform heat generation rate is not overly conservative.

The temperature gradient within a sphere is increased as the unfueled shell thickness is increased, keeping the fuel element diameter and heat generated constant. This is due to both the higher gradient in the fueled region and the additional temperature gradient in the unfueled shell. The temperature drop in an unfueled spherical shell is:

$$T_i - T_o = \frac{Q}{4\pi K}\left(\frac{1}{r_i} - \frac{1}{r_o}\right) \qquad (3\text{-}4)$$

Combining eqs. 3-2 and 3-4 gives

$$T_{center} - T_{surface} = \frac{Q}{8\pi K r_o}\left(\frac{3}{x} - 2\right) \qquad (3\text{-}5)$$

where $x = r_i/r_o$ for the unfueled shell.

Note that when x = 1 (i.e. no unfueled shell) eq. 3-5 is identical with eq. 3-2. The correction factors for converting ΔT in a uniformly loaded sphere to ΔT for a shelled sphere is plotted in Figure 3-2 as a function of $x = r_i/r_o$. The thermal conductivity of the fueled and unfueled regions are taken as being equal.

A typical case in the use of Figures 3-1 and 3-2 is illustrated by the FA-5 element (see Section 4.0). The unfueled shell thickness is 0.15 in and a value of k = 20 BTU/hr-ft^2-°F is taken. From Figure 3-1 at 3 KW/ball, ΔT within a uniformly loaded 1-1/2 in sphere of this material would be 326°F. Since x = .60/.75 = 0.8, Figure 3.2 becomes 1.75 so that the temperature gradient in an FA-5 type element at 3 KW would be (1.75)(326) = 570°F.

The tangential thermal stress at the surface of a sphere with internal heat generation is given by

$$\sigma_t = \frac{Q \alpha E}{20\pi K r_o (1-\nu)} \qquad (3\text{-}6)$$

If the heat is generated in a central-spherical region of the sphere, eq. 3-6 must be modified to give

$$\sigma_t = \frac{Q \alpha E}{8\pi K r_o (1-\nu)}\left(1 - \frac{3}{5}x^2\right) \qquad (3\text{-}7)$$

Again, the properties of the unfueled and fueled regions are taken to be identical. Figure 3-3 is a plot of the tangential thermal stress at the surface of a 1-1/2 in diameter sphere with 3 KW total heat generation and properties as listed on the graph. The influence of the thickness of the unfueled shell is shown by plotting σ_t vs. r_i/r_o. For x = 1.0 (uniformly loaded sphere), σ_t = 1100 psi while for a fuel element such as the FA-5 type, σ_t = 1600 psi. These values compare with modulus of rupture values of 3000 to 5000 psi reported for good grades of graphite.

3.2 Surface Coatings

Section 4.0 describes several types of coatings which can be applied to the surface of a fueled graphite sphere to retard fission product diffusion. However, these coatings cause an additional temperature gradient in the sphere. Figure 3-4 shows the effect of coating thickness on temperature gradient through the coating for various thermal conductivities of the coating material. Silicon carbide coatings of interest range in thickness from .003 to .030 in and have thermal conductivites of 10 to 15 BTU/hr-ft-°F. At a maximum, the additional temperature gradient would be about 50°F. Thermal conductivities as low as 2 BTU/hr-ft-°F have been used in Figure 3-4 to include the pyrographite coating discussed in Section 4.3. This material is highly anisotropic, having a low radial and a high circumferential thermal conductivity. Coatings of .060 in of this material would result in about a 590°F temperature gradient. However, it is expected that small amounts of metal additives (100-200 ppm) can increase the thermal conductivity to the range of 5 to 10 BTU/hr-ft-°F thus reducing the coating temperature gradient to 100°F - 200°F.

3.3 Coated Particles

As described in Sections 4.4 and 5.1, various types of metal or ceramic coatings can be applied to the fuel particles in an admixture fuel element. Possible deleterious effects of these coatings could include displacement of moderator and increase in fuel particle temperature.

Figure 3-5 has been prepared to show the inter-relation of diameter of the fuel particle and thickness of a carbon-free coating on the carbon: uranium ratio of a fuel element. The specific values shown are for a test element loaded with UO_2 only and having a graphite density of 1.7. The same relative reductions in carbon:uranium ratios would apply to the case of the reference element where thorium is also present. As can be noted, massive coating thicknesses on small particles can seriously reduce the carbon:uranium ratio in a fuel element. However, if thick coatings prove desirable, then larger fuel particles must be used. In the absence of nuclear calculations, a limit of 10-15% reduction in carbon:uranium ratio has been set as the objective.

Figure 3-6 shows the influence of fuel particle diameter and coating thickness on the volume fraction of the fuel element occupied by the coated particle. Since fuel loadings higher than 20 v/o in graphite can significantly affect the properties of the graphite, this value has been set as a desirable upper limit.

Figure 3-7 shows the relatively minor effect of coating thickness on temperature gradients within the particle. This is for the specific case of alumina coated particles discussed in Section 5-1. The temperature gradients are plotted for the case of an equivalent 1.0 KW heat generation per 1-1/2 in diameter fueled sphere. For the case of the maximum 3 KW heat generation per sphere, 250 μ alumina coating on a 500 μ UO_2 particle would increase the UO_2 temperature by only 12°F.

Nomenclature for Section 3.0

E = Modulus of Elasticity, psi

k = Thermal Conductivity, BTU/hr-°F-ft

Q = Heat Generated per Sphere, BTU/hr

q = Volumetric Heat Generation Rate, BTU/hr-ft^3

r = Sphere Radius, ft.

T = Temperature, °F

V = Sphere Volume, ft^3

x = r_o/r_i for unfueled shell

α = Coefficient of Thermal Expansion, °F^{-1}

ν = Poisson's Ratio

σ_t = Tangential Thermal Stress at Sphere Surface, psi

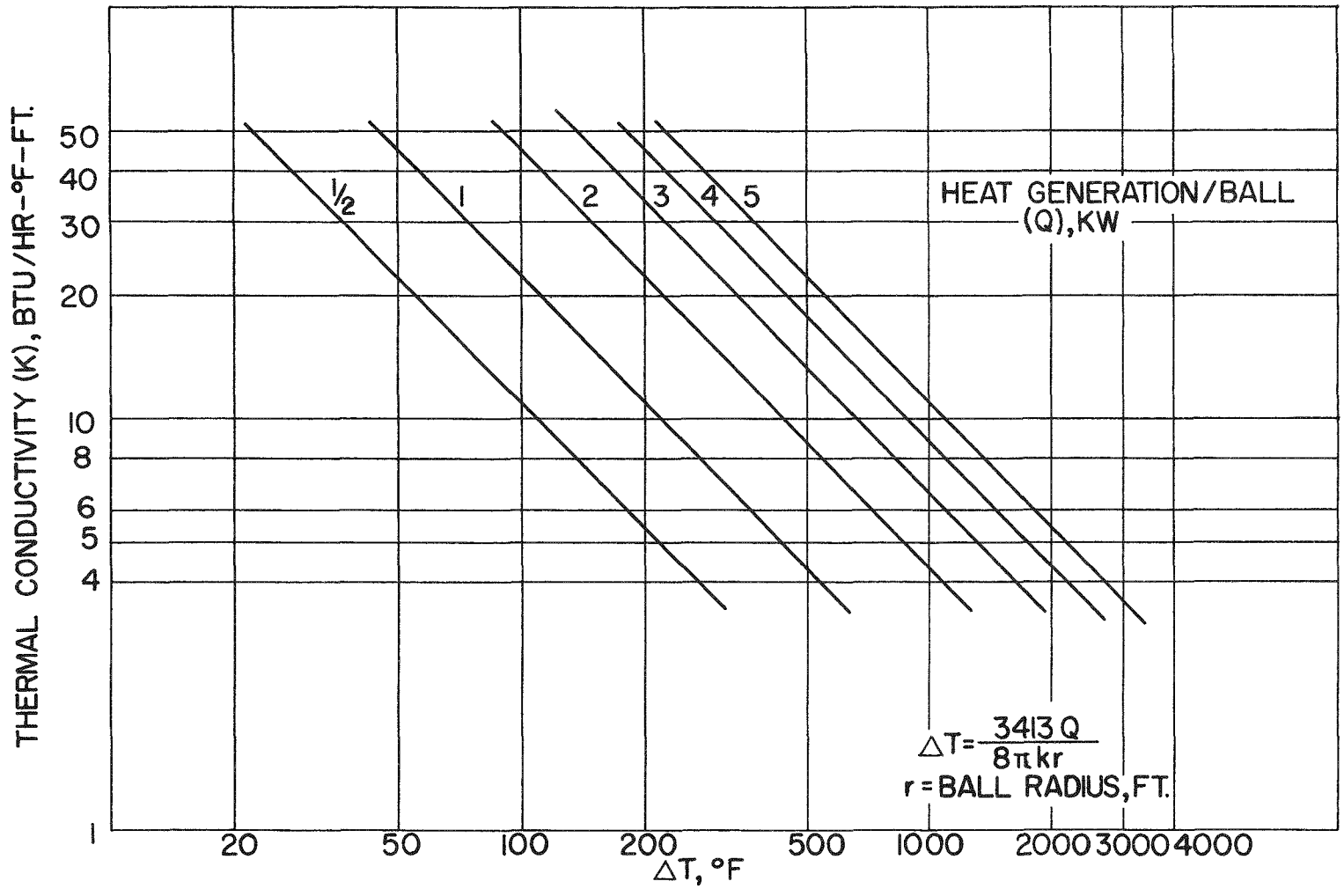

FIG. 3-1 TEMPERATURE RISE (ΔT) IN 1½" DIAMETER BALL WITH UNIFORM HEAT GENERATION, °F

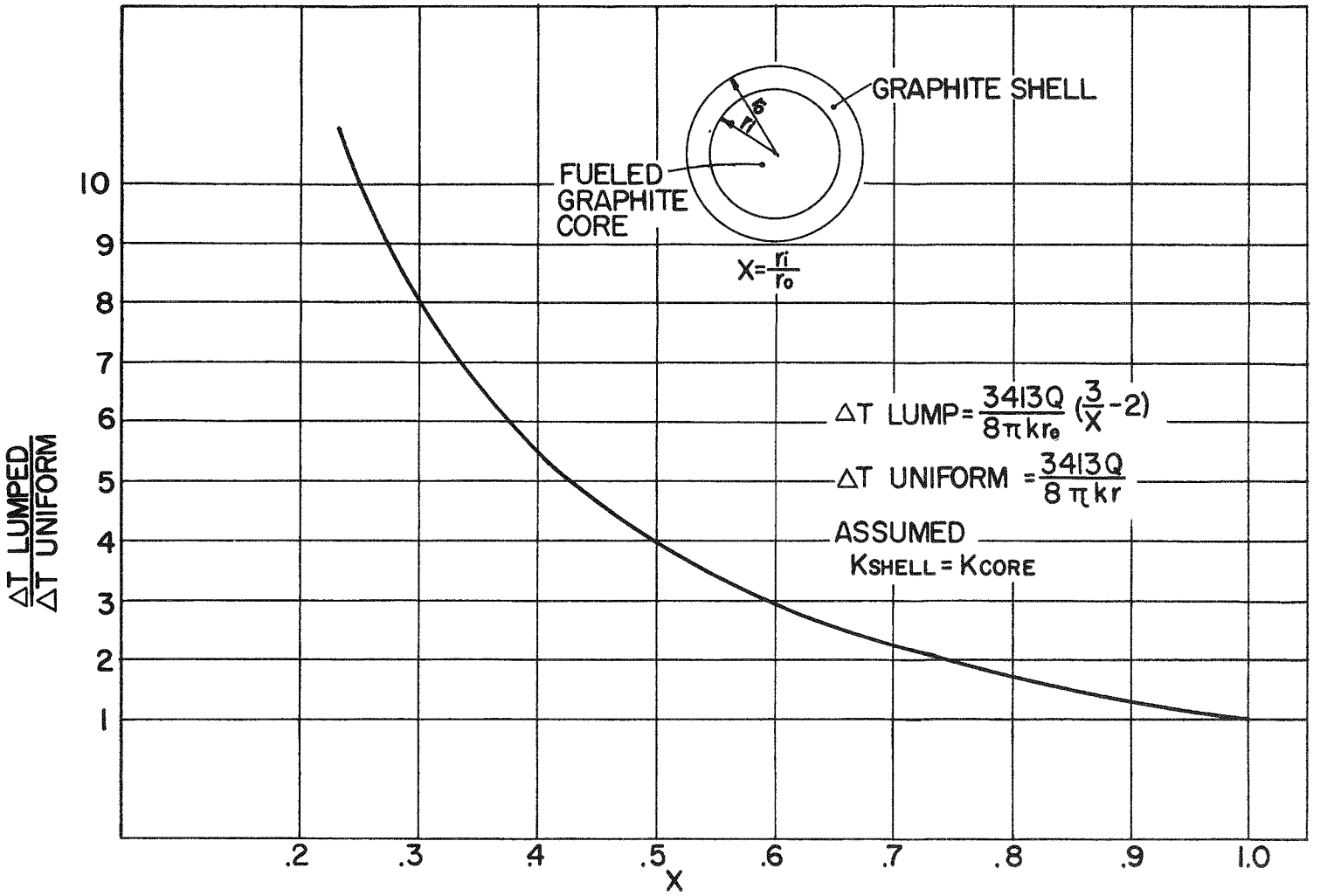

FIG.3-2 RELATIVE EFFECT OF UNFUELED SHELL THICKNESS ON SURFACE–CENTER TEMPERATURE DIFFERENCE FOR SPHERICAL FUEL ELEMENTS

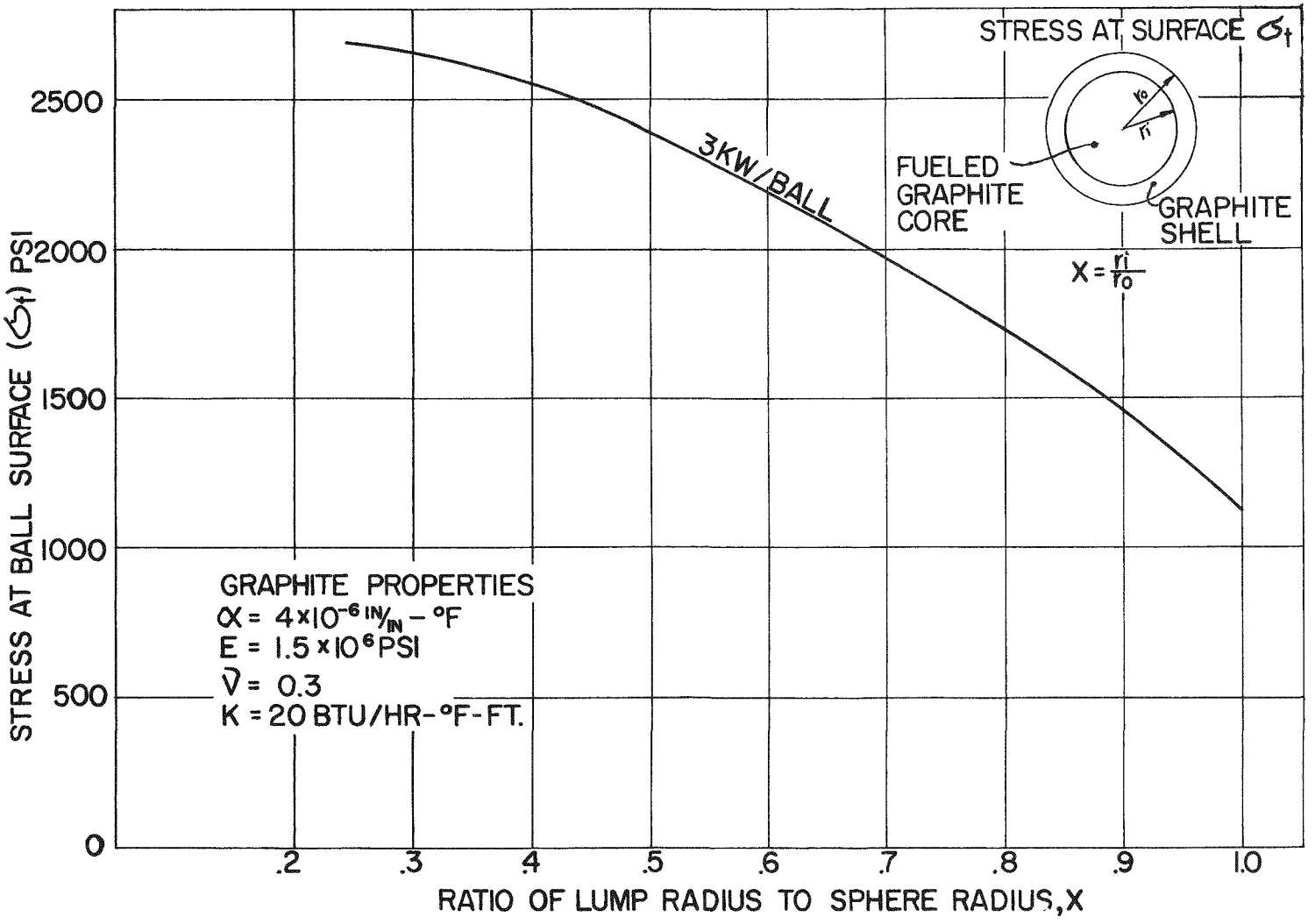

FIG. 3-3 EFFECT OF UNFUELED SHELL THICKNESS ON STRESS AT BALL SURFACE

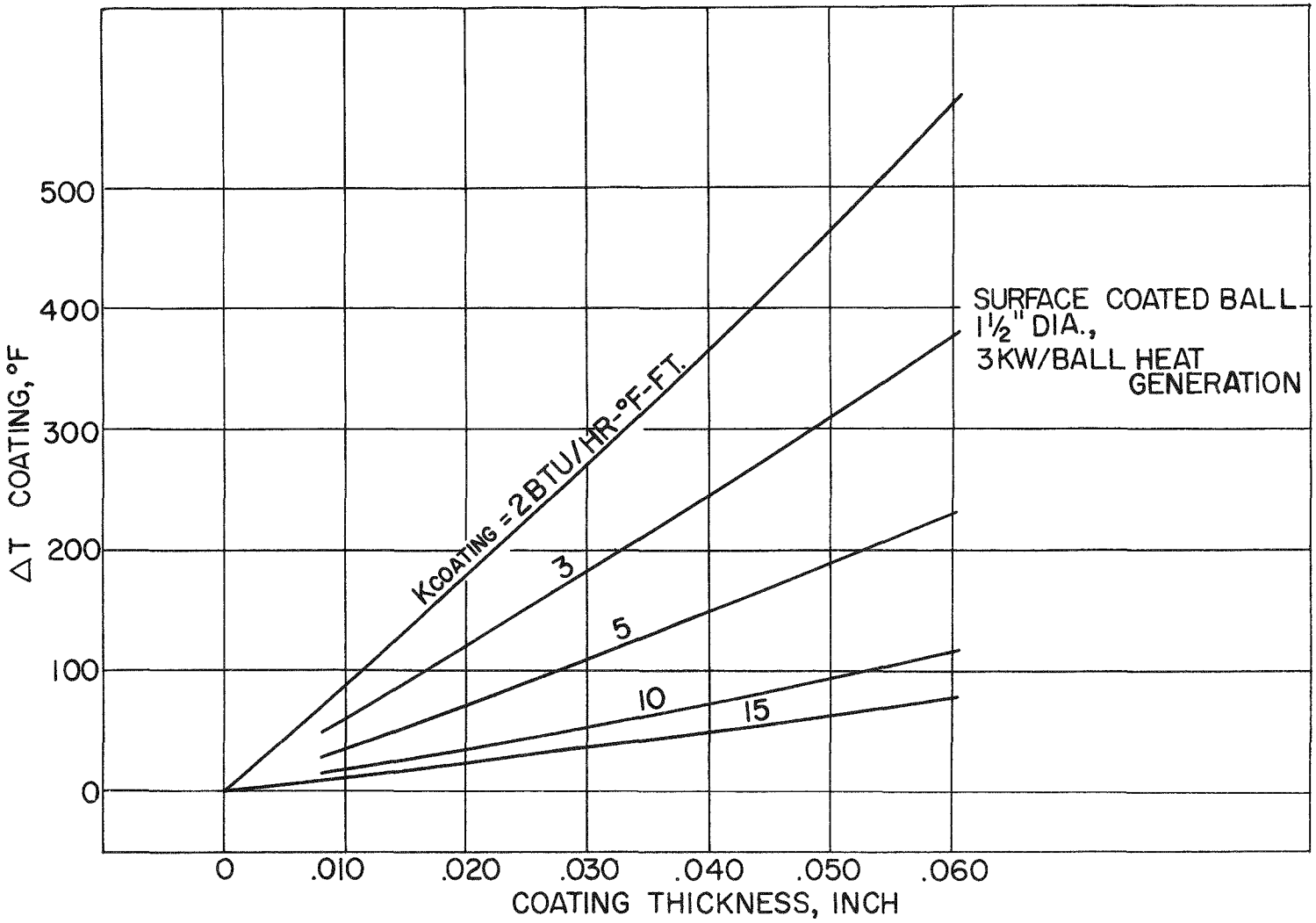

FIG. 3-4 TEMPERATURE GRADIENTS THROUGH SURFACE COATINGS

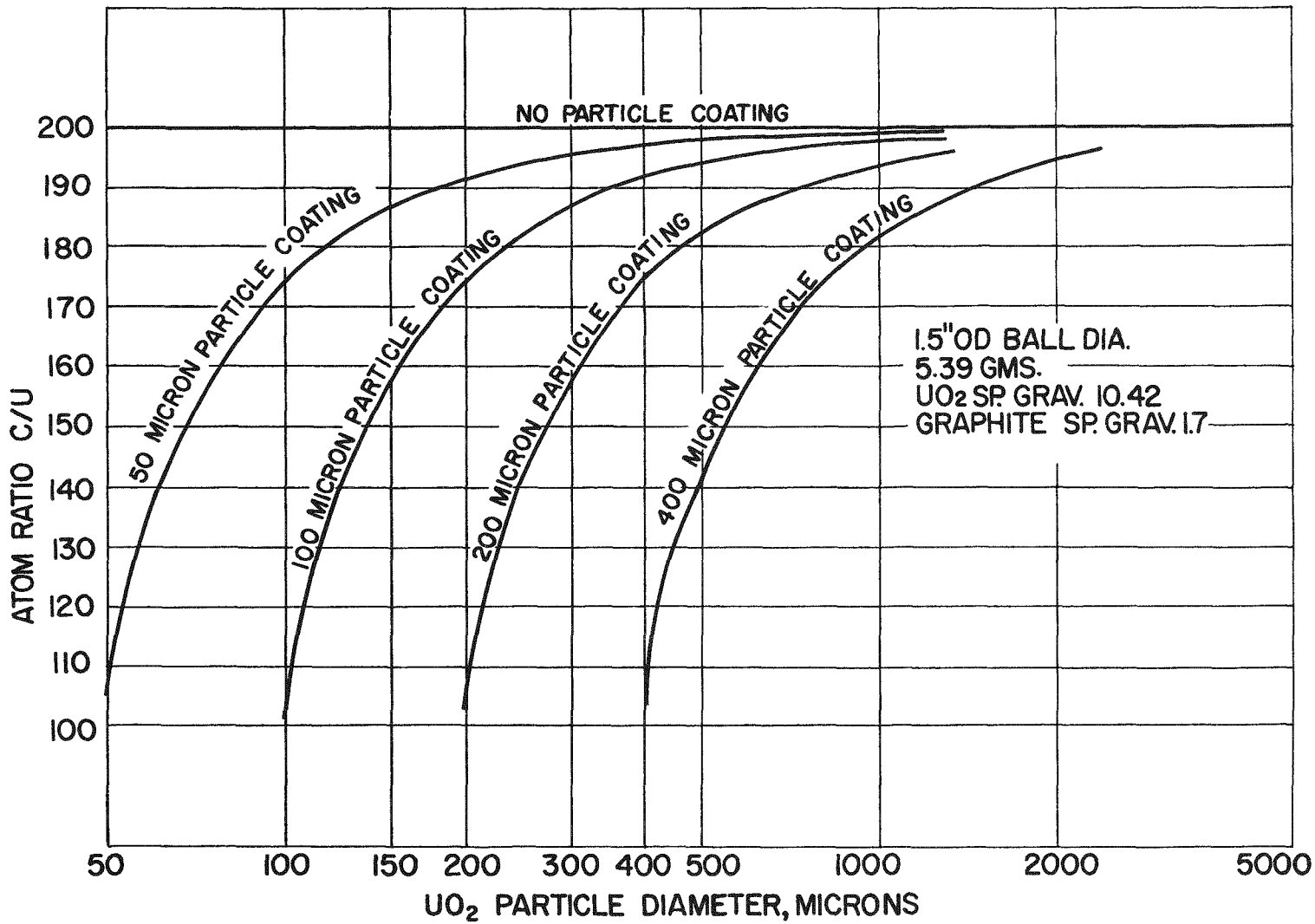

FIG. 3-5 INFLUENCE OF PARTICLE COATING ON CARBON URANIUM RATIO

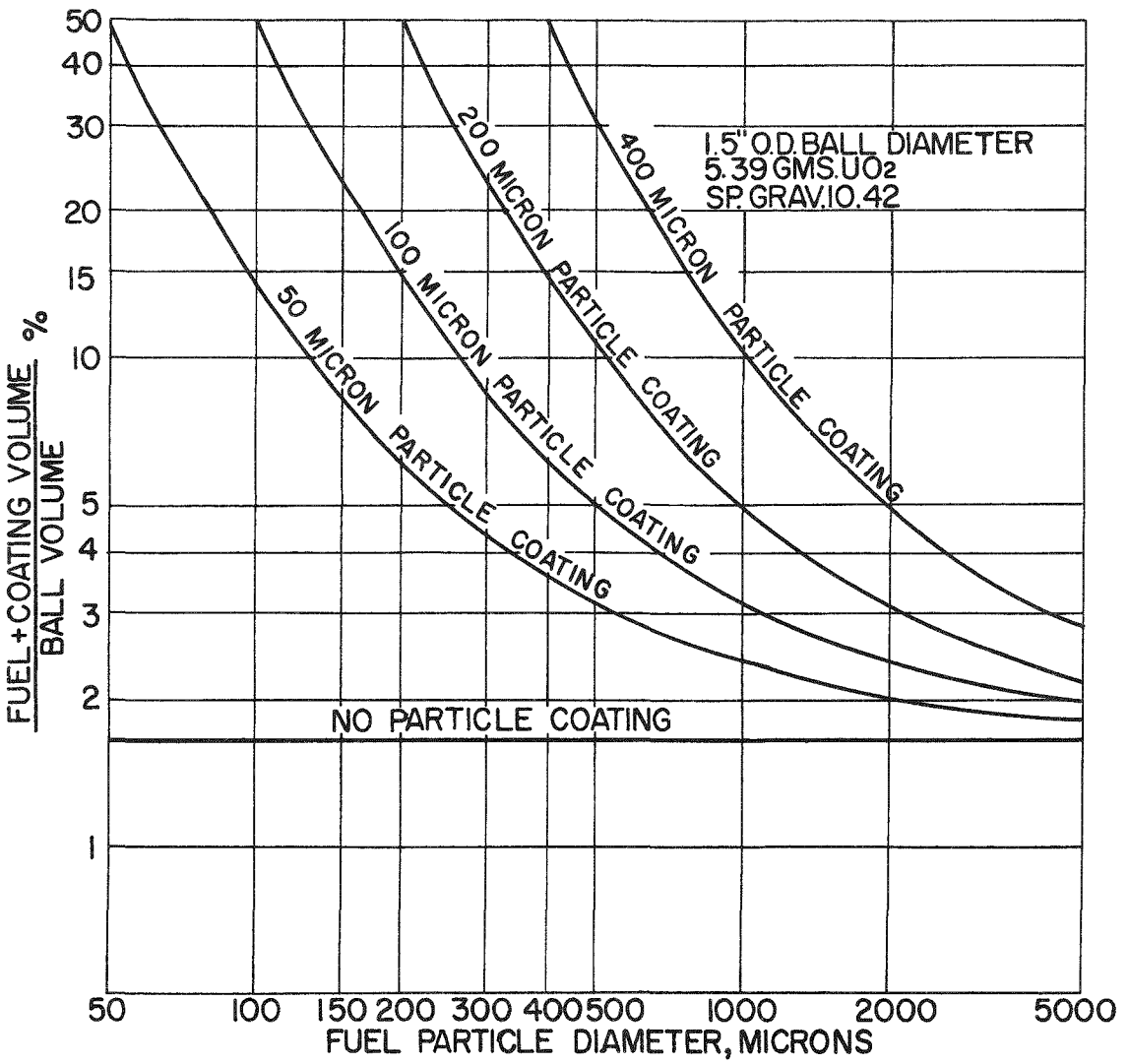

FIG. 3-6 EFFECT OF COATING THICKNESS ON COATED PARTICLE VOLUME FRACTION

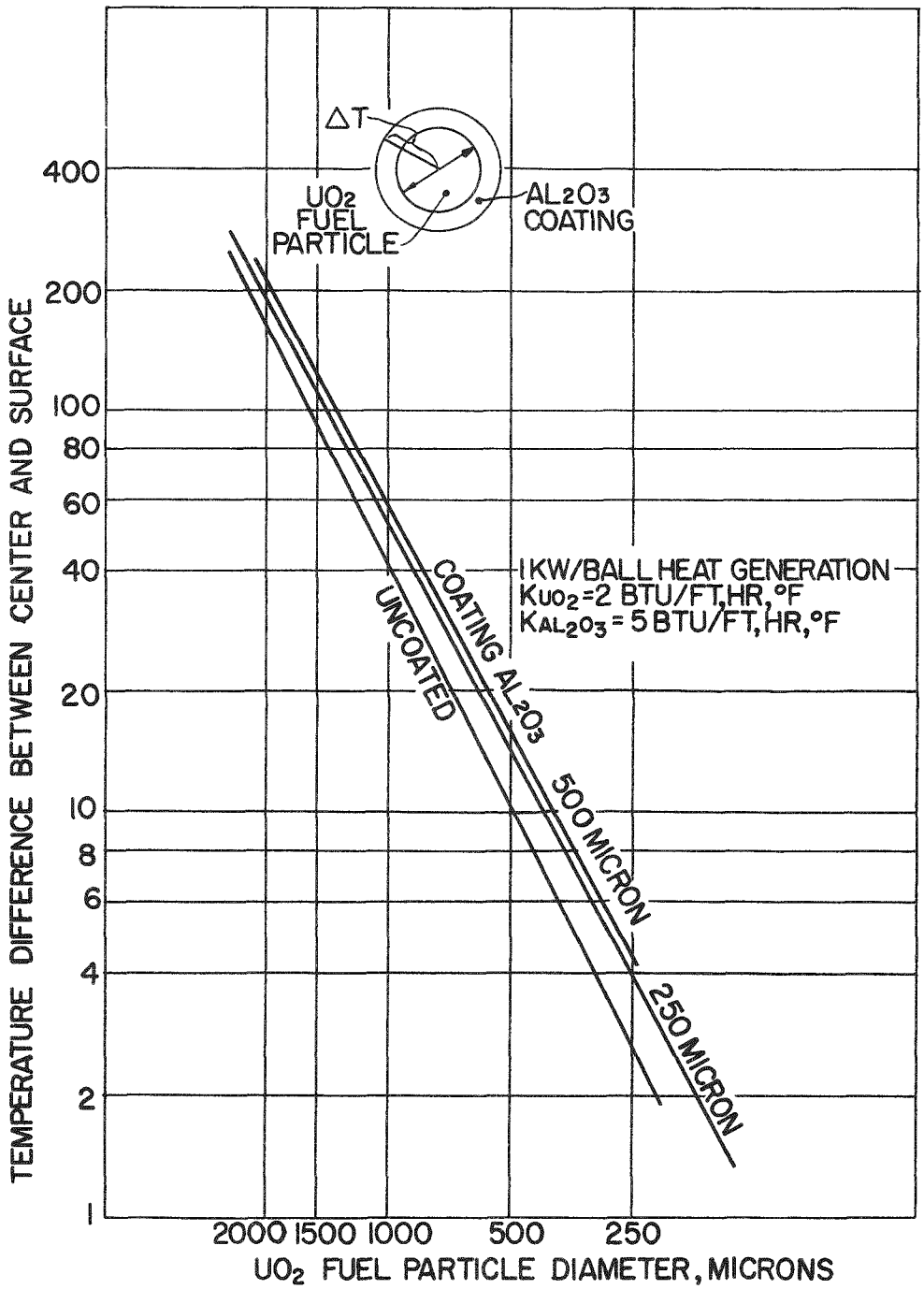

FIG.3-7 TEMPERATURE GRADIENTS IN COATED FUEL PARTICLES

4.0 Fuel Element Types

The major emphasis in Phase I of the present PBR Fuel Cycle Development Program has been on the retention of fission products. Prior to the present program, Sanderson & Porter conducted an experimental program to evaluate the structural integrity and fission product leakage characteristics of uncoated graphite spheres fueled by three different methods: (1) admixture of ceramic fuel particles with the graphite, (2) infiltration of the graphite sphere with a uranyl nitrate solution, and (3) lumping of a ceramic fuel pellet in a graphite shell. The relative merits of these fuel types have been discussed in NYO 8753 and the encouraging results of both pre- and post-irradiation tests on these types of uncoated fuel elements have been described in NYO 2373.

Fission product diffusion from these basic types of fueled graphite spheres can be influenced by conditions in any of six regions in the fuel elements.

1. The fuel particle itself,
2. A metallic or ceramic coating on the fuel particle,
3. A low permeability graphite matrix,
4. An internal coating between the fueled and unfueled region,
5. A low permeability graphite shell around the fueled region,
6. A surface coating on the fuel element.

Fuel particles will lose a fraction of the fission fragments by recoil from the particle surface, and the diffusion coefficient of the fuel particle material (i.e. UO_2, UC_2, etc.) will influence the rate of leakage of the remainder of the fission products. Particle coatings will prevent recoil fission fragments from coming to rest in the graphite matrix and will retard the diffusion of those fission fragments which diffuse from within fuel particles. A low permeability graphite matrix will further retard most of the fission products except for those arising from fuel particles located at the surface of the fuel element. However, an unfueled graphite shell surrounding the fueled graphite core, a coating on the inside of the unfueled shell, and a coating on the outside of the fuel element would each retard all of the fission products.

The underlying philosophy of Sanderson & Porter in applying these techniques to Pebble Bed Reactor fuel elements has been to stimulate private enterprise in the manufacture of high temperature ceramic fuel elements since economic nuclear fuel elements can only come eventually through the broad participation of private manufacturing companies on a competitive basis. Many of these companies have already developed certain proprietary techniques which appear applicable to PBR fuel elements. It is possible to procure specimens from these manufacturers on either a no-cost or a fixed-price-sample-lot basis. Proposed operating conditions, established during design studies of the Pebble Bed Reactor and described in procurement specifications, clearly establish the objectives for the manufacturers in the fabrication of the fuel element specimens. Then, the performance characteristics and evaluation of all fuel element types in a uniform testing program are made available to the entire industry. In this manner, improved specimens can be manufactured and all companies will have the opportunity of developing and providing specimens of the more promising types.

Table 4-1 has been prepared to show the various types of specimens procured during the past period. The manufacturer and pertinent characteristics of the fuel elements are listed. Each type of specimen has been assigned a type number. The letters, FA, FI, and FL refer the method of fueling the graphite (i.e. admixture, infiltration, and lumping, respectively). In the case of certain unfueled specimens, the designation FX is used, and for coated fuel particles, the designation FP is used. Numbers are assigned serially within each group, and have no special significance. Occassionally, when it is desired to identify a particular ball within a group, an additional identification number in parentheses will be added to the type number. Throughout this report, specimens are referred to only by type number. Consequently, the specimens have been listed numerically in Table 4-1 to permit rapid identification.

As discussed in Section 2.0, the test specimens are all 1 1/2-in diameter spheres fueled with 4.75 gms of uranium in the form of either UO_2, UC, or UC_2. Normal enrichment uranium is used in all types. Where a specimen type shows sufficient promise to warrant a high level irradiation test, additional specimens of that type containing fully enriched uranium are used.

In addition to the many coatings listed in Table 4-1, it will be noted that a number of variables are included in such other areas as type and size of the fuel particle, method of fueling density of graphite, and degree of carburization. However, not every graphite and fuel variable has been included with each coating since the number of specimens would otherwise be unmanageable. By testing the various coating specimens, data on the performance of all the various graphites and fuel particles will also be obtained. It would be expected that desirable features could ultimately be combined in an optimum fuel element.

It is felt that the more promising techniques for retaining fission products are the use of surface coatings and/or fuel particle coatings. Consequently, the description of fuel element types has been divided into sections according to the various types of coatings. It will be noted that within each category, uncoated specimens and variations in such things as fuel particles, type of graphite, etc. are included which are pertinent to that category. The categories are:

1. Silicon Carbide Surface Coatings
2. Metal Carbide Surface Coatings
3. Carbonaceous Surface Coatings
4. Coated Fuel Particles
5. Miscellaneous Uncoated Specimens

4.1 Silicon Carbide Surface Coatings

Two types of silicon carbide coatings, made by 3M and Carborundum, have been extensively investigated during the past period.

Minnesota Mining and Manufacturing Co. - Types FA-5, FA-6, FA-16

The FA-6 fuel element, the principal type of this group which was tested during the past period, consists of a 1.2 in diameter fueled core surrounded by a 0.15 in thick unfueled graphite shell. A .003 in coating of siliconized silicon carbide was applied to the outside of the unfueled shell. The FA-5 specimens were identical to FA-6 except that no SiC-Si coating was applied.

The core was initially loaded with UO_2 particles in the size range of 105 to 210 microns (i.e. -70, +140 mesh). This material was obtained from the Mallinckrodt Chemical Works who crushed and sieved some residual fully enriched UO_2 cake. This material was contaminated with a significant concentration of iron. Several separations techniques such as heating to 3000°F and magnetic separation were used to reduce the iron concentration to 3.24 w/o in the final UO_2 product. Therefore, in order to produce the desired loading of 5.39 gms of UO_2 per specimen, 5.57 $\pm$ .001 gms of material were weighed out and added to each specimen.

The core piece consisted of an admixture of the UO_2 together with Graphite Specialties Grade W filler and binder. In order to enhance the bonding between the core and the shell, the same type of graphite was used in each region. The sphere was isostatically molded under a pressure of 5000 psi and baked. The sphere was reimpregnated several times and rebaked at a top temperature of 3600°F. A final graphite density of 1.80 gms/cc was achieved. X-ray diffraction patterns revealed that the UO_2 had been converted to UC. The .003" coating of siliconized silicon carbide was then applied to the sphere.

Photomicrographs of the 3M specimen are shown in Figure 4-1. The 10x view shows the coating, unfueled shell, and fueled core. The small bright spots in the core are fuel particles while the dark spots are places from which fuel particles have been removed during cutting and polishing. No difference can be noted between the uniform graphite matrix of the core piece and the unfueled shell. This section was cut from a specimen which had been impacted to failure, causing the crack in the left side of the picture. The excellent degree of bonding between the core and shell has prevented a discontinuity of this crack at the interface. The thin whitish crack near the right side occurred during manufacture and became filled with silicon carbide. The 100x view shows the two-phase coating consisting of the light gray silicon carbide particles in the white silicon matrix. The ability of the coating to completely penetrate crevices in the graphite can be noted.

The FA-16 specimens were prepared during the latter part of the past period in view of the serious flaws which developed in the FA-6 type while under irradiation in capsule SP-3 (See Section 7.2.1). Since it appeared that the source of these flaws was small cracks, probably of

the type noted in the 10X view in Fig. 4-1, a revised manufacturing procedure was used in preparing the FA-16 specimens. In addition, an unfueled shell thickness of 0.060 in was used. A large number of specimens made by the revised procedures were examined by sectioning and were found to contain no cracks. Further evaluation data on the FA-16 type is not yet available.

Carborundum Co.: Types FA-7, FA-8

The FA-8 fuel element, the principal type of this group which was tested during the past period, consists of an admixtured sphere and a 0.030 in SiC-Si coating. The FA-7 specimens are identical to FA-8 except that no SiC-Si coating was applied.

The uranium dicarbide fuel particles for this type were made by the Carborundum Company by reacting stoichiometric amounts of -200 mesh UO_2 powder and high purity graphite powder. Pellets of this material were heated to 2400°C and then crushed and screened so that 100 to 200 micron particles could be selected for incorporation in the fuel element. The carbon content of the fuel particles varied from 9.2 to 9.3% compared with 9.16% for pure uranium dicarbide. These fuel particles were admixtured with an isotropic grade of graphite (Speer Carbon Grade 901S) sieved through a 20 mesh screen. A resin type binder (Varcum 82-51) was used. Spherical shapes were then molded under 1000 psi and baked up to a maximum temperature of 3600°F. A .030 in silicon carbide coating containing an excess of silicon was then applied to the fueled graphite spheres.

Photomicrographs of an FA-8 specimen are shown in Fig. 4-2. The 10x view shows the coarse-grained matrix used in this specimen. The bright spots in the matrix are fuel particles while the smaller dark spots are spaces from which fuel particles have been removed during cutting and polishing. The larger dark spots appear to be voids and fissures in the matrix. A small crack can be noted in the outer surface of the coating. The disruption of the inner surface of the coating near the right side is possibly an area where the silicon has reacted with the fuel particles. The 100x view shows the larger proportion of silicon carbide in the coating with respect to the FA-6 specimen.

4.2 Metal Carbide Surface Coatings

Metal carbide surface coatings include zirconium carbide and titanium carbide. Several types were obtained on fueled spheres while several others were obtained on unfueled spheres.

American Metal Products: Types FI-6, FL-1, FL-2

This group includes two types of fueled graphite bodies to which a .001 in thick zirconium carbide coating was applied. The fuel is uniformly dispersed through the graphite matrix in the FI-6 type. Fuel particle size is 1 to 5 microns and a high density graphite is achieved by carbonaceous reimpregnation of the matrix. The ZrC coating is applied directly to the fueled sphere.

In the FL-2 specimen, all of the fuel is lumped in the center of the sphere in the form of a uranium dicarbide pellet. The fuel pellet is mounted inside a graphite cylinder which is threaded into the center of the sphere. After reimpregnation, the sphere is coated with ZrC. FL-1 is an uncoated version otherwise similar to FL-2. Figure 4-6 is a radiograph of the FL-2 specimen which clearly shows the centrally located 3/8 in diameter cylindrical fuel pellet. Some undesirable gaps around the fuel pellet cylinder can be noted. The ZrC coating is shown in Figure 4-7. The ZrC appears to be in a continuous phase with unconnected void spots although there is some evidence of continuous voidage at what are probably grain boundaries.

Plasmakote Corp.: Types FX-1 and FX-2

Plasmakote Corp. have developed techniques for depositing metal or metal carbide coatings by a flame-spraying technique. In order to evaluate this type of coating process, several unfueled specimens with two types of coatings were obtained. Type FX-1 was titanium carbide and type FX-2 was zirconium carbide. Unfueled 1-1/2 in diameter graphite spheres, machined from Speer Graphite Co. Moderator Grade B stock, were supplied to the manufacturer. Coating thickness ranged from .005 to .010 in. The coatings were given a high temperature fusing treatment, after being flame-sprayed on the graphite, in an attempt to form a continuous impermeable coating. However, as shown in

Figure 4-8, the coating appeared quite porous. As noted in Section 7.1, impact tests on both types showed poor adherence to the matrix, however, this could be partially attributable to the type of graphite surface.

4.3 Carbonaceous Surface Coatings

This type of coating contains no metal or metal carbide phase and consists solely of carbon deposited on the fuel element surface from the reduction of a hydrocarbon gas such as methane. The crystal structure of the coating can be that of a highly ordered graphite or a randomly ordered carbon structure, depending primarily on the temperature at which the coating is deposited. No attempt has been made to identify the crystal structure of either of the two types of coatings obtained during the past period. The National Carbon coating is referred to as a "pyrolytically deposited carbon coating" and abbreviated as "Pyro-C". The Raytheon coating is referred to as "Pyrographite", a company trade name, and is abbreviated as "Pyro-G". These titles are not necessarily meant to imply a difference in carbon structure.

National Carbon: Types FA-1, 9, 11, 14, 17, 19 and 20

This group of admixtured fuel elements have all been made of the same basic materials. They differ in such areas as the use of a re-impregnation treatment to increase the carbon density, the degree of graphitization, the type of fuel particle, and the application of a Pyro-C surface coating. Figure 4-3 has been prepared to illustrate the principal variables between fuel element types within this group.

The basic fuel element type within this group is FA-1. This type is made from an admixture of UO_2 fuel particles, graphite filler and a coal tar pitch binder. The UO_2 fuel particles were prepared by the Mallinckrodt Chemical Works in the form of high-fired shot of 94% theoretica density. The filler component was National Carbon Type 2301 graphite powder sized so that 98.5% would pass through a 200 mesh sieve. The mixture was then molded and baked up to a maximum temperature of 2560°F. At this temperature, the fuel particles were preserved as UO_2 but the matrix was not fully graphitized except for the filler component which was initially graphite powder.

As can be noted in Figure 4-3, two major variations of the basic FA-1 type were the reimpregnation of the graphite matrix and the complete graphitization of the matrix. The FA-9 specimens were prepared by successive reimpregnation with a carbonaceous pitch and rebaking of FA-1 specimens until the net density of the graphite matrix had been increased from 1.62 to 1.68 gm/cc. The FA-11 specimens were prepared by applying a .005 in thick pyrolytically deposited carbon coating to the FA-9 and FA-11 types.

The second major variation involves the full graphitization of the matrix. The FA-19 specimens were prepared by baking FA-1 specimens at 4800°F. At this temperature, the UO_2 fuel particles reacted with the graphite matrix to form UC_2 fuel particles. Full graphitization also causes a greater degree of shrinkage during baking so that the net graphite density is increased from 1.62 to 1.65 gm/cc. A slightly larger diameter FA-1 specimen was first prepared so that the final graphitized sphere would still be a nominal 1-1/2 in in diameter sphere. The FA-20 specimens were prepared by applying a .002 in thick pyrolytically deposited carbon coating to the specimen and rebaking at graphitizing temperatures. Photomicrographs of this type of coating are shown in Figure 4-4. A dense continuous coating can be seen except that the conical growth patterns of the carbon structure can be distinguished. The coating appears to adhere closely to the graphite matrix except in one area where a void has occurred. The bright spots in the region of this void have not been identified.

Two other variations, types FA-17 and FA-14, have also been prepared. Type FA-17 consists of a pyrolytic carbon coating applied directly to the type FA-1 specimen. Some difficulty had been encountered in getting a Pyro-C coating to adhere to a matrix which had been reimpregnated and it was found that type FA-17 coatings generally adhered better to the graphite matrix than did the type FA-11 coatings. Since the reference design for the 125 eMW Pebble Bed Reactor called for the addition of thorium to the core fuel elements, a batch of specimens containing the specified thorium and uranium content were prepared. This was done to check whether any significant differences or unanticipated problems would arise, since uranium was used in place of the thorium for all other test specimens. The type FA-14 specimens were prepared as uncoated specimens using the same graphite materials as in the basic FA-1 specimens. The fissile-fertile particles were prepared by the Mallinckrodt Chemical Works as high-fired shot, screened to -100 +140 mesh. Each particle contained thoria and urania in an 11:1 Th-U atom ratio, the reference design requirements.

A complete characterization of all these 7 types was not done during the past phase, however, pertinent test data is reported for each type, with the emphasis being on the basic FA-1 type and the graphitized and coated FA-20 type.

Raytheon Co.: Type FX-3

Two unfueled graphite spheres coated with Raytheon's "Pyrographite" were obtained during the past period. This material has found application as a rocket nozzle material primarily because of its superior strength and highly anisotropic properties. Tensile strengths of 25,000 psi are reported compared with values of 5000 to 8000 psi for normal high strength graphites. Thermal conductivity values of 200 and 2 BTU/hr-°F-ft in directions respectively parallel and perpendicular to the plane of the coatings are reported. The manufacturer also reports that this coating exhibits no detectable leakage at 1 atm. helium and room temperature under a mass spectrometer leak test.

In the application of this material to coatings for PBR fuel elements, two problems are significant. The low thermal conductivity in the radial direction can cause significant temperature gradients as discussed in Section 3.2. Also the coefficient of thermal expansion is somewhat lower for Pyrographite than for most other graphites. It is expected the addition of trace amounts of metal to the Pyrographite structure can improve the radial thermal conductivity to an acceptable degree. The lower thermal expansion can lead to one of two concepts. In one case, an unbonded spherical shell of high strength Pyrographite can surround a simple fueled body. The Pyrographite shell would possess all of the strength and fission product retention characteristics of the fuel element, irrespective of the type of fueled body or the irradiation damage to the fueled body. In the other case a special fueled graphite body would be developed having a matched thermal expansion so that no gap would develop during fabrication.

The FX-3 spheres consisted of unfueled graphite spheres, identical to the matrix of the FA-19 specimen, to which a .060 in thick Pyrographite coating was applied. One specimen was coated while being supported on a graphite rod and the other was coated while being tumbled. Figure 4-5 is a photomicrograph of a separate piece of the Pyrographite coating which had not been bonded to a graphite sphere. Both views in Figure 4-5 are at

250x, the upper view being taken in a bright field and the lower view taken under polarized light. Again, a dense continuous coating is seen. Under polarized light, the conical growth patterns of graphite crystals are readily seen. The only tests of the FX-3 specimens during the past period were a hot oil test which showed no leakage from either specimen.

4.4 Coated Fueled Particles

Four types of coated UO_2 particles were obtained during the past period. Three types of metal coatings were furnished by NUMEC. The fourth type was an alumina coating being developed by BMI and development progress for this type is described in Section 5.1.

Nuclear Materials & Equipment Corp.: Types FP-1, 2 and 3

Metal coatings for UO_2 particles are being developed by NUMEC for other applications under another AEC contract. A quantity of these coated fueled particles were obtained from NUMEC to determine whether they could be applied to Pebble Bed Reactor requirements. Although the available metals have a significant thermal neutron adsorption cross-section and are known to react with carbon, it was desired to see whether a metal or metal carbide coating on the fuel particles would offer a significant degree of fission product retention. The three types of metal coatings were nickel (FP-1), nickel-chromium (FP-2) and niobium (FP-3). The nickel (FP-1) and niobium (FP-3) coatings were 10μ thick. The FP-2 particles were made by depositing first a 2μ nickel layer and then an 8μ Cr layer. Two batches of the FP-1 and FP-2 particles having different manufacturing procedures were received.

Figure 4-9 is a photomicrograph of the Nb ciated particles in the as-received condition. Figures 4-10 and 4-11 are photomicrographs of the Ni and Ni-Cr coated particles from the second batch, also in the as-received condition. In addition to the standard screening tests, coated particles from the first batches were incorporated in graphite at BMI for carburization studies as described in Section 7.1.

4.5 Miscellaneous Uncoated Specimens

One of the high temperature irradiation tests started during the past period was in Capsule SP-4 (see Section 7.2.2). The purpose of this test

was to determine the stability of four types of UO_2 particles in graphite under irradiation. In addition to the FA-1 specimen (100μ)UO_2 described in Section 4.3, the other types were an infiltrated specimen (FI-1), a 67 μ UO_2 admixtured specimen (FA-2), and a 400μ UO_2 admixtured specimen, (FA-10). All these types were uncoated.

Sylvania Corning Nuclear Corp: Type FI-1

This type of specimen was prepared by infiltrating AGOT graphite spheres with a uranyl nitrate solution followed by a drying and a denitration step. The final fuel form was a uniform dispersion of 1μ UO_2 particles in the graphite. Details of the process as developed by Sylcor are described in Appendix B of NYO 2373.

Battelle Memorial Institute: Type FA-2

This type of fuel element was made by an admixture of UO_2, coke filler, and a pitch binder. The UO_2 particles averaged 67 microns in diameter. A Texas coke filler and a standard coal tar pitch binder were used. The mixture was molded into a spherical shape under 10,000 psi pressure. The spheres were then baked at 2000°F in order to preserve the UO_2 particles. At this bake temperature only a small degree of graphitization was achieved since neither the filler nor the binder were in graphite form prior to making the specimens.

Great Lakes Carbon: Type FA-10

This type was made by an admixture of UO_2 particles, graphite filler, and a coal tar pitch binder. The UO_2 fuel particles were prepared by the Davison Chemical Co. from U_3O_8 powder. The material was fired at 3100°F for 2 hrs and a top density of 5.06 gm/cc was achieved. The particles were sieved through 40 mesh on 45 mesh to give a particle size range of 350 to 420 microns. The graphite filler was Great Lakes Carbon Grade 1008 graphite flour, sized so that 5 % would pass through a 200 mesh sieve. After molding, the specimens were baked at 2000°F. The spheres were reimpregnated several times and rebaked to give a net graphite density of 1.8 gms/cc.

TABLE 4-1

SUMMARY OF FUEL ELEMENT TYPES

	INFILTRATED		LUMPED		UNFUELED			COATED PARTICLES			
Number	FI-1	FI-6	FL-1	FL-2	FX-1	FX-2	FX-3	FP-1	FP-2	FP-3	FP-4
Mfgr.	Syl.	AMP	AMP	AMP	Plas.	Plas.	Ray.	NUMEC	NUMEC	NUMEC	BMI
FUEL											
Loaded As	UNH	UNH	UC_2	UC_2	—	—	—	UO_2	UO_2	UO_2	UO_2
Final Form	UO_2	UC_2	UC_2	UC_2	—	—	—	UO_2	UO_2	UO_2	UO_2
Particle Size, μ	1	1	3/8"	3/8"	—	—	—	100	100	100	500
MATRIX											
Reimpreg.	no	yes	yes	yes	—	—	—	—	—	—	—
Net Density	1.65	1.85	1.85	1.85	—	—	—	—	—	—	—
Shell Thick.	0	0	0.35"	0.35"	—	—	—	—	—	—	—
Bake Temp, °F	1470	3500	3500	3500	—	—	—	—	—	—	—
COATING											
Material	—	ZrC	—	ZrC	TiC	ZrC	Pyro-G	Ni	Ni-Cr	Nb	Al_2O_3
Thickness	—	.001"	—	.001"	.010"	.010"	.060"	10μ	10μ	10μ	250μ

Manufacturers

- AMP - American Metal Products
- BMI - Battelle Memorial Institute
- Carbo - Carborundum
- GLC - Great Lakes Carbon
- 3M - Minnesota Mining and Manufacturing
- NC - National Carbon
- NUMEC - Nuclear Materials and Equipment Corp.
- Plas - Plasmakote
- Ray - Raytheon
- Syl - Sylvania-Corning Nuclear

	ADMIXTURED													
Number	FA-1	FA-2	FA-5	FA-6	FA-7	FA-8	FA-9	FA-10	FA-11	FA-14	FA-16	FA-17	FA-19	FA-20
Mfgr.	NC	BMI	3M	3M	Carbo	Carbo	NC	GLC	NC	NC	3M	NC	NC	NC
FUEL														
Loaded As	UO_2	UO_2	UO_2	UO_2	UC_2	UC_2	UO_2	UO_2	UO_2	ThO_2/UO_2	UO_2	UO_2	UO_2	UO_2
Final Form	UO_2	UO_2	UC	UC	UC_2	UC_2	UO_2	UO_2	UO_2	ThO_2/UO_2	UC	UO_2	UC_2	UC_2
Particle Size, μ	100/150	67	100/200	100/200	100/200	100/200	100/150	350/420	100/150	100/150	100/200	100/150	100/150	100/150
MATRIX														
Reimpreg.	no	no	yes	yes	no	no	yes	yes	yes	no	yes	no	no	no
Net Density	1.62	1.63	1.80	1.80	1.63	1.63	1.68	1.80	1.68	1.62	1.75	1.62	1.65	1.65
Shell Thick	0	0	0.15"	0.15"	0	0	0	0	0	0	.060"	0	0	0
Bake Temp, °F	2560	2000	3600	3600	3600	3600	2560	2000	2560	2560	3600	2560	4800	4800
COATING														
Material	—	—	—	SiC-Si	—	SiC-Si	—	—	Pyro-C	—	SiC-Si	Pyro-C	—	Pyro-C
Thickness	—	—	—	.003"	—	.030"	—	—	.005"	—	.003"	.002"	—	.002"

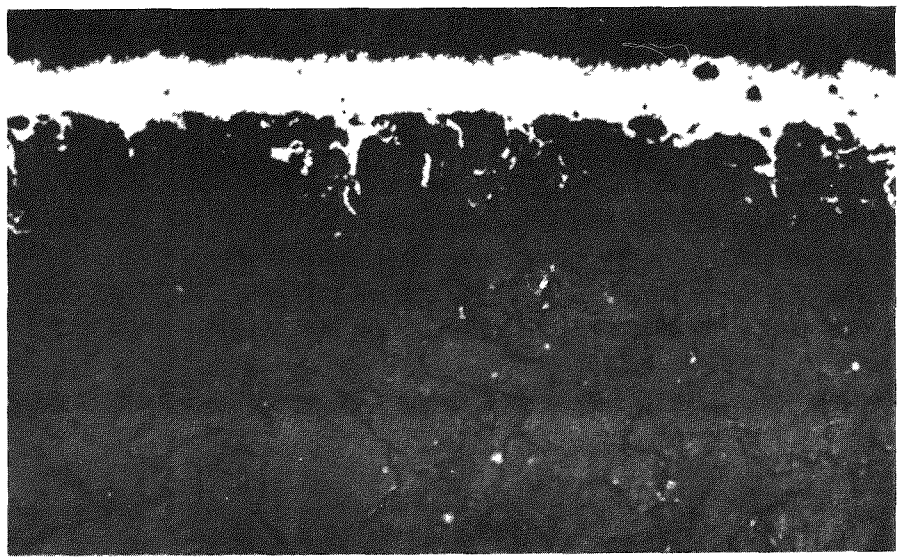

100x

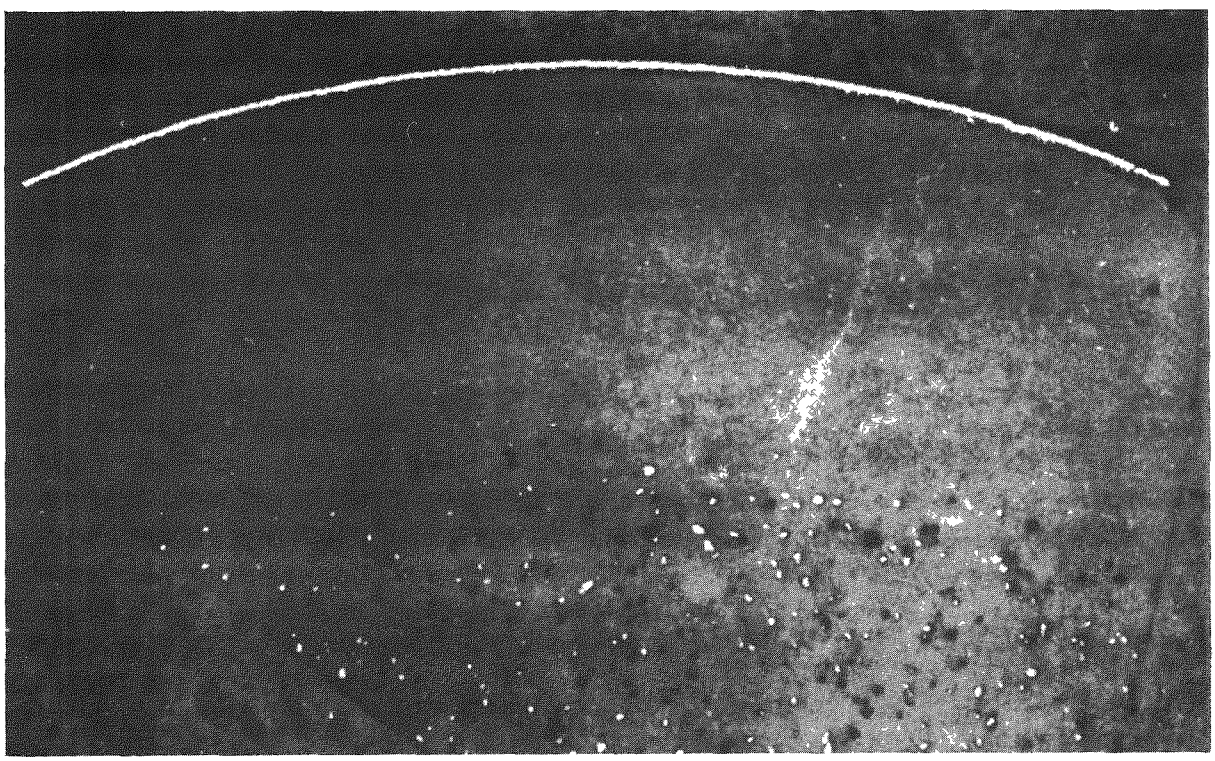

10x

FIG. 4-1 SiC-Si Coated Specimen FA-6 Before Irradiation.

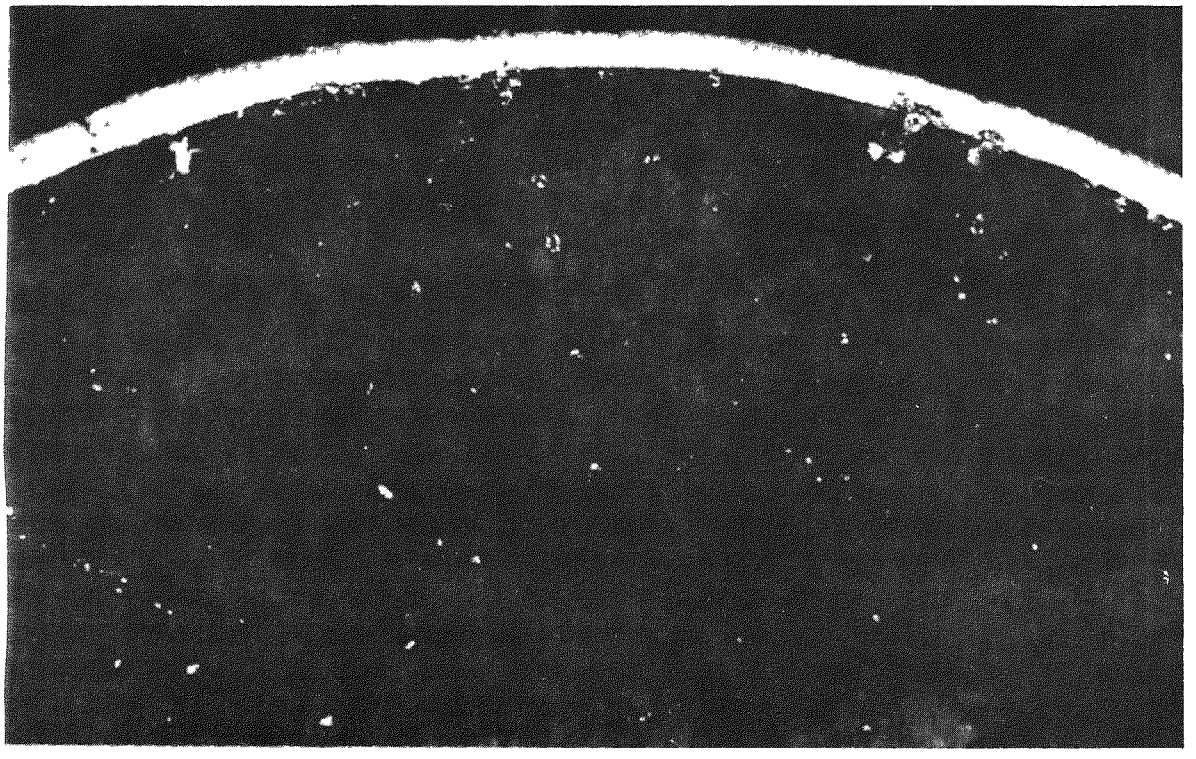

10 x

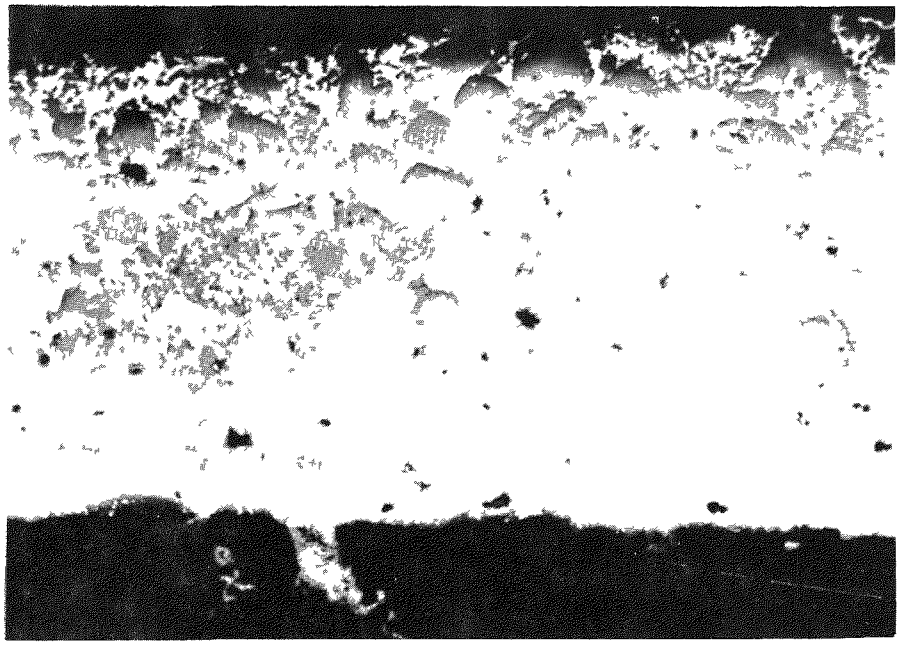

100x

FIG. 4-2 SiC-Si Coated, Specimen FA-8 Before Irradiation.

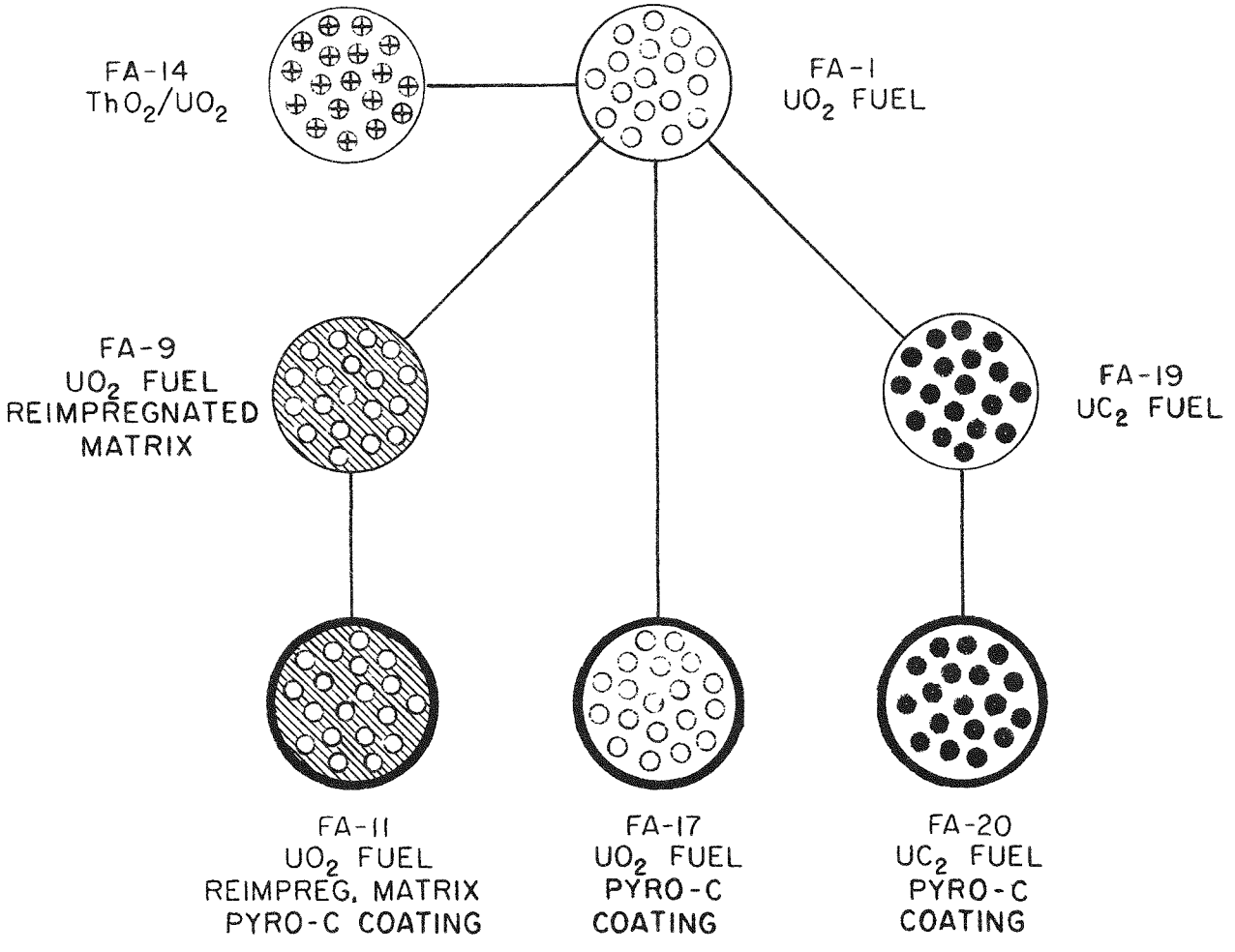

FIG. 4-3 PRINCIPAL VARIABLES BETWEEN ADMIXTURED PBR FUEL ELEMENT SPECIMENS SUPPLIED BY THE NATIONAL CARBON CO.

(a) 250X

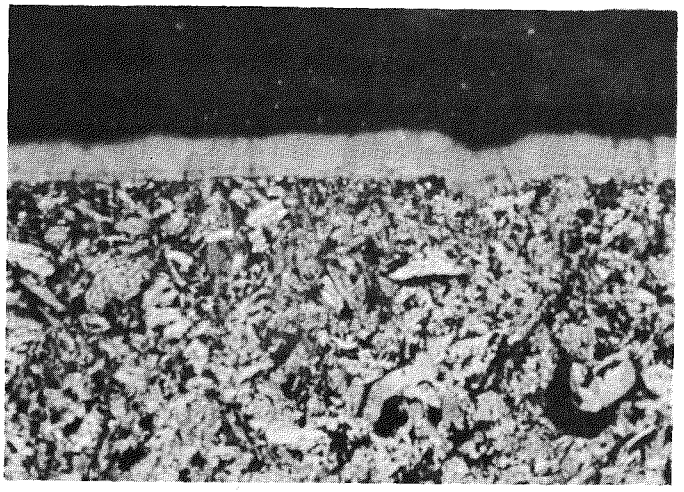

(b) 100X

FIG. 4-4 Pyrolytically Deposited Carbon Coating, on the FA-20 Specimen.

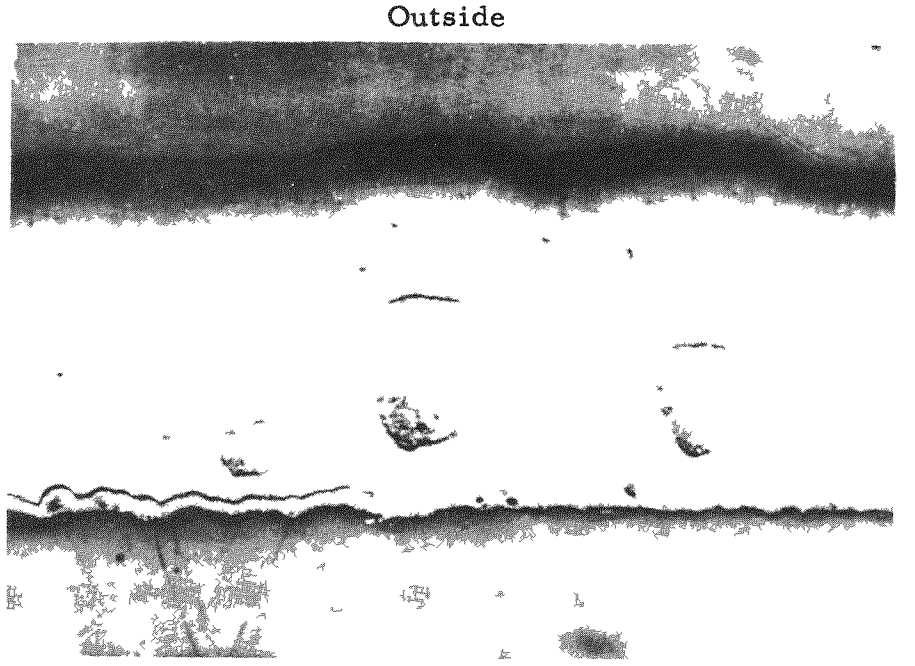

(a) 250X in bright Field

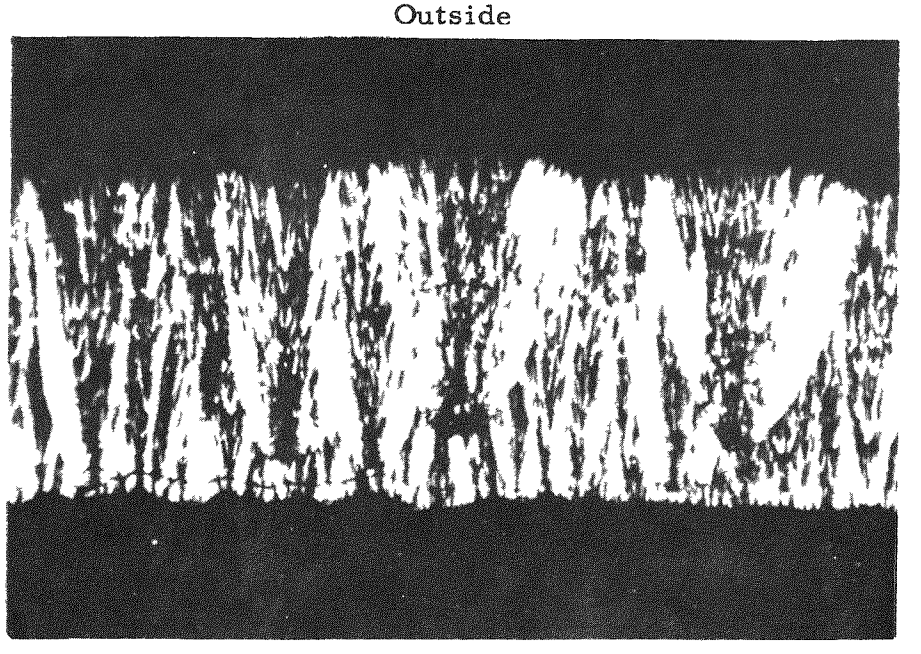

(b) 250X under polarized light

FIG. 4-5 Pyrographite Coating, Similar to Coating on FX-3 Specimen, Not Mounted on Graphite Matrix.

FIG. 4-6 Radiograph of FL-2 Specimen

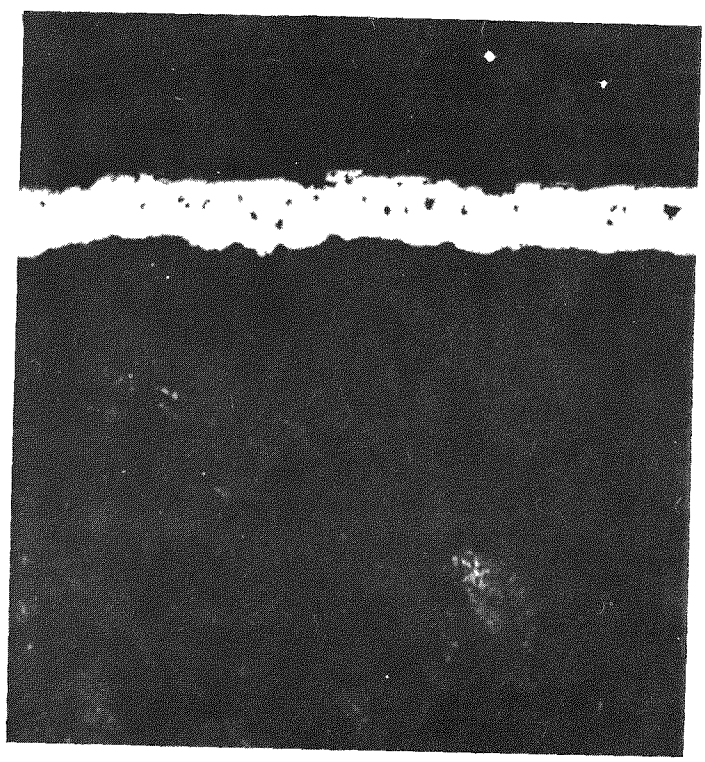

FIG. 4-7 Zirconium Carbide Coating on Type FL-2 Specimen (250X).

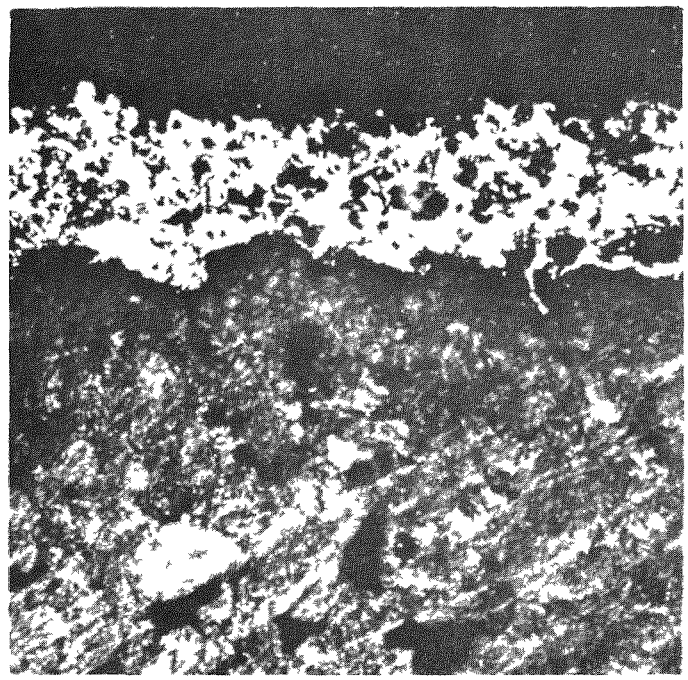

FIG. 4-8 Flame Sprayed and Fused Zirconium Carbide Coating on FX-2 Specimen (100X).

FIG. 4-9 Niobium Coated UO_2 from First Batch (250X).

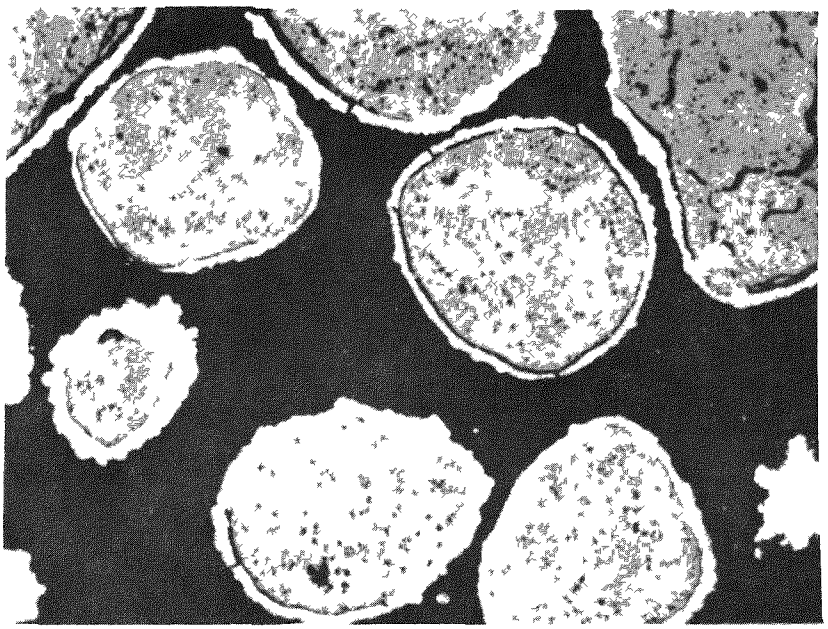

FIG. 4-10 Nickel Coated UO_2 from Second Batch (250X).

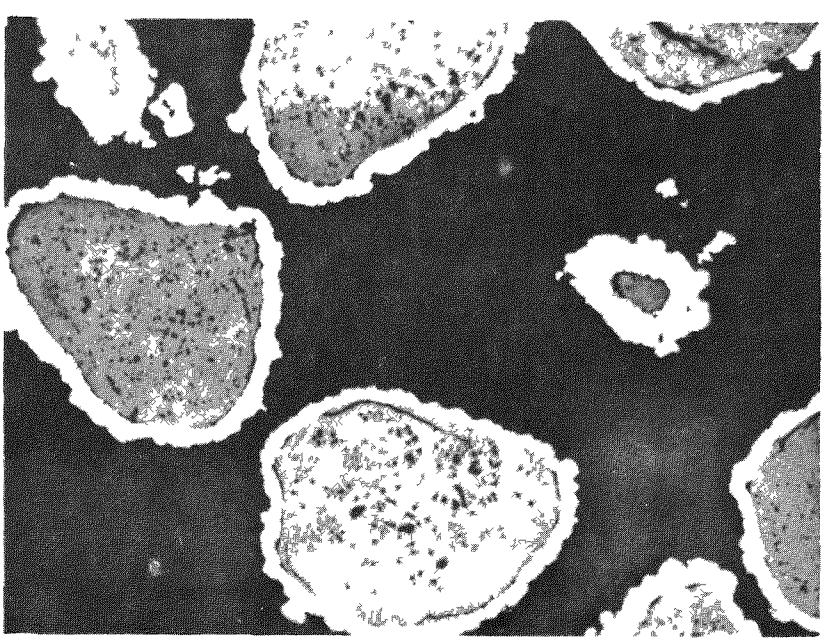

FIG. 4-11 Chromium-on-Nickel Coated UO_2 from Second Batch (250X).

5.0 Development of Alumina & Sub-surface Coatings

The fuel element types and components described in Section 4.0 were all procured from private manufacturers on a no-charge basis or on a sample-lot-fixed-price basis. During the past period the development of two additional concepts were carried on at the Battelle Memorial Institute. These were alumina coatings for UO_2 particles and an internal coating concept conceived by S & P and known as the "freeze-seal" concept. Progress in the development of these types and test results obtained during the past period are described in this section.

5.1 Alumina Coated UO_2 Particles

A technique for applying high density alumina coatings on UO_2 particles had been conceived at Battelle and described in BMI-1321. A small batch of coated particles had been made by using irregular UO_2 particles, crushed from a sintered compact. Due to the differential sintering shrinkage of the alumina (about 17 linear percent) and the UO_2 (about 10 linear percent), it was necessary to introduce an organic layer (gum arabic) between the coating and the fuel particle which would burn out during sintering and thus allow the alumina to shrink without restraint.

At this point, further development work on this concept was undertaken for the PBR program during the past period. The objectives in this work were to employ spherical UO_2 to overcome the uneven coating thickness caused by irregular UO_2 particles; to investigate other methods of enhancing the shrinkage of the UO_2 particles which would be more amenable to control of the coating process than the use of the organic "burnout" layer; to refine the fabrication process in order to permit production of reproducible coatings; and to investigate the reaction of alumina with graphite.

5.1.1 Fabrication Development

The basic process for fabricating alumina coated particles consists of first building up spherical uranium oxide particles from sinterable oxide powder and organic binder in a planetary mixer and a pelletizing drum. After screening the particles to the desired size, they are again placed in a pelletizing drum where a slip of organic binder and alumina powder are dusted on until a suitable coating thickness has been deposited. The coated particles are then isostatically pressed and sintered.

Numerous variables in this procedure were tested in order to produce a uniformly acceptable coating. In order to increase the sintering shrinkage of the UO_2 particles, two approaches were tried. One was the use of UO_3 which has a considerable shrinkage when reduced to UO_2. The other was the addition of 10 w/o alumina monohydrates to the UO_2. Various organic binders, such as polyvinyl alcohol, Carbowax 4000, and gum arabic, each up to 10 w/o were tried for both fuel and coating. Fuel particles were used both with and without a compacting step prior to coating. A special devolatilization step prior to sintering was tried by holding the formed particles at 1200°F for 0, 1, 2 and 4 hours. Both calcined and fused alumina were tried as the pressing matrix during the isostatic pressing step.

One of the more promising fuel particles produced is shown in Figure 5-1. The UO_2 particle diameter and the alumina coating thickness are both about 400μ. The 50μ gap between the UO_2 and the alumina results from the high degree of fuel particle shrinkage achieved during sintering. Some unconnected porosity can be seen in the alumina coating.

The most promising fabrication procedure based on work to date involves either the use of UO_2-UO_3 mixture or less than 10 w/o of alumina monohydrate in the UO_2 since both of theses materials have been found to produce sufficient shrinkage to leave a gap between the final UO_2 and the alumina. A 2 w/o polyvinyl alcohol binder would be used for the fuel particle. The UO_2 particle would be compacted before coating and a 5 w/o gum arabic binder would be used with the alumina coating. Isostatic pressing would be done at 100,000 psi using a fused alumina pressing matrix. Devolatilization of the binder would be accomplished by soaking for 4 hours at 1200°F. Coated particles would be sintered for 1 hour at 2800°F.

5.1.2 Evaluation

Two pre-irradiation tests have been used to evaluate the coated particles. In one, the particles are heated in air at 1200°F for several hours so that the presence of faults in the coating will oxidize the UO_2 to U_3O_8. This result can often be observed visually. However, weight gain is used as the criterion of acceptance. Typical weight gains of greater than 20% are noted for extremely poor batches. A weight gain of less than 1% is considered acceptable.

In one batch, a weight gain of 0.14% was noted. The exposed U_3O_8 was leached from this batch by boiling in 6N HNO_3. The empty alumina shells were separated by a heavy-liquid flotation. In order to test for

uranium contamination at the coating surface of these particles, an alpha count was performed using the gas flow counter described in Section 6.1. An alpha count rate of <0.5 cpm per gm was noted. This is equivalent to 1×10^{-4} mg U per gm of particle or 4×10^{-7} gms U at the surface per gm of U in the particle.

A neutron activation test was also performed using the apparatus described in Section 6.2. Both coated and uncoated UO_2 particles were tested for comparison. Results are given in Table 5-1.

TABLE 5-1.

Results of Neutron Activation Test on Al_2O_3 Coated & Uncoated UO_2.

	Test Temp. °F	Time Min.	Fraction of Xe133 Released
Uncoated UO_2	1600	15	0.3×10^{-2}
	1800	15	(a)
	2500	30	2.0×10^{-2}
Al_2O_3 Coated UO_2	1500	30	(a)
	1800	30	2.4×10^{-5}
	2000	60	1.4×10^{-5}
	2200	30	(a)
	2450	30	5.5×10^{-5}

(a) Activity level included as part of the subsequent reading.

5.1.3 Carburization Studies

In addition to development work on the coated particle itself, the reaction of alumina coatings with a graphite matrix was also investigated during the past period. This was done by incorporating alumina coated UO_2 particles in graphite and heating at various temperatures of interest. The graphite matrices were made with an AGOT graphite flour and a Barrett pitch binder, pressed at 24,000 psi, and baked at 1700°F. Separate specimens containing dispersions of alumina coated UO_2 particles were then heated in helium at 2500°F for 168 hrs and at 3000°F for 6 hrs.

The specimens were examined by metallographic techniques in order to determine the extent of reaction between the graphite, alumina and UO_2.

Figure 5-2 shows the coated particle in graphite as baked at 1700°F. The coarse granular nature of the alumina on one side of the coating is probably due to uneven pressure during the pressing step. No evidence of reaction between the UO_2, Al_2O_3 and the graphite is noted. The dark band on the inside and outside of the alumina coating is a gap. Figure 5-3 shows the results of heating at 2500°F. Again, no alumina-graphite reaction can be detected. There is some evidence of an alumina-urania reaction at the inner surface of the alumina, although this could be a residue from the fabrication process. At 3000°F, complete disintegration of the particle was noted, as seen in Figure 5-4. No attempt was made to identify the reaction products. Light gray particles are noted in the center as distinguished from the graphite crystals near the edges. The white metallic-like phase outlining the original particle is probably a complex uranium-aluminum carbide.

5.1.4 Conclusions

Fabrication studies have shown that a feasible approach to the differential shrinkage problem during fabrication of the particles is through the use of UO_2 blended with either UO_3 or alumina monohydrate and that a reasonably spherical shape can be obtained in the process. Study of other variables in the fabrication process indicates that coatings of reproducible integrity can be made. Reaction studies with graphite have shown that a fuel element of this type will be limited to 2500°F which means that partially graphitized bodies would be used. A fission product diffusion screening test has shown that at 2500°F, the presence of the alumina coating reduces the fission product leakage by nearly three orders of magnitude.

Based on these results, it is planned to continue development work during the next period with emphasis on preparing particles with a minimum gap between the alumina and the UO_2, on the reduction of coating thickness to about equal the UO_2 particle radius, on long time reaction rates between alumina and graphite at 2500°F, and on the preparation of sufficient quantities of normal and possibly enriched particles to permit testing of 1-1/2 in diameter fueled graphite spheres.

5.2 Sub-Surface Coatings

A third method of applying coatings to uranium-graphite fuel elements, in addition to surface coatings and fuel particle coatings previously described, is to locate the coating between a fueled pellet and an outer shell of unfueled graphite. This technique has two basic advantages.

(1) The coating is not directly subjected to external loads during handling and coating contamination requirements can be relaxed because of the unfueled graphite barrier.

(2) A coating material can be used which becomes plastic or molten at reactor operating temperatures, flowing into the pores and fissures of the unfueled shell and solidifying because of the temperature gradient. This concept has been identified as a "Freeze-Seal".

Two of the major problems encountered to date in the use of surface coatings have been uranium contamination of the coating and damage during handling. The use of a sub-surface coating, i.e. a coated fueled core with an outer shell of unfueled graphite offers a solution to these problems.

A further extension of this concept is the "Freeze-Seal" element. Such an element consists of a spherical pellet containing fissile and/or fertile material dispersed in graphite. This pellet is jacketed with a suitable material and the whole encased in a graphite shell. Lumping the fuel in a small spherical pellet results in a high central temperature and a large temperature gradient through the graphite shell. By selecting a material for the jacket which is plastic or molten at reactor operating temperatures, the pressure generated by the fission product gases in the fueled pellet will drive the molten jacket material into the pores of the graphite where it freezes and seals, due to the temperature gradient. A fissure in the graphite shell would be sealed in the same manner.

5.2.1 Sub-Surface Coating Program

The program for development of this fuel element type has been set up in three phases, as follows:

1 - Compatibility and Fabrication Studies - A series of scoping experiments will serve to define problem areas and promising materials.

2 - Proof Testing - The question of the efficacy of the concept(s) in preventing the leakage of fission products by pre- and post-irradiation testing will be answered.

3 - Design Optimization - Assuming basic feasibility has been demonstrated by item 2, this phase of the program will be concerned with design optimization.

Work done during Phase I of this contract has been on compatibility and fabrication studies.

5.2.2 Compatibility Studies

Compatibility studies have been made between several metals and ceramics and graphite. The basic object was to obtain data on the wettability of these materials. Table 5-2 lists the materials tested. Table 5-2a lists the detailed composition of the four glasses used.

TABLE 5-2

Materials Used in Graphite Wettability Studies

Material	MP - °F	σ_a, barns
4 glasses (Table 5-2a)	1800-2500	-
$MoSi_2$	2165	2.76
Cu	1980	3.69
Ni	2640	4.6
Si	2600	0.13

TABLE 5-2a

Composition of Glasses(w/o)

Material	Glass #1	Glass #2	Glass #3	Glass #4
$CaSiO_3$	27.4	19.2	19.2	35.6
Al_2O_3	8.6	6.0	6.0	18.0
SiO_2	21.2	14.8	14.8	-
BaO	42.8	60.0	55.0	-
MoO_3	-	-	5.0	-
KNO_3	-	-	-	19.6
MnO	-	-	-	9.0
TiO_2	-	-	-	4.4
CaF_2	-	-	-	13.4
σ_a, barns	.655	.979	.778	3.275

In selecting these materials the glasses were included for the reason that they represent a ceramic that can be tailored in melting point and wettability by adjusting composition. They were considered to be potential jackets for freeze-seal elements. $MoSi_2$, which was known to be compatible with graphite, was included to provide a common material in the compatibility and fabrication studies. Copper, nickel and silicon were selected as metals for possible freeze-seal application because of the range of melting temperatures, their reactions with graphite, and compatibility characteristics with graphite. While there was a desire to include beryllium it was omitted because of the setup costs that would be incurred in handling a toxic material.

To test wettability with graphite, the metals and glasses listed in Table 5-2 were placed in small graphite crucibles and held at controlled temperatures for short periods of time after which they were cooled, sectioned and examined metallographically. The temperatures used were 1800°F, 2200°F and 2600°F, while the time at temperature was 5 minutes.

The results of these tests are summarized in Table 5-3. It can be seen by examination of this table that at 1800°F there was no penetration of the graphite by any of the materials tested. There was some wetting of the surface by copper as well as silicon, as determined by metallographic examination of the interface between the crucible and the melt. At 2200°F there was definite wetting of the graphite by copper, silicon and #3 glass and there may have been some penetration by the metals but not by the glass. At 2600°F the copper, silicon, nickel and #1 and #3 glasses all wet the surface. The copper, nickel and #1 glass all showed slight penetration while the silicon showed a greater penetration probably in the form of silicon carbide. The #2 glass showed some adherence to the graphite surface with slight penetration. The #4 glass neither wet nor penetrated the graphite, however there was some slight erosion of the crucible The #1 glass penetrated slightly but seriously eroded the crucible. The molybdenum disilicide showed selective adhesion to the graphite.

Figures 5-5 and 5-6 show typical photographs of the sectioned crucibles after heating to 2600°F. The metal had been removed in each case (though the glass is still present in the photograph) and all that shows in the photographs is that which had adhered to the graphite surface or worked its way into the pores.

TABLE 5-3

Results of Melts in AGOT Crucibles

Type of Metal	Wet Graphite at Crucible Interface	Degree of Penetration into Graphite Crucible	Observations
		Heated at 1800 F for 5 minutes	
Copper	Yes	Slight	Some particles adhered to wall.
Silicon	Slight	None	
No. 1 glass	None	None	
No. 2 glass	None	None	
No. 3 glass	None	None	
No. 4 glass	None	None	
Nickel	None	None	
$MoSi_2$	None	Slight	Some particles adhered to crucible wall.
		Heated at 2200 F for 5 minutes	
Copper	Yes	Slight	Particles adhered to crucible wall.
Silicon	Yes	Very slight	
No. 1 glass	None	None	
No. 2 glass	None	None	
No. 3 glass	Slightly	None	Some adherence in small area.
No. 4 glass	None	None	Slight erosion of crucible.
Nickel	None	None	
$MoSi_2$	None	Slight	
		Heated at 2600 F for 5 minutes	
Copper	Yes	Slight	Adhered to graphite.
Silicon	Slightly	1/8 in. or greater	
No. 1 glass	Yes	Slight	Crucible badly eroded.
No. 2 glass	None	Slight	Adhered to graphite.
No. 3 glass	Yes	None	
No. 4 glass	None	None	
Nickel	Yes	Slight	
$MoSi_2$	None	None	

The above results are not conclusive, however they do indicate that copper, nickel (or cupro-nickel alloys) and $MoSi_2$ have the necessary materials-compatibility characteristics to function as the seal in graphite fuel elements. The #2 and #3 glasses also seem to be satisfactory. It must be remembered however, that since these tests were intended primarily to study wettability and penetrability, the materials were held at temperature for only a short time interval. Chemical reactions and other kinetic effects therefore cannot be reported from this program.

5.2.3 Fabrication Studies

While the above compatibility studies were under way, the fabrication of several spherical fuel elements containing a sub-surface seal was attempted to determine whether any unforeseen problems would arise during the fabrication cycle. If no problems developed, it was expected that one or more of these elements might be used during the proof testing phase of the work. Two types of fuel elements were prepared, with the following approximate dimensions: one having a 1 in fueled graphite core covered with a 1/8 in thick metal jacket which is in turn covered by a 1/8 in thick graphite shell; and the other having a 1 in fueled graphite core with a very thin metal seal and a 1/4 in thick graphite shell. These seal thicknesses represent extremes within which the desired seal thickness will probably fall, and were selected to bracket the desirable range rather than to be representative of finished elements. In preparing these balls, the seal material was incorporated in the ball by mixing powdered metal with a binder (carbopol or 79L resin) and compacting under pressure. This technique was used in an attempt to prepare a ball in which all three regions would shrink a like amount during fabrication. The use of a solid metal sheath in the intermediate region of a freeze-seal ball would give more positive leakage protection but presents the problem of the outer graphite jacket shrinking during fabrication while the inner regions are unyielding. It is believed that this can be handled by incorporating a burnout layer between the seal metal and the outer shell, however this does represent a manufacturing complexity which it was thought best to avoid at the outset.

The materials chosen for this series of tests were selected because of prior experience by others indicating compatibility with graphite. $MoSi_2$ and Cr were selected because of the known ability of $MoSi_2$ and chromium carbide to prevent UC_2 migration in graphite. Titanium was selected because of the known penetrability of graphite by titanium and because of the knowledge that titanium carbide coatings have been successfully applied to graphite.

A total of 22 fuel elements were prepared using natural UO_2 in the fueled region. Five balls had no seal layer and were used as controls. Three were prepared with a thick chromium seal and one with a thin chromium seal. Four had a thick molydisilicide seal and one had a thin molydisilicide seal. Five had a thick titanium seal and two had a thin titanium seal. These fuel elements were all fabricated by molding the inner core piece, then molding on the metallic seal layer and finally molding on the outer graphite shell.

After fabrication these balls were first cured at 350°F to set the binder then baked for 8 days at 200°F to devolatilize the ball. Degassing of all three regions of the ball occurred at the same time.

All of the balls looked satisfactory after the 350°F cure. After the 8 day bakeout however, many of the balls had severely cracked outer shells and in several cases had cracked seal regions as well. The results are summarized in Table 5-4.

The chromium and titanium thick-seal balls which had severe cracks in the outer shell were deshelled manually and the metal-jacketed inner cores were subjected to the hot-oil test. The seal layer was found to leak in the characteristics manner of a porous body. This is really not surprising since the metal particles in the seal layer were not fused.

To determine whether the seal layer could be made to fuse into a leak-tight coating, new graphite shells were molded onto the damaged samples and the samples were brought to 4660°F to melt the metal layer. The molten chromium ran out a crack which developed in the outer shell. The titanium layer failed to penetrate the graphite structure, probably due to the presence of a titanium carbide layer formed during the 8 day bake-out at a lower temperature. The $MoSi_2$ layer fused together and whereas the layer was actually broken into several discrete pieces before this last heat, after heating the hot-oil test showed but one pinhole leak.

5.2.4 Conclusions

The studies conducted to date indicate the compatibility of copper, nickel, molydisilicide and #3 glass with graphite at the temperature of interest to the Pebble Bed Reactor. These studies have also indicated that it is possible to fabricate a ball with a fusible seal material contained within it. Furthermore, there is evidence which leads one to be optimistic that such a fusible seal layer can in fact form a barrier to the leakage of fission product gases.

On the basis of these results, it is planned to continue this work in the next period with emphasis on the cupro-nickel alloys, $MoSi_2$ and #3 glass. Modifications in the fabrication technique will involve baking out (degassing) of the inner fueled core prior to jacketing, and the use of preformed metal jackets. It is expected that a satisfactory fuel element will be prepared during this period and that it will be proof-tested by neutron activation.

TABLE 5-4

Spheres Baked at 2200 F

Sample No.	Seal Material	Seal Thickness inches	Observations after Bake	Further Treatment	Further Observation
1	Chromium	.027	Small crack at equator		
3	Titanium	.014	Two small cracks at equator		
4	Titanium	.019	Small crack at equator		
5	Chromium	.049	Shell cracked--metal seal intact	Fabricated new shell--being baked at 1500 F	
7	$MoSi_2$	.046	Badly cracked--some erosion of graphite on both sides of seal	Fabricated new shell--being baked at 1500 F	
8	$MoSi_2$	.049	Badly cracked--some erosion of graphite on both sides of seal	Fabricated new shell--heated to 4660 F	Excellent adherence of seal to both inner sphere and shell.
9	Titanium	.018	Shell cracked--metal seal intact	Fabricated new shell--being baked at 1500 F	
10	Titanium	.034	Shell cracked--metal seal intact	Fabricated new shell--being baked at 1500 F	
11	Chromium	.052	Shell cracked--metal seal intact	Fabricated new shell--heated to 4660 F	Seal melted and ran through cracks in shell.
12	Chromium	.029	No apparent cracks		
16	Titanium	.056	Cracked at equator		
17	Titanium	.049	Cracked across equator		
18	MoSi	.037	Badly cracked--some erosion of graphite on both sides of seal	Fabricated new shell--being baked at 1500 F	
21	MoSi	.138	Badly cracked--some erosion of graphite on both sides of seal	Fabricated new shell--being baked at 1500 F	
23	Titanium	.100	Badly cracked	Fabricated new shell--heated at 4660 F	Cracks in seal but good adherence to graphite.
26	MoSi	.048	Badly cracked--some erosion of graphite on both sides of seal	Fabricated new shell--being baked at 1500 F	
31	Standard spheres containing no metal seal	--	Very good--no apparent cracking		
32	Ditto	--	Good except for mold tear near equator		
33	"	--	Good--fine hairline crack		
34	"	--	Very good		
35	"	--	Good--hairline crack at equator		

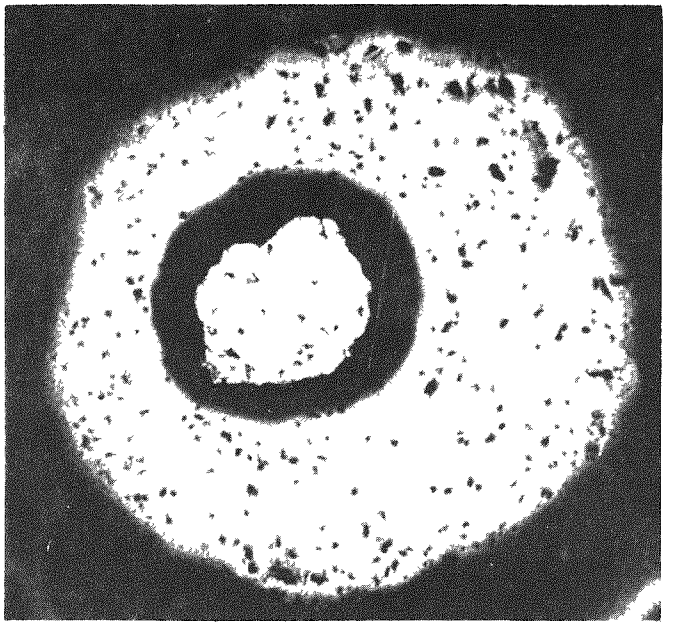

FIG. 5-1 Al_2O_3 Coated UO_2 as Fabricated (50X)

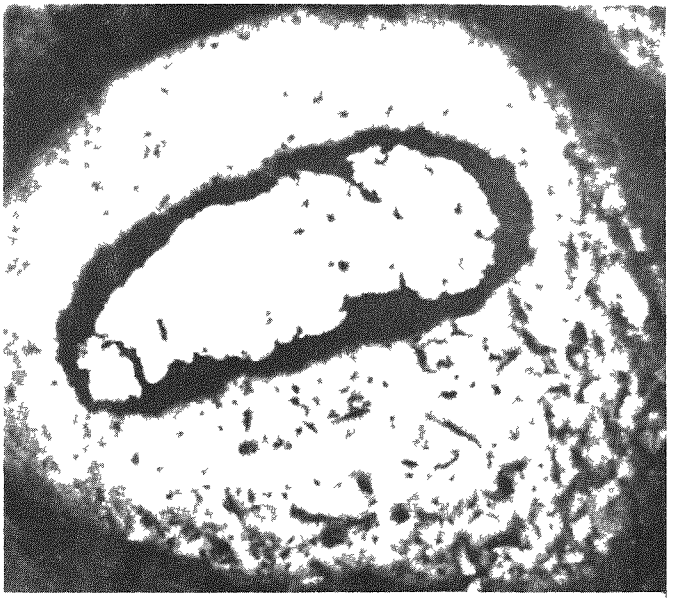

FIG. 5-2 Al_2O_3 Coated UO_2 in Graphite Baked at 1700°F (50X).

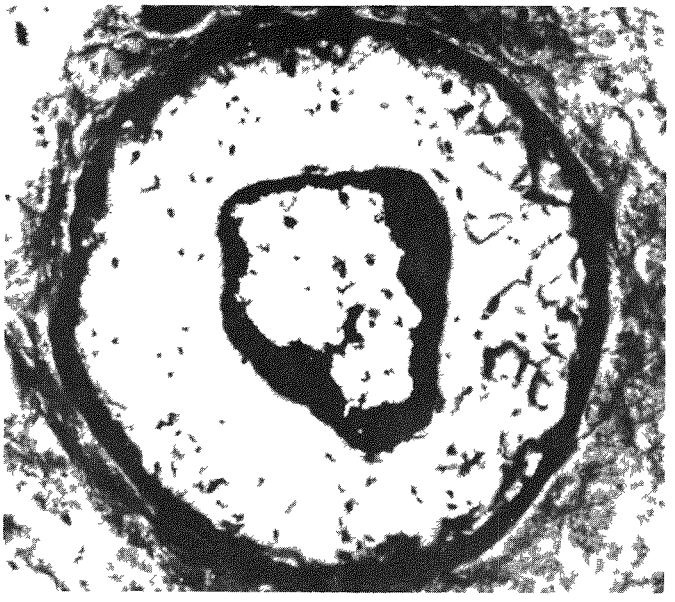

FIG. 5-3 Al_2O_3 Coated UO_2 Heated in Graphite at 2500°F for 168 hrs. (50X).

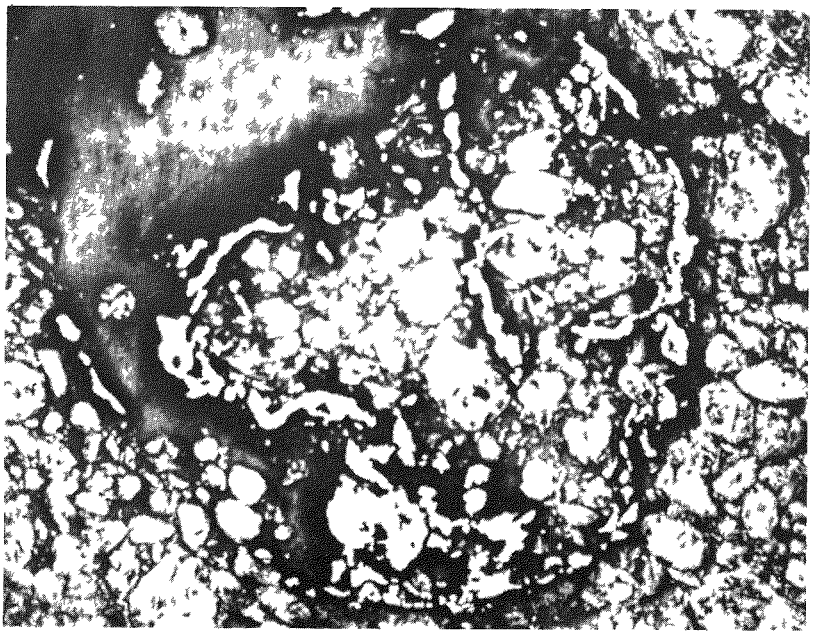

FIG. 5-4 Al_2O_3 Coated UO_2 Heated in Graphite at 3000°F for 6 hrs. (50X).

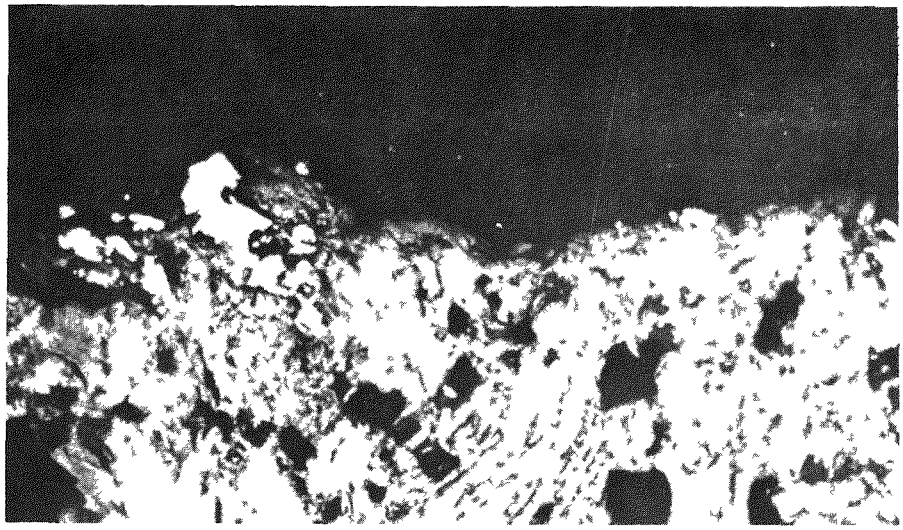

(a) Nickel: Note penetration of pore structure by nickel and possibly some nickel carbide formation

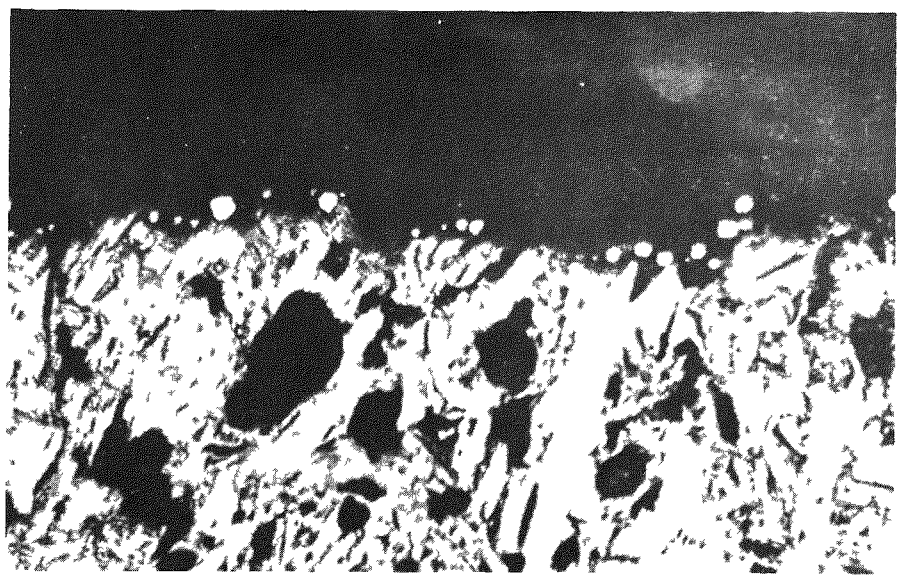

(b) Copper: Note particles of copper adhering to graphite surface

FIG. 5-5 Sections Through Graphite Crucibles at Graphite-Metal (Ni and Cu) Interface (250X).

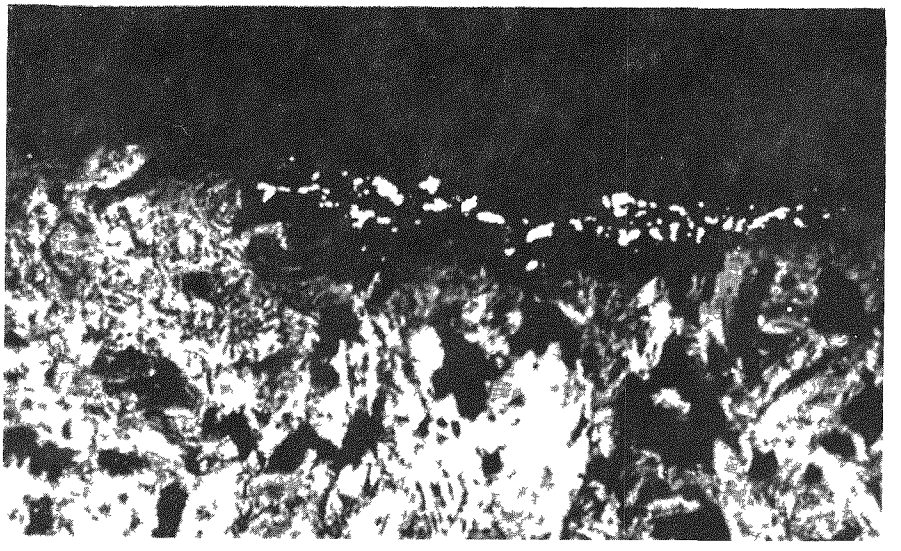

(a) $MoSi_2$: Note selective reaction of $MoSi_2$ with graphite (250X)

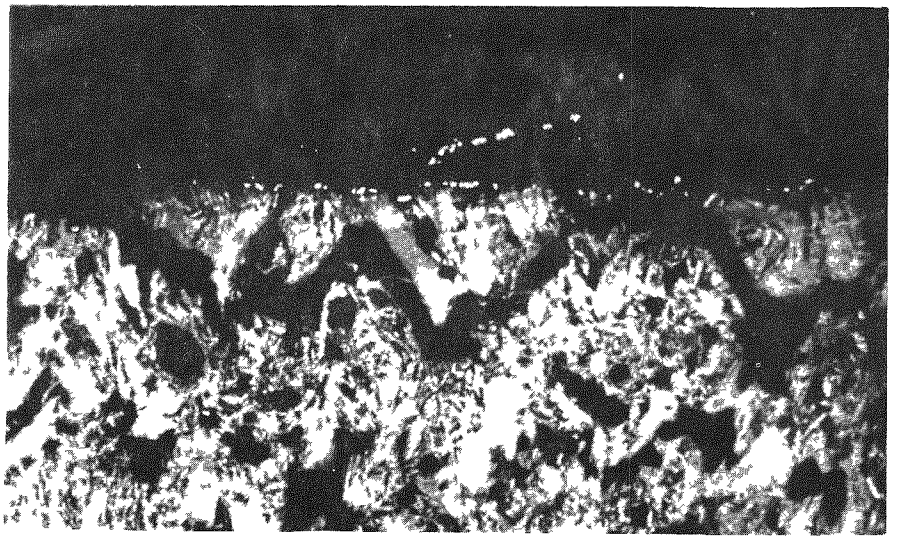

(b) #3 Glass: Note adhesion of glass to graphite (100X)

FIG. 5-6 Sections Through Graphite Crucibles at Graphite-$MoSi_2$ and Graphite-Glass Interfaces

6.0 Test Apparatus

There are four areas in which fuel element types must be evaluated before they can be considered for use in a reactor.

1. Preliminary screening and evaluation of physical characteristics.
2. Fission product retention characteristics.
3. Effect of irradiation on physical characteristics.
4. Radioactivity levels in a recycled helium stream.

An evaluation program encompassing these four phases has been set up under subcontracts to the Battelle Memorial Institute for the first three areas and the Nuclear Science and Engineering Corp. for the fourth area. These evaluations are based on a number of testing phases. Figure 6-1 illustrates how a fuel element type progresses through the test phases and the relationship of the test phases to the evaluation areas.

In general, work for a given fuel element concept is initiated in the basic study phase and is graduated to other test phases and areas of evaluation. Basic studies include development of portions of a complete fuel element. Work being done on coated fuel particles or surface coatings on unfueled graphite spheres are examples of investigation considered part of the basic study phase. Test apparatus used in the basic study phase is generally the same as used in other phases of the program. For this reason it is not discussed here separately.

Pre-irradiation characterization testing consists of physical testing of fueled 1-1/2 in graphite spheres which employ the results of the basic studies. These tests are designed to simulate, to a degree consistant within reasonable laboratory capabilities, the mechanical and thermal environments which would occur in the 125 eMW PBR. Certain simple tests, which are performed early in the pre-irradiation testing phase, are designed to show up inherent weakness in the specimens in order to avoid performance of the more elaborate and costly tests when not warranted.

Fission product retention studies are carried out on those specimens which had satisfactory pre-irradiation characteristics. Data are obtained by neutron activation experiments and by irradiation in two types of sweep capsules. In the neutron activation experiments fueled specimens are given a dose of neutrons sufficient to generate enough fission products for analysis when the specimen is subsequently heated in an out-of-pile

apparatus. Sweep capsules, in which a helium gas stream is passed around a specimen during irradiation, permit a continuous method for measuring released fission products during irradiation. The furnace capsule is a type of sweep capsule in which the specimen is irradiated at a relatively low flux and is heated to the desired temperature by an electrical heater. The regular sweep capsules which contain no auxiliary heaters, operate in a flux sufficiently high so that the specimen heat generation is comparable to the maximum design value for fuel elements in the 125 eMW PBR. The relative cost of a sweep capsule test is such that specimen types are first screened in the less expensive neutron activation and furnace capsule tests before selection for testing in the regular sweep capsule. The higher level of irradiation in the regular sweep capsule yields data on radiation damage in addition to fission product release data.

Static capsule irradiations, which are performed in lieu of or as a supplement to irradiation in the regular sweep capsules, are tests to detect radiation induced changes in the physical properties of test specimens. Static capsules operate at specimen power levels and to burnups which are equal to or exceed the maximum design conditions for the 125 eMW PBR. These capsules can be left in the reactor for an indefinite period since no maintenance or external control is required. The desired temperature during irradiation is achieved by close design of the heat flow path between the heat generating specimen and the pool water heat sink. Two static capsules have been operated in the 2 MW Battelle Research Reactor. A new type of static capsule is in design which will operate in a higher flux reactor.

The most promising specimens will be subjected to an in-pile loop test. Here the behavior of fission products escaping into a recycled helium stream will be studied.

In many cases the same testing apparatus, or a similar piece of apparatus, is used in more than one phase of the program. For instance a fuel element concept might be tested in compression first in the basic study phase (i.e. before fuel is added to the matrix), again in the pre-irradiation testing of fueled specimens and finally, with similar apparatus, in the hot cell evaluation following capsule irradiation. Apparatus is not discussed separately here when it is applicable to more than one phase.

The majority of the test work is performed on 1 1/2 in fueled and unfueled graphite spheres. For this reason apparatus and techniques are

not discussed separately when applicable to test specimens other than spheres, such as encountered in the basic study phase. Some of the apparatus has been described in previous Sanderson & Porter progress reports (NYO 2373 and NYO 8753). In this case, the apparatus is described here briefly. A more detailed description is given to apparatus of more recent development.

6.1 Pre-irradiation Characterization

Visual Inspection: All spheres supplied for testing are visually inspected for surface irregularities. Some of the irregularities which are evident from visual inspection are cracks, large holes in the coating, and coating uneveness. Microscopic inspection is used where warrented.

Physical Measurements: Weight is measured to 0.1 mg and dimensions, across three mutually perpendicular diameters, to 0.0001 in. These measurements, which are taken before and after long term capsule irradiation, can detect changes of 0.02 and 0.006 per cent in weight and diameter, respectively. Density is calculated from these dimensions. The reported density is a net graphite density which corrects for the weight and volume of fuel contained in the specimen.

Metallography: Fuel element specimens are sectioned and examined microscopically to determine the nature of the graphite structure, the nature of the fuel particles, the presence of cracks or voids in the graphite, and the degree of bonding, uniformity and apparent soundness of the surface coating. Coated fuel particles are examined to determine the character and thickness of the coating and to detect chemical reactions between the graphite matrix, the coating and the fuel. Photomicrographs are taken when appropriate.

Impact: Resistance to impact is measured by dropping a 1 pound steel weight onto specimens from increasing heights. This apparatus is shown in Figure 6-2. The ball is held in a lucite cylinder to restrict motion following impact. For more exact representation of conditions within the PBR, the ball is rotated following each impact event. Coating fracture is determined by the "hot oil" permeability test performed after each impact.

Compression: Compression tests are performed by loading the specimen at a rate of 200 lbs/min in a Universal Testing Machine. The specimens are tested in the lucite cylinder with a movable plunger at one

end, which is the same one used for impact testing. Coated specimens are tested for compression while immersed in a bath of hot silicone oil. Figure 6-3 shows the apparatus for compression testing of irradiated, coated specimens in the Battelle Memorial Institute Hot Cell.

Abrasion: Specimens are tested for abrasion resistance in the apparatus shown in Figure 6-4. The specimens are tumbled together with a number of dummy elements in a drum 8" diameter, 4 3/4" long and at a speed of 52 rpm. Visual observations and weight loss are the criteria for abrasion resistance.

Self Welding: A vertical row of specimens is subjected to an axial load (typically 50 pounds) while in a furnace capable of heating the specimens to 2500°F. Specimens are visually examined and "hot oil" tested to determine whether a tendency exists for self welding. The self welding apparatus is shown in Figure 6-5.

"Hot Oil" Permeability: This test is a simple and inexpensive method for the determination of coating integrity. The specimen is immersed in 400°F silicone oil. Absorbed gases on the underlying graphite coating form a readily visible stream of bubbles if the coating has a fault. Figure 6-6 shows a specimen undergoing the "Hot Oil" permeability test.

High Temperature Permeability: The apparatus shown in Figure 6-7 measures coating permeability at temperatures up to 2000°F. A test sphere is sealed in a glass system which is subsequently purged with inert gas at atmospheric pressure. A sample of this purged gas is obtained and then the sphere is electrically heated to the desired temperature. A second gas sample is taken after the temperature has been maintained for five minutes. Both gas samples are then analyzed by a mass spectrograph. Changes in the gas analysis indicate gas evolution through the coating.

Surface Contamination: Uranium contamination in the surface of fuel specimens is obtained by counting gross alpha activity in a flow type alpha proportional counter. The counter is a shielded hemispherical volume which contains a wire electrode in the form a loop and a base plate on which the specimen rests. The specimen is covered with a flat sheet of lucite which exposes one-seventh of the surface. A methane-argon mixture (Q-gas) is passed through the chamber. The counter is operated at a voltage which excludes betas and counts only alphas. Data can be reported on two bases: (1) that the alphas originate from uranium which is only on the surface and (2) that the alphas originate from uranium which is

evenly dispersed in the coating. These two bases represent the upper and lower limits of surface contamination with the correction for absorption in the surface coating resulting in a reported alpha count which is about twice that reported under the assumption that all the uranium is located on the surface. When specimens are fueled with enriched uranium rather than natural, a correction is made for the shorter-lived U-234 which is present in significant quantities in enriched fuel. Generally only one portion of the specimen surface is counted. In cases where there is reason to suspect that the surface contamination is not uniform, the sphere is rotated to expose other segments for counting.

Internal Pressure: An out-of-pile testing procedure has recently been developed for establishing surface coating integrity with respect to internal pressure. Internal pressure is expected to build up within fuel elements as fission product gases are retained. In this test procedure, a 1/16 inch diameter hole is drilled ultrasonically through the coating to the center of the sphere. Ultrasonic drilling produces a hole free of edge cracks. The pressurizing apparatus is sealed to the ball by the modified C-clamp shown in Figure 6-8. The pressure seal consists of a polyethylene gasket fused to the area around the hole and a lead O-ring gasket which is seated in the pressuring apparatus. The ball is pressurized while in hot silicone oil so that leakage under pressure can be immediately noticed.

Tests for Coated Fuel Particles: Two simple tests are performed to determine the suitability of various metallic and ceramic coatings for fuel particles. The first is an air oxidation test, known as the "popcorn test", in which as-received particles are heated in air at 1200°F. Cracks or open pores in the coating permit oxidation of the UO_2 cores which result in an observable rupture of the coatings. Weight gain is also used as an index of coating failure. The second test is for the compatibility of particle coatings in graphite. Coated UO_2 particles are dispersed in graphite, and pressed at 24,000 psi. The specimens are then baked in a Globar furnace. Variables in the carburization test are type of graphite matrix, and baking temperature and time. A series of carburization studies was made in which specimens of AGOT graphite-Barrett pitch containing Ni, Ni-Cr, Nb and alumina coated UO_2 particles were heated in helium to 2500°F for 168 hours and to 3000°F for 6 hours. Results for the Ni, Ni-Cr and Nb particles are given in Section 7.1. The results for the alumina specimens are given in Section 5.1.

6.2 Fission Product Retention

Neutron Activation: Neutron Activation testing provides an inexpensive and rapid method for the preliminary determination of fission product retention ability. By controlling test variables, the neutron activation tests could provide clues to the mechanism for fission product release in addition to establishing the relative leakage rates for various test specimens.

The procedure is generally the same for Neutron Activation Experiments with either fueled graphite spheres or fuel particles. Specimens containing natural uranium are given a dose of neutrons sufficient to generate a measurable amount of fission products (up to 6×10^{15} nvt). This exposure is accomplished in periods of less than one hour in the Battelle Research Reactor Weasel Tube, a hydraulically operated tube which is placed vertically near the edge of the core. A holder used for irradiation of graphite spheres in the weasel tube is shown in Figure 6-9. Fuel particle experiments use a similar holder. A dosimeter wire is placed around or near the specimen to determine the total exposure.

The activated specimens are allowed to decay for 3 to 7 days in order to achieve a better resolution of the 5.27 day Xe 133 isotope which has been selected for measurement in the single channel gamma ray spectrometer.

Figure 6-10 is a general view of the apparatus for heating the specimen and for collecting the evolved fission gas. A schematic diagram for this apparatus is given in Figure 6-11. The specimen is placed in a 2 inch diameter quartz tube (shown on the left of Figure 6-10) which is then lowered into the furnace below. The furnace is an induction coil capable of heating the specimen to 2500°F. The quartz tube has a hemispherical bottom, a quartz holder for the specimen and a ground joint connector at the top which contains helium inlet and outlet lines, and a thermocouple well. Helium at atmospheric pressure is swept over the heated specimen at a rate of 3 liters per hour (NTP). The gas stream is then cooled to remove condensibles in a dry ice-acetone trap and then passed through an on-stream gamma spectrometer. Here gas is passed through a charcoal trap, at dry ice temperature, which is sunk in the well-type scintillation crystal. The remainder of the gas train includes cleanup and safety apparatus.

Furnace Capsules: Furnace capsules contain a heating element which permits selection and control of specimen temperatures up to 2000°F and helium sweep gas connections for measurement of fission product release. Furnace capsules are designed to provide an economical method for obtaining fission product release data while the specimen is being irradiated.

Isotopes measured are Xe133, Xe135, Kr87, Kr88 and Kr85m. the relative abundance of these various isotopes can be used to estimate the overall diffusion coefficients. A hundred channel analyzer is first used for qualitative scanning of gas specimen. Quantitative analysis is obtained with a calibrated single channel analyzer with appropriate corrections made for time delays. Furnace capsules operate at the edge of the Battelle Research Reactor and hence their external dimensions, 3-1/2 in diameter by 12-1/8 in. in length, are not confined to a size determined by a vacant fuel element position. The furnace capsules can be irradiated in a maximum flux of 10^{12} nv which is limited by fission heat generation in the specimen. At this flux and with specimens fueled with natural uranium, ratios of the rate of fission products released to the rate at which fission products are created (known hereafter as the R/B factor), as low as 10^{-7} to 10^{-8} can be detected. Ratios of this magnitude are well down into the range of interest for the PBR fuel element development program.

The first furnace capsule, designated SPF-1, has been in operation in the Battelle Research Reactor since October 14, 1959. It contains a single FA-20 specimen. Fission product release data have been obtained for this specimen and are reported in Section 8.2 of this report.

The salient features of the SPF-1 capsule are shown in Figure 6-12. This same design will be used for future furnace capsules. The test sphere is supported by a pin on the bottom and held horizontally at 120 degree intervals by vertical tubes, one of which is a helium sweep tube. The ball temperature is measured in three locations by sheathed thermocouples which also aid in the support of the specimen. The helium outlet tube enters the test chamber from above. The test chamber is wound with a Kanthal heater with a rating of 1 KW. Insulation between the heater wound test chamber and the exterior wall of the capsule is attained by an evacuated annulus containing a radiation barrier. The flux level is measured periodically by a dosimeter wire external to the capsule. The flux depression when the capsule contains a normally enriched specimen is negligible.

Figure 6-13 is a schematic diagram of the gas train for SPF-1. Helium, regulated at the cylinder, is swept through the capsule at a rate of about 18 cc/sec (NTP). The sweep gas containing the volatile fission products is first monitored by a gross activity counter. The monitor is connected to a recorder-controller which both scrams the reactor and shuts off helium flow in the event of excessively high gas activity. The gas is next cooled in a dry ice trap which removes condensible gases and then is fed to either of two quantitative charcoal traps in parallel. These traps are similar to those used in the neutron activation experiments. The

remainder of the gas train is cleanup apparatus, which consists of large activated charcoal traps, a Cambridge absolute filter and a holdup tank. A monitor measures gross gamma activity before the gas is released to the stack.

Sweep Capsules: The primary purpose of the sweep capsules is to obtain direct fission product leakage data from fuel element specimens operating under very nearly the design conditions of the 125 eMW PBR. Helium sweep gas is passed over the specimens at a low flow rate and then analyzed by methods similar to those for the furnace capsules or neutron activation experiments discussed previously in this section.

One sweep capsule, designated SP-3, was operated in the Battelle Research Reactor this period. The basic design features of this capsule are shown in Figure 6-14. Two separate inner capsules each contain a pair of 1-1/2 in diameter specimens. Each sphere is surrounded by a 0.03 in layer of powdered graphite and encased between two graphite blocks. The use of graphite powder permits a good and uniform thermal contact between the test sphere and the graphite blocks, while at the same time it provides for relative expansion or contraction during irradiation. The inner capsule has fins on its outer surface which provide a method for controlled thermal contact between the inner capsule and the shell which forms the outer surface of the capsule. The number and width of these fins is chosen on the basis of the desired specimen temperature during irradiation. Separate sweep helium inlet and outlet connections are provided for each of the inner capsules. The gas train for SP-3, essentially the same gas train as now in use for SPF-1, is shown in Figure 6-13. This is a dual gas train and both sections were used for SP-3. A bypass line has been installed around the gas train so that when high leak rate specimens are being tested, most of the off-gas flow can be diverted through the bypass in order to decrease the activity level in the gas train. Details of the operation and experimental results are discussed in sections 7.2.1 (irradiation effects) and 8.3 (fission product retention).

6.3 Static Capsules

Static Capsule SP-4: The irradiation of a static capsule, designated SP-4, was started on August 25, 1959 in the Battelle Research Reactor and is scheduled for completion in December 1959. This capsule, illustrated in Figure 6-15, holds six 1-1/2 in diameter test spheres in a vertical row, all within a common inner capsule. The design features of capsule SP-4 are essentially the same as SP-3 except that no provision is made for

sweep helium. The operation of SP-4 and basis for the selection of test specimens are discussed in Section 7.2.2.

Figure 6-16 is a photograph of an out-of-pile thermal history apparatus used to duplicate the thermal environment of SP-4. These data are being obtained so that the effects of the thermal environment and radiation environment can be distinguished. The history apparatus contains fuel elements specimens identical to those in SP-4. The heater for this apparatus is programmed by the temperature chart recorded for a central fuel specimen in SP-4. In this way, the out-of-pile specimens are subjected to very nearly the exact temperature level and temperature variations experienced by the in-pile specimens.

High Flux Static Capsules: Preliminary design was done on a 10 specimen capsule to operate at power densities of 5 KW per ball. The capsule will be 2-1/4 in OD and 28 in long. Several capsules of this type will be irradiated in a reactor having a higher flux than the Battelle Research Reactor. The 5 KW/ball power level is 60% higher than peak PBR power and full scale burnup will be achieved in a 3 month irradiation.

6.4 In-Pile Loop

The design of an in-pile loop to study the behavior of fission products escaping from a PBR fuel element was started during the past period under subcontract to the Nuclear Science & Engineering Corp. The purposes of this loop are to study the equilibrium activity levels in a recycle stream, methods of lowering gas stream activity, level, the amount, location and nature of deposited fission products and methods of decontaminating equipment surfaces.

A schematic diagram of the loop is shown in Figure 6-17. A single PBR fuel specimen will be irradiated in an effective flux of 1 to 3 x 10^{12} nv at 1800°F. Special test sections to study plate-out at 1250°F and 550°F (PBR design conditions) will be provided. A canned positive displacement blower will recycle atmospheric pressure helium at a pumping temperature of 250°F. An in-line analytical system will permit measurement of gas-phase activity levels and a bypass cleanup system will be used to study reduction of gas-phase activity levels. The experimental program will include deliberately violated PBR specimens in addition to good PBR specimens.

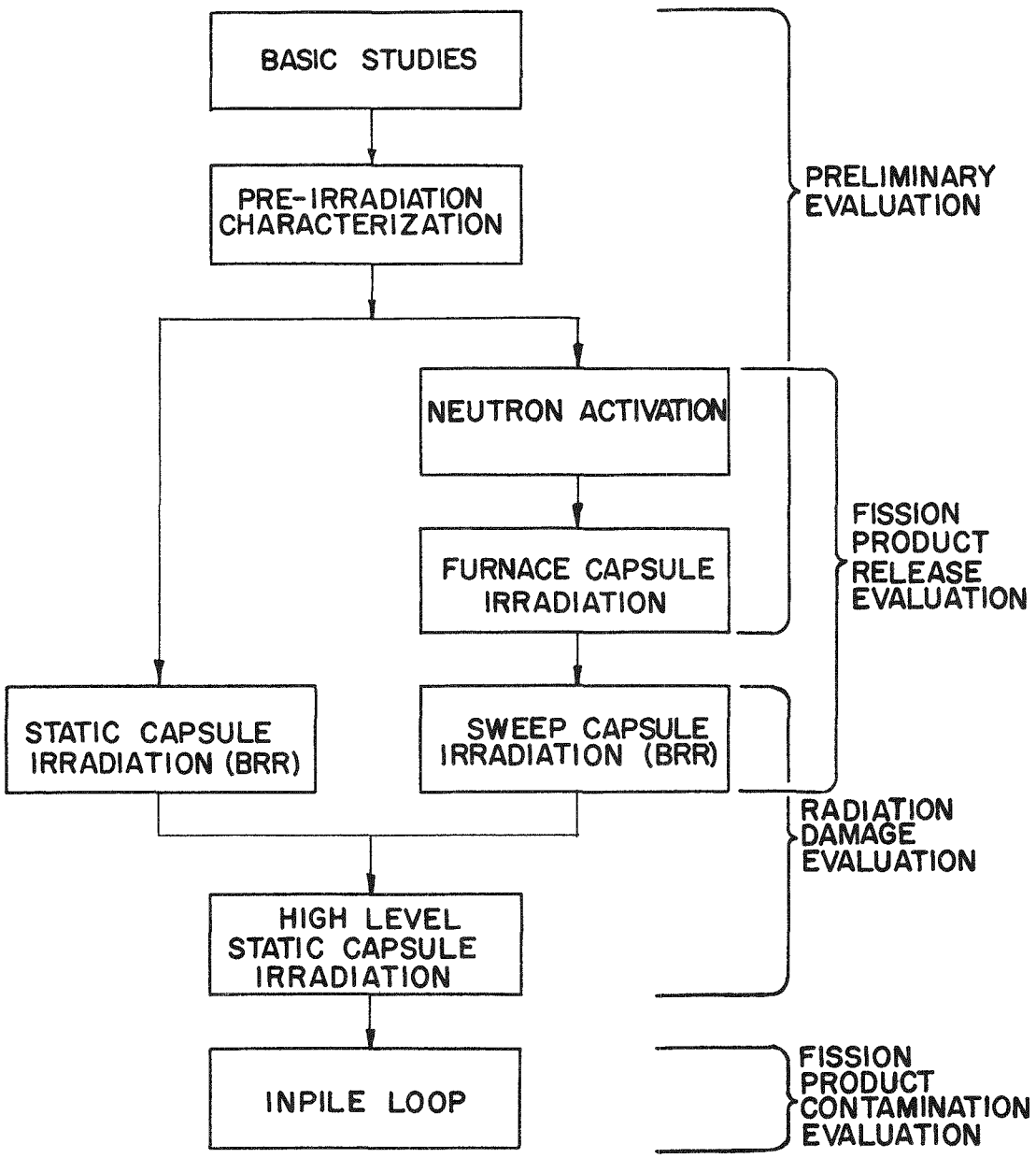

FIG. 6-1 PBR FUEL ELEMENT DEVELOPMENT PROCEDURE

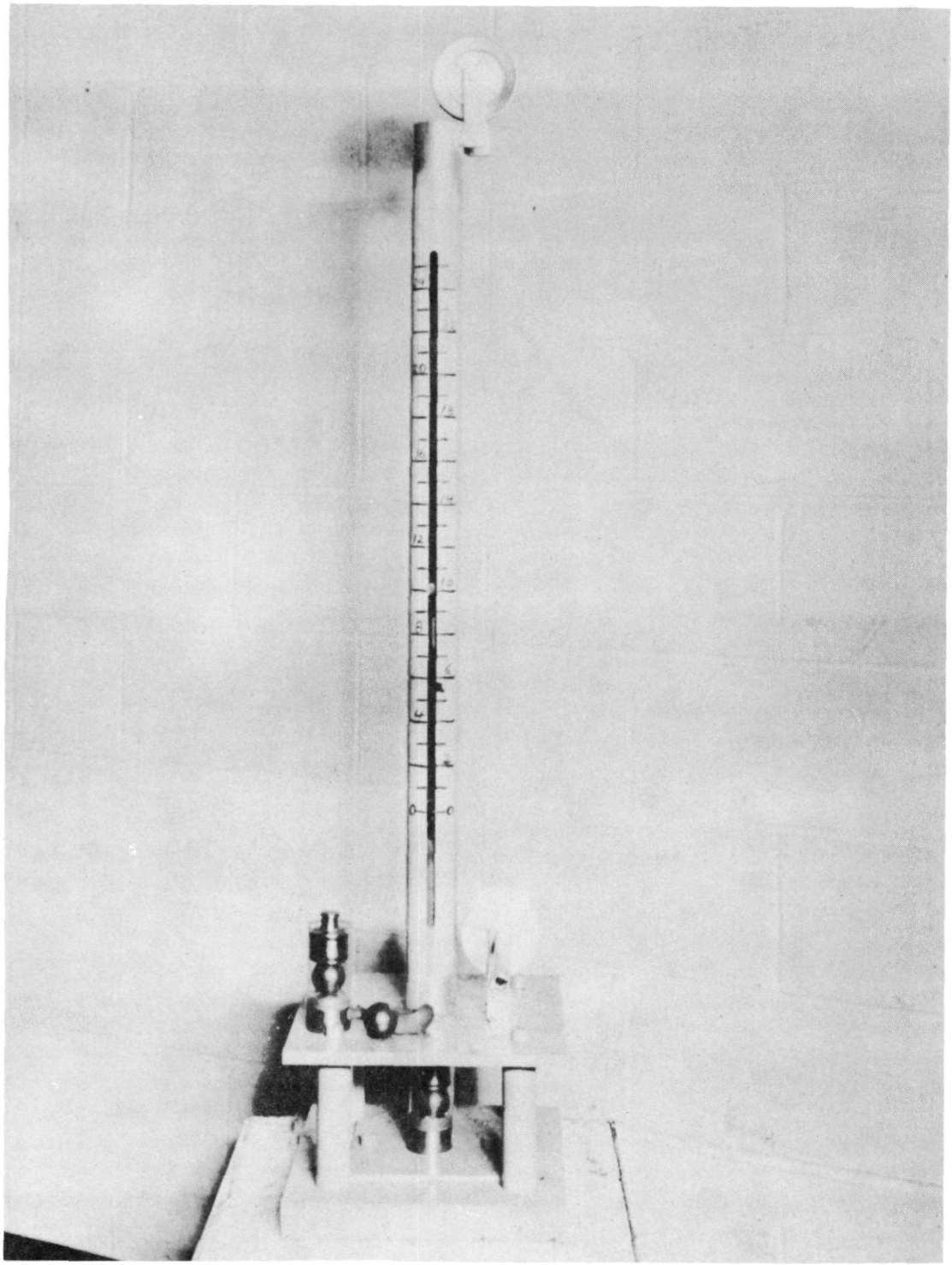

6-2 Impact Testing Apparatus

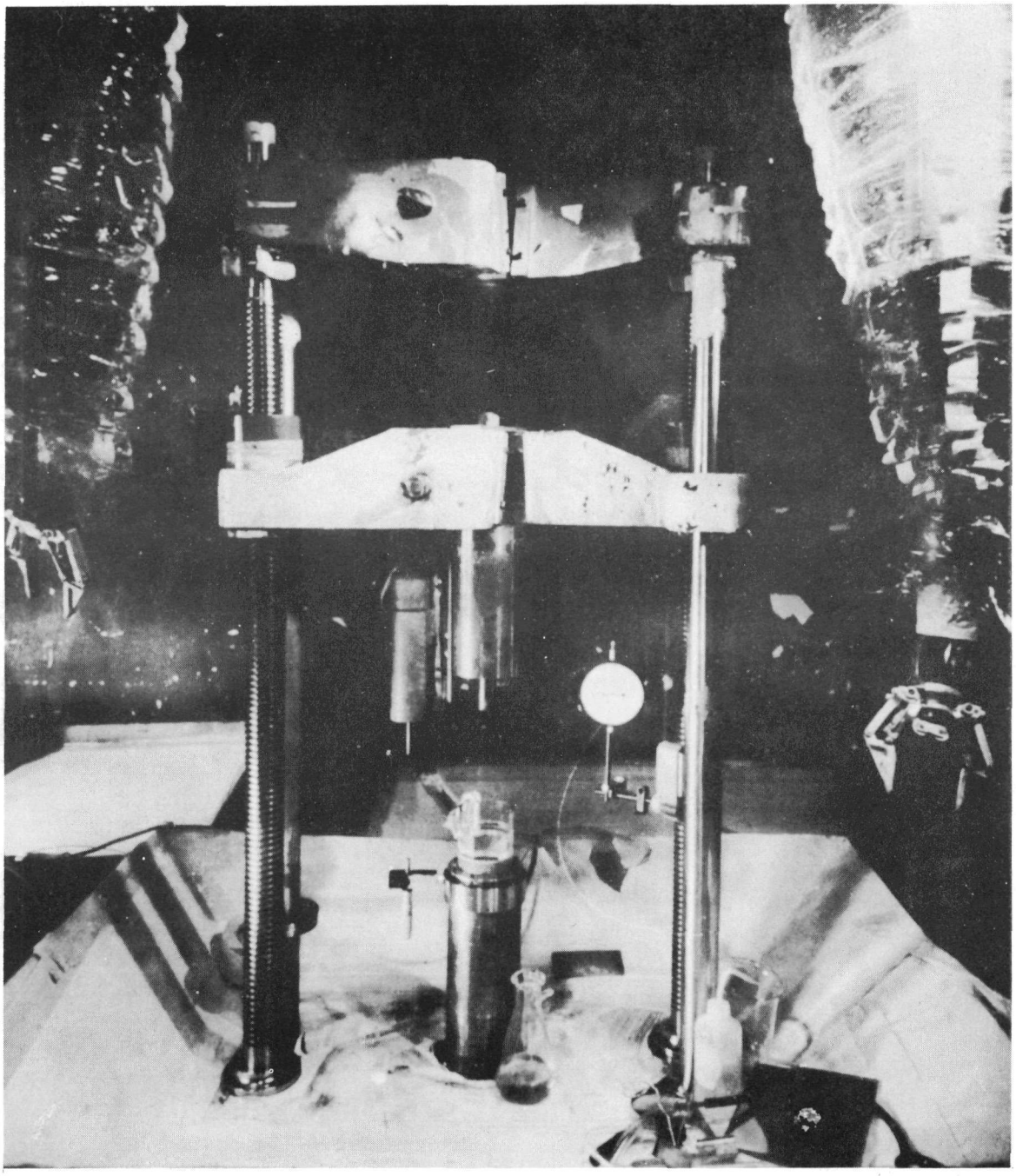

6-3 Compression Testing Apparatus in Hot Cell

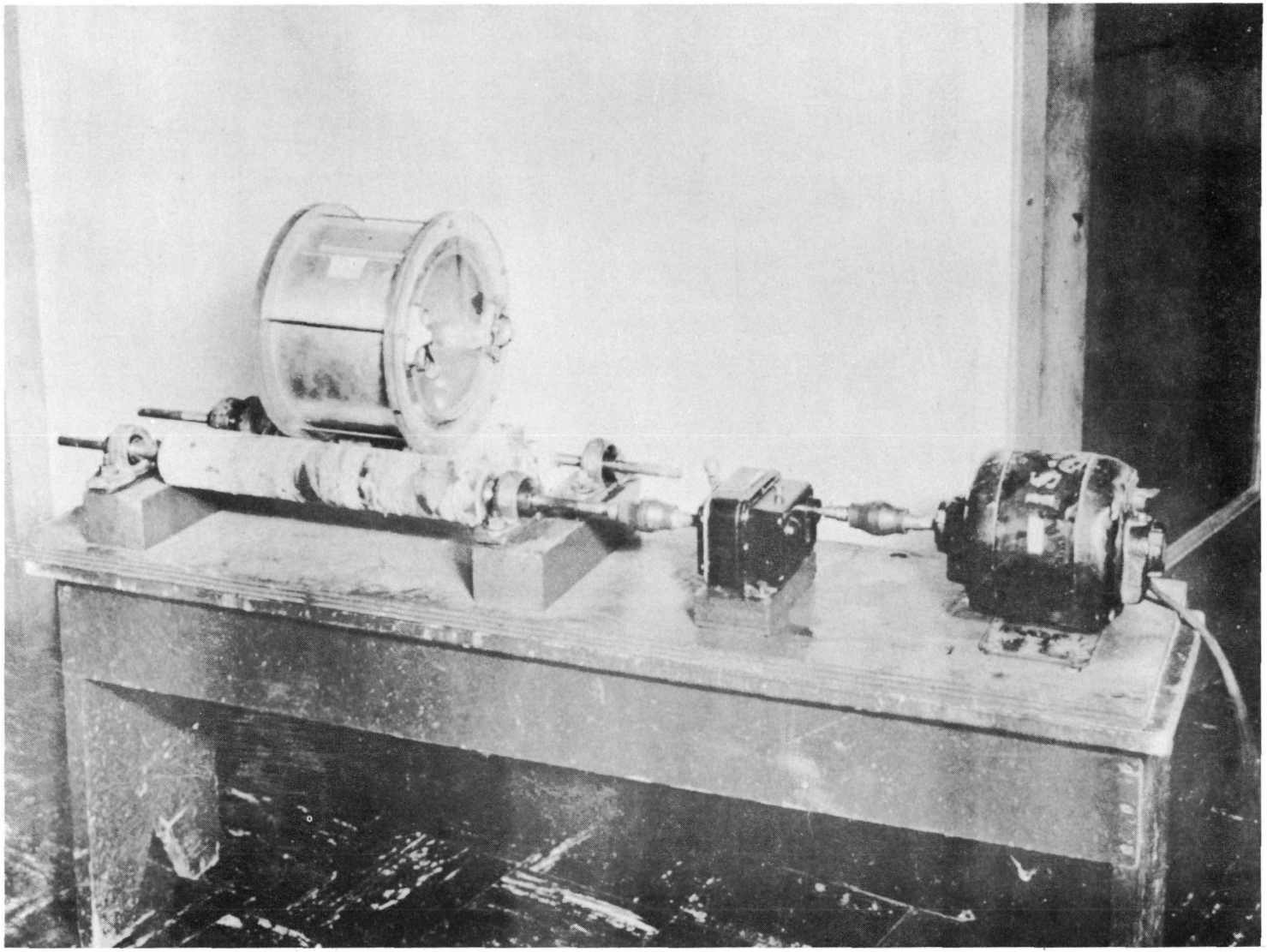

6-4 Abrasion Testing Apparatus

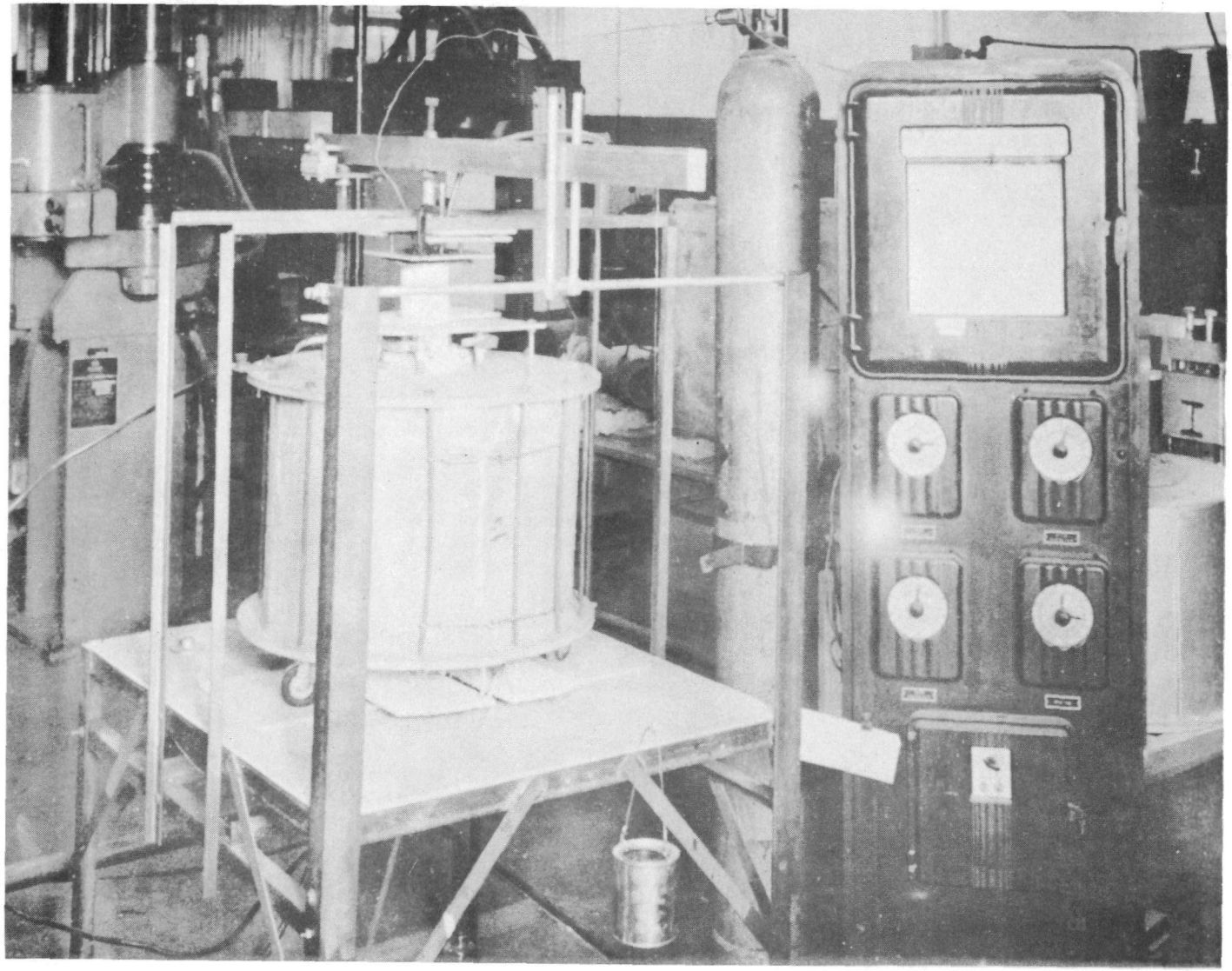

6-5 Self-Welding Testing Apparatus

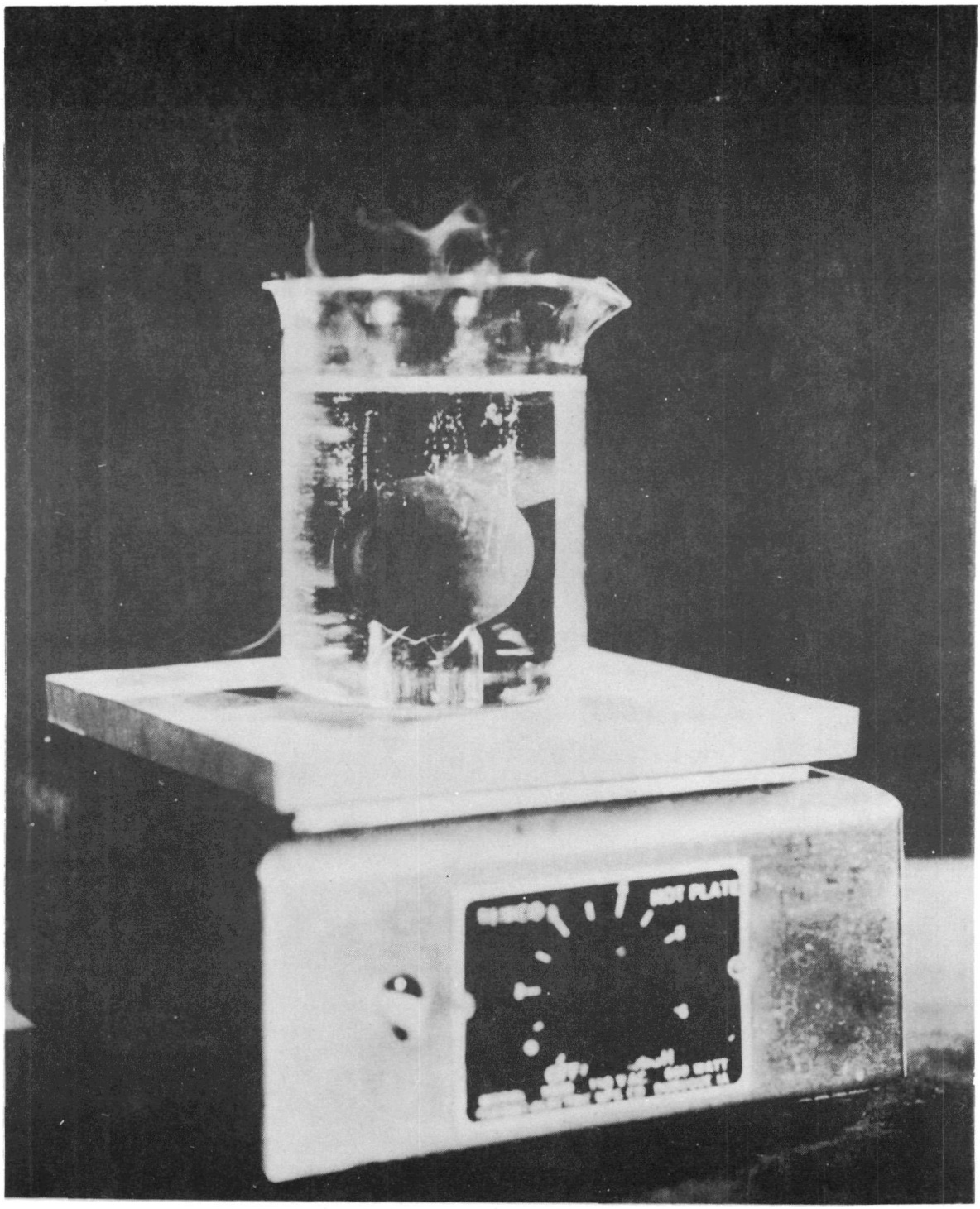

6-6 Hot Silicone Oil Test for Coated Fuel Specimens

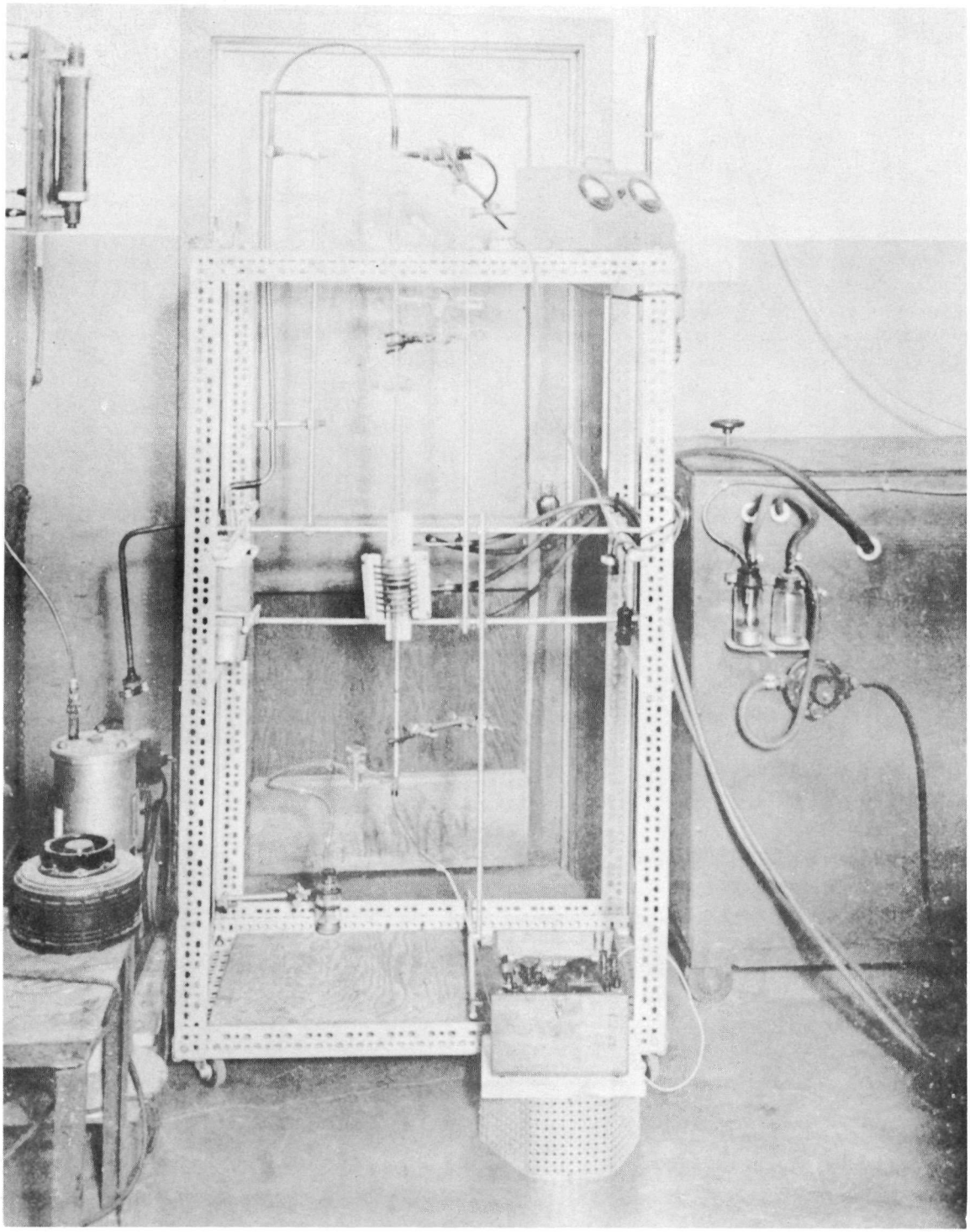

6-7 High Temperature Permeability Testing Apparatus

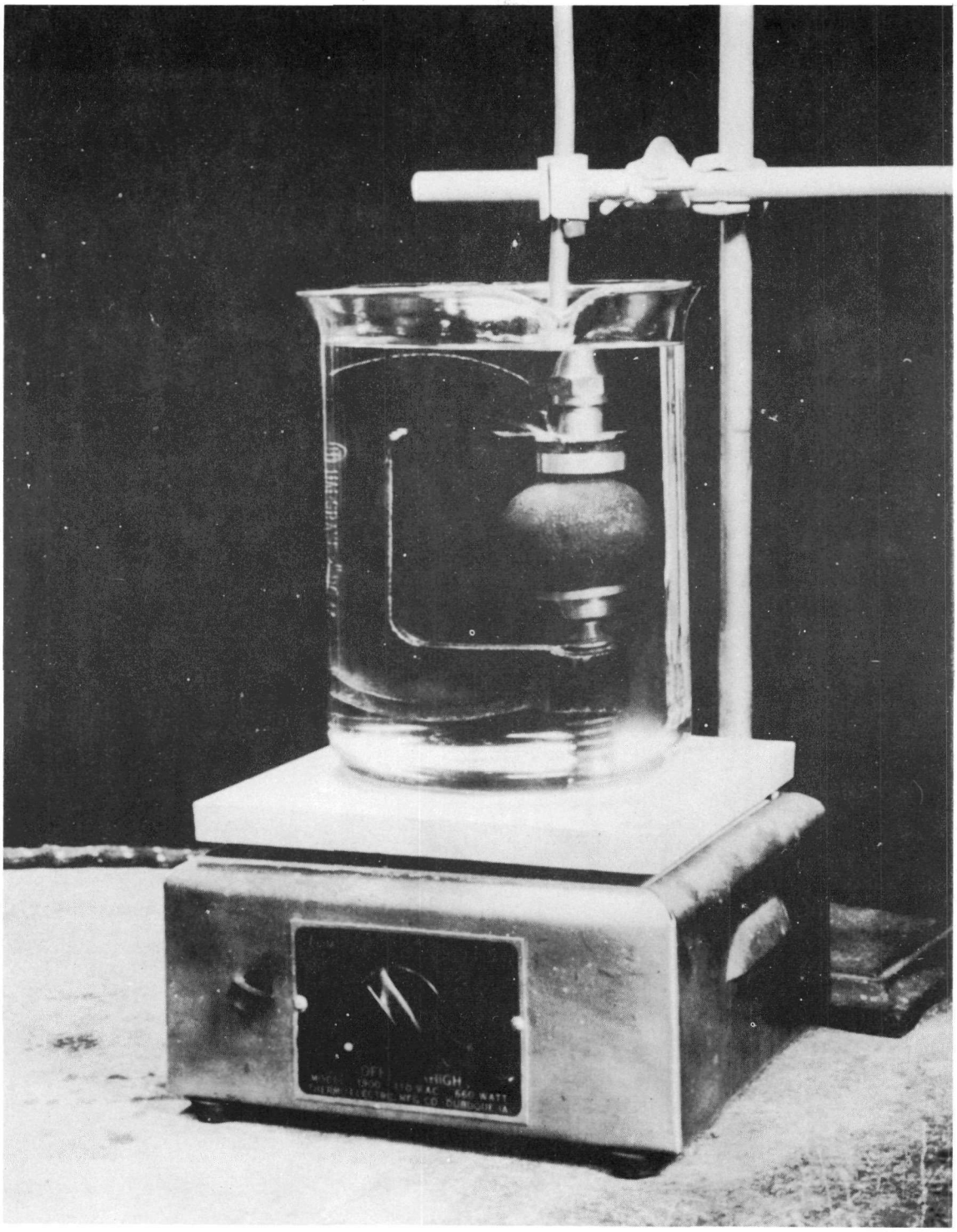

6-8 Internal Pressure Testing Apparatus

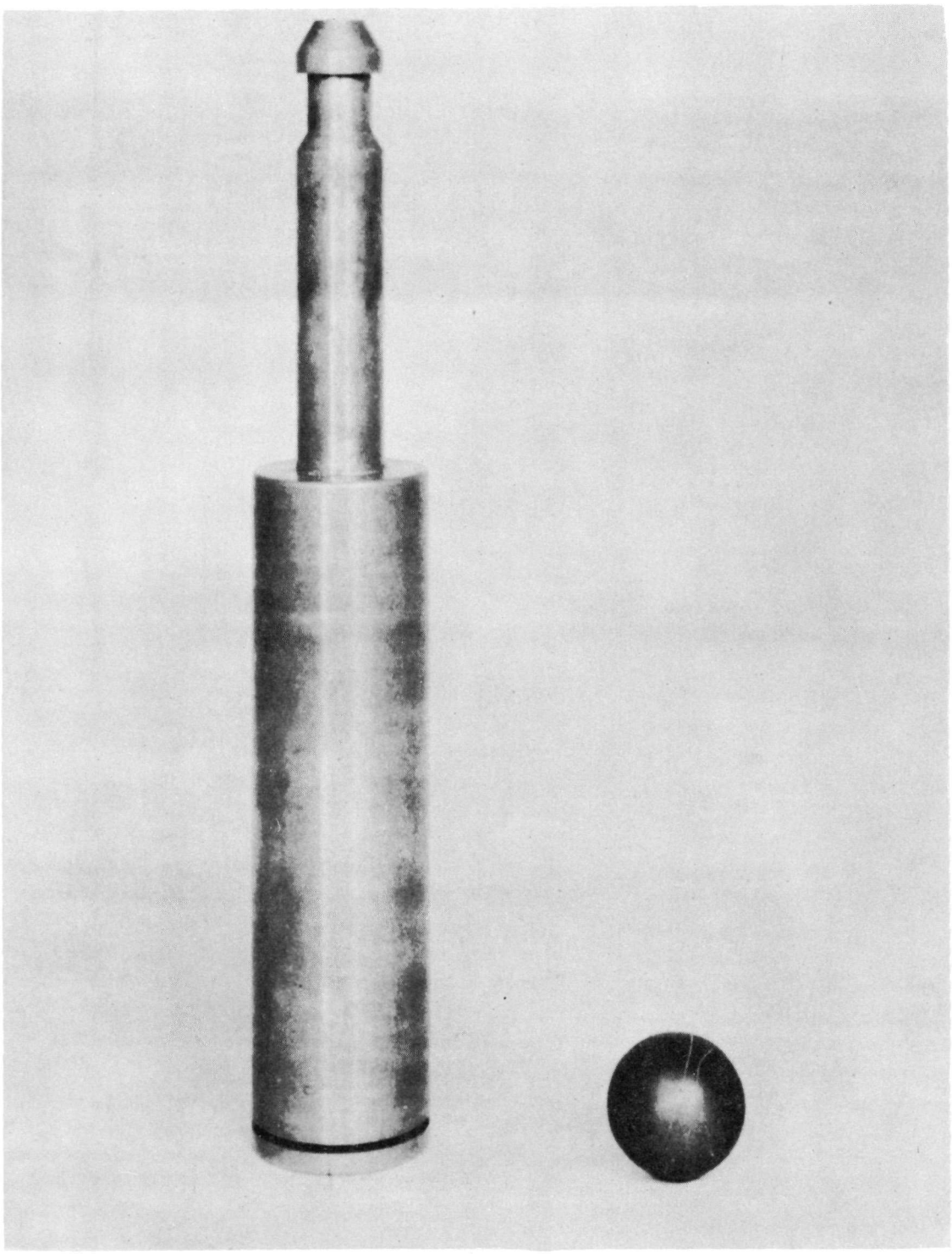

6-9 Holder for Neutron Activation of Specimens in BRR Weasel Tube

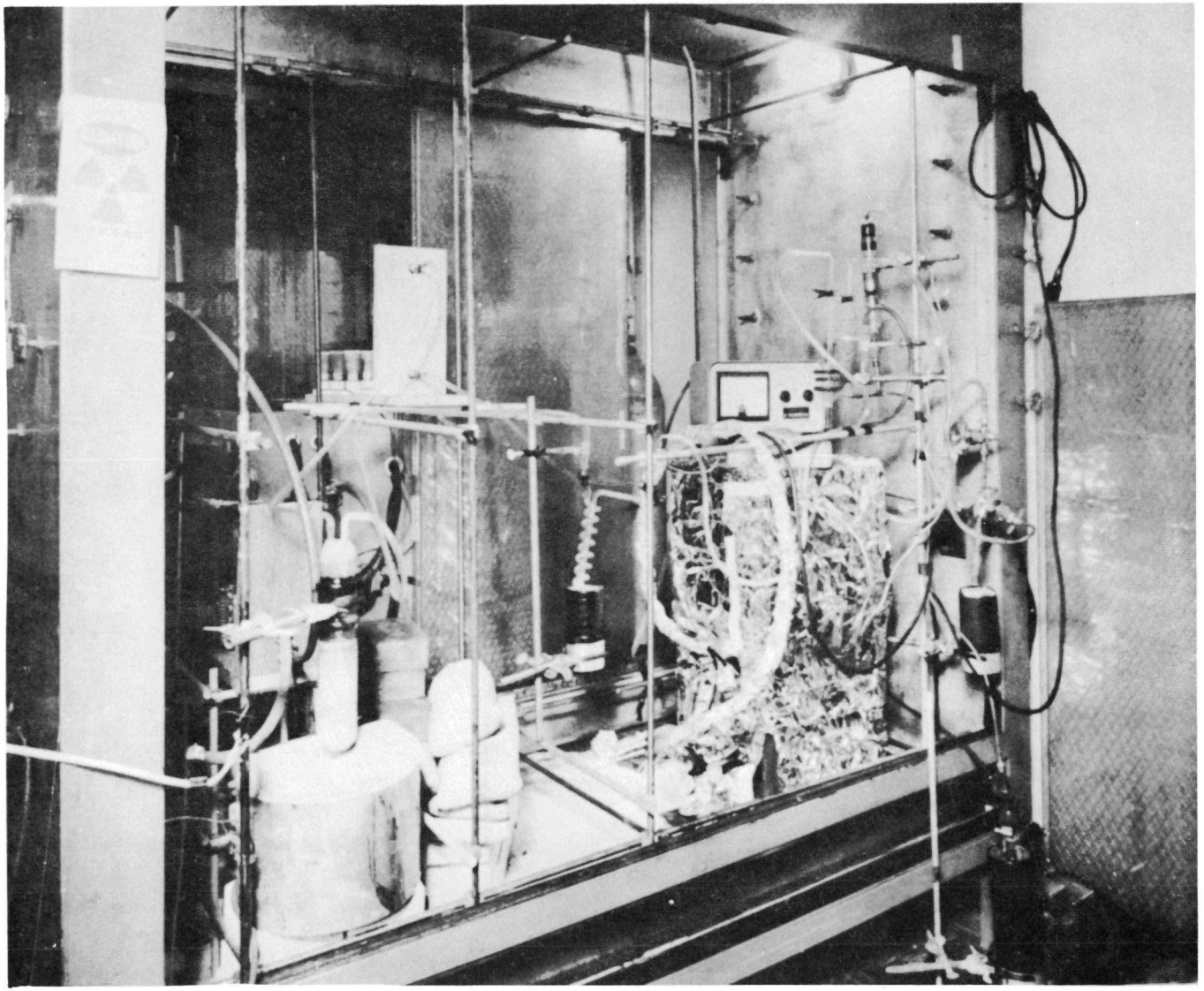

6-10 Gas Train for Neutron Activation Experiments

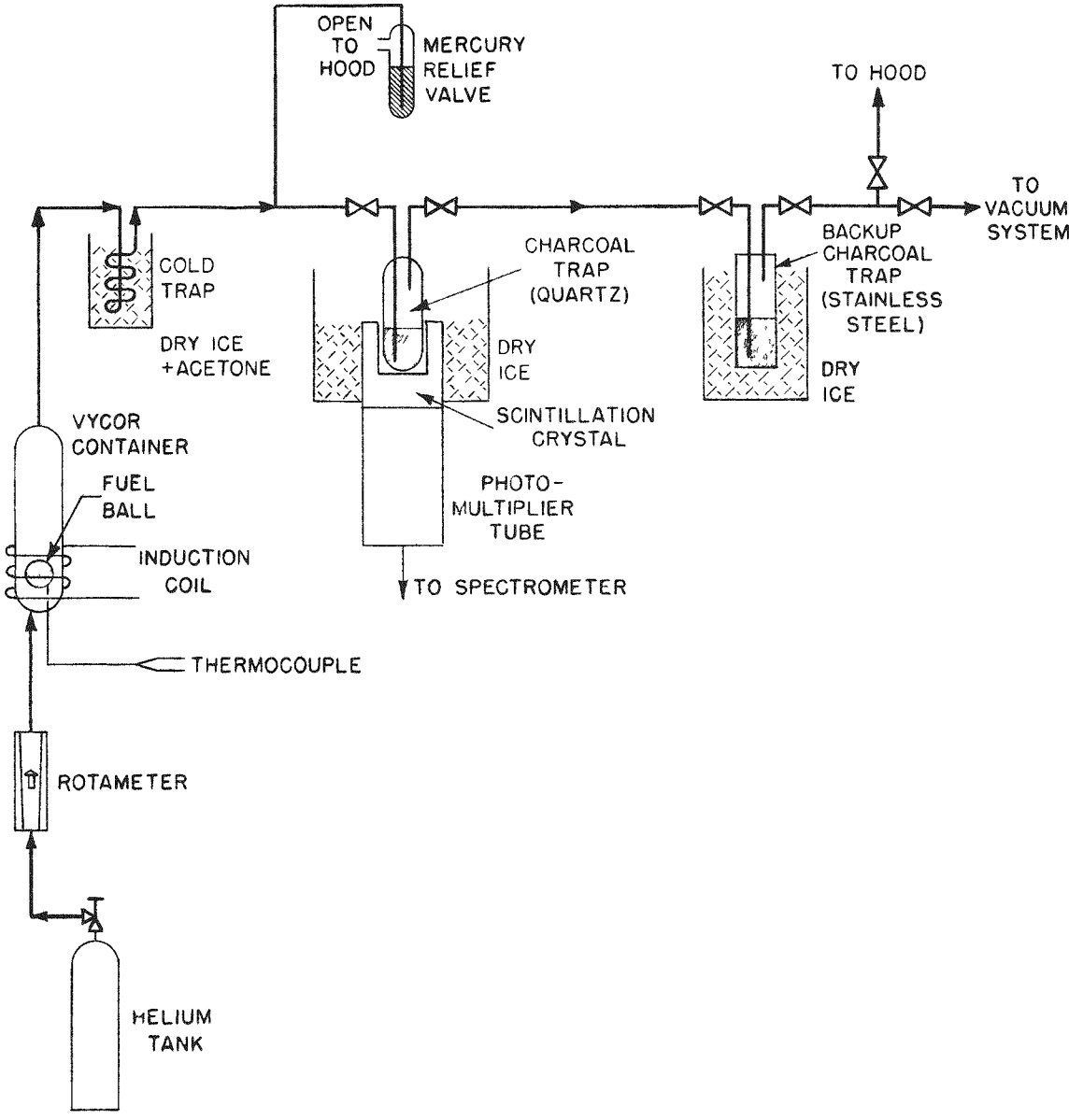

FIG. 6-11 SCHEMATIC DIAGRAM OF GAS TRAIN FOR NEUTRON ACTIVATION EXPERIMENTS

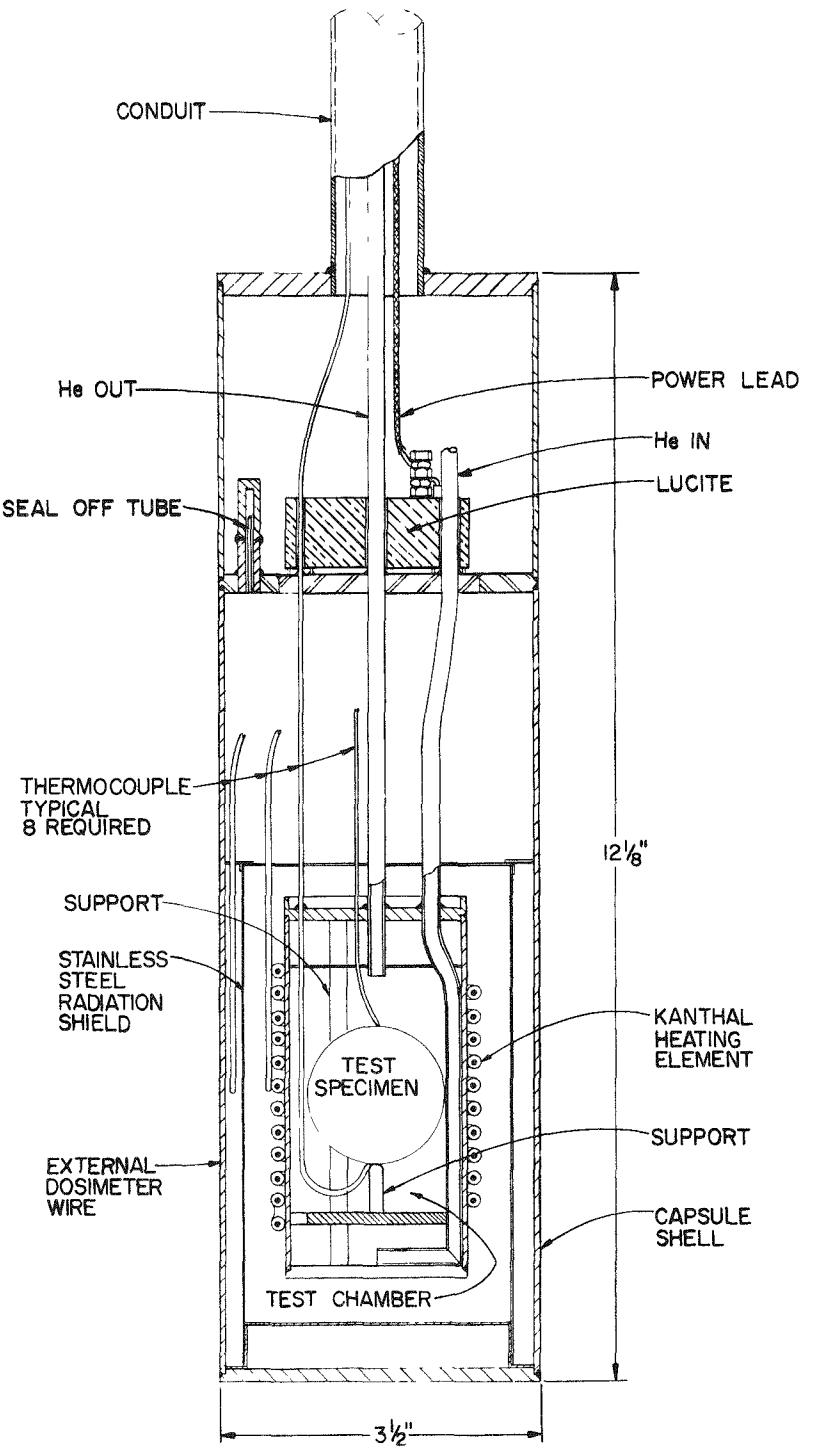

FIG. 6-12 FURNACE CAPSULE SPF-1

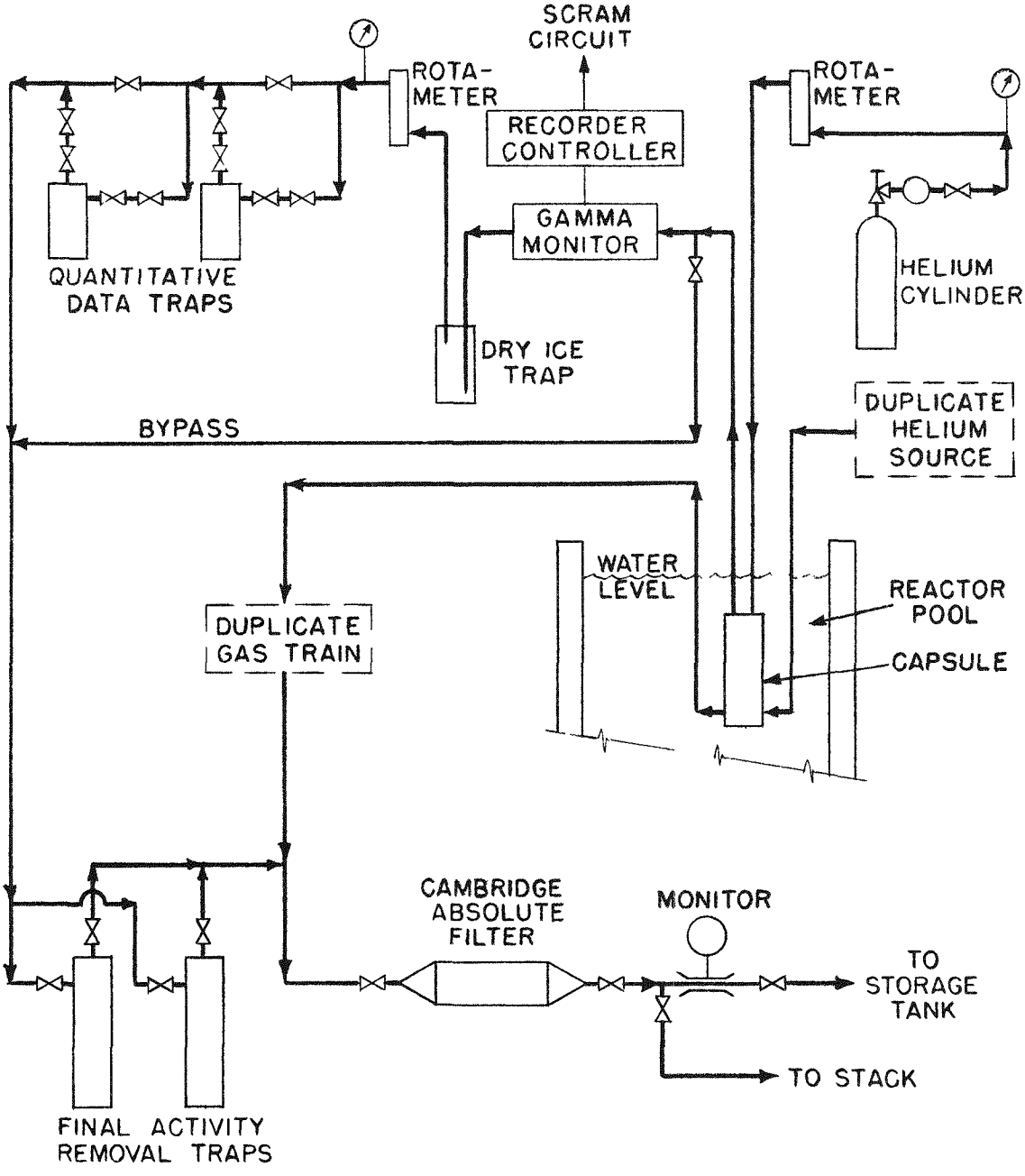

FIG. 6-13 GAS TRAIN FOR FURNACE CAPSULES AND SWEEP CAPSULES

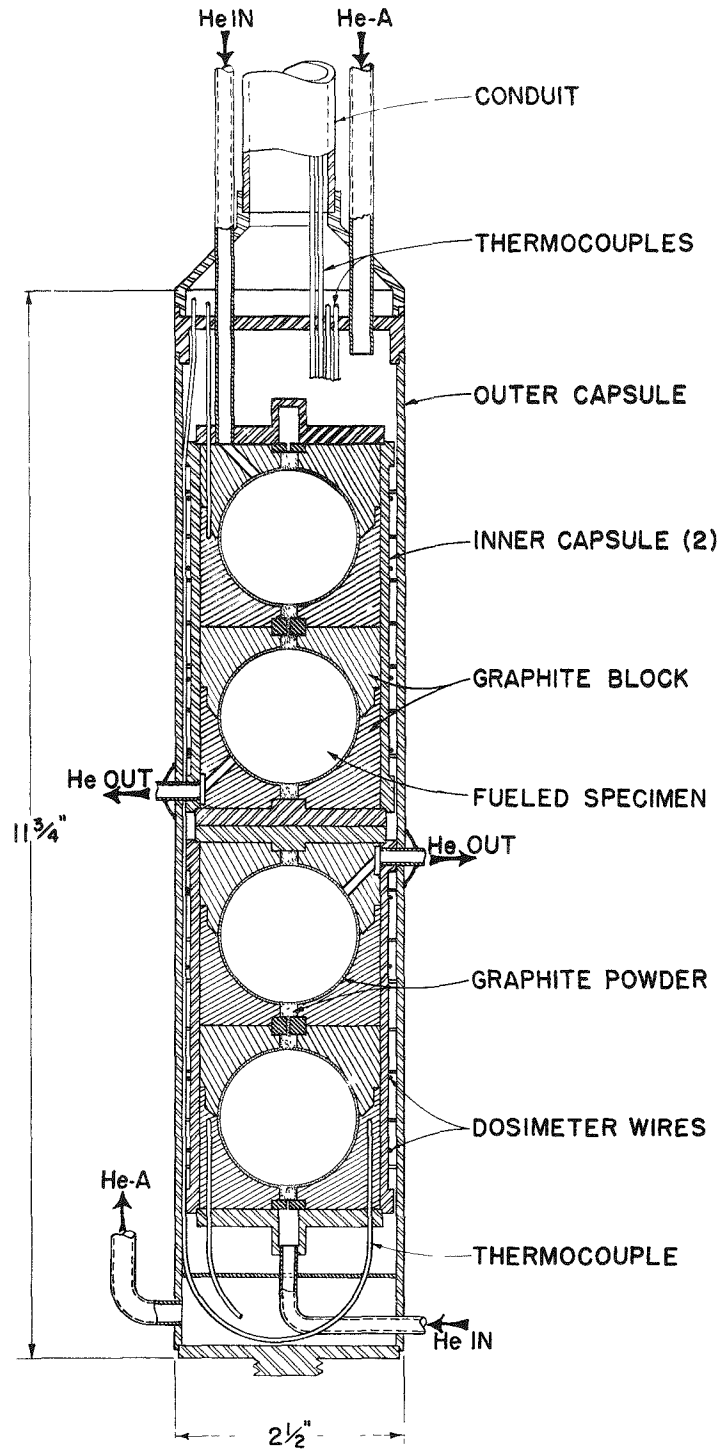

FIG. 6-14 SWEEP CAPSULE SP-3

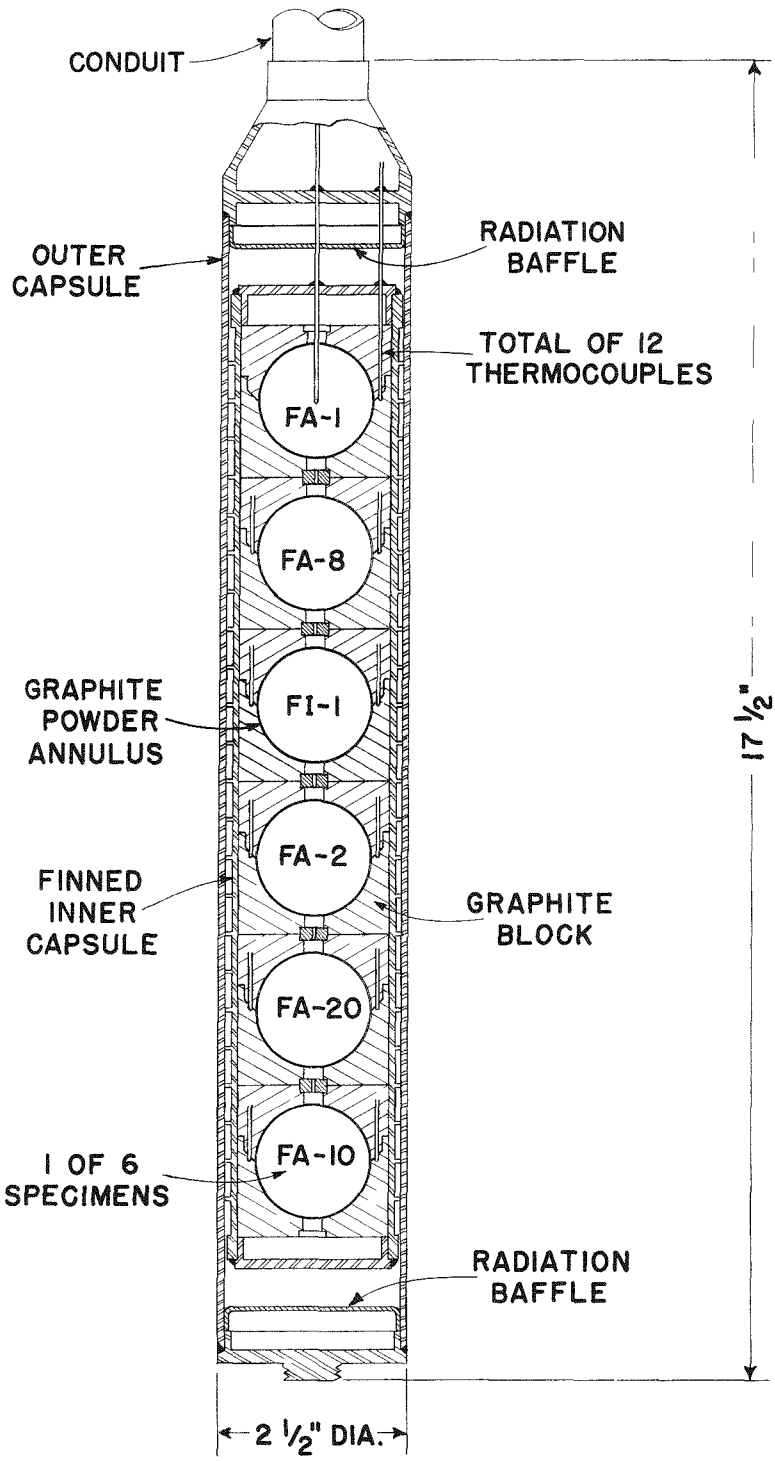

FIG. 6-15 STATIC CAPSULE, SP-4

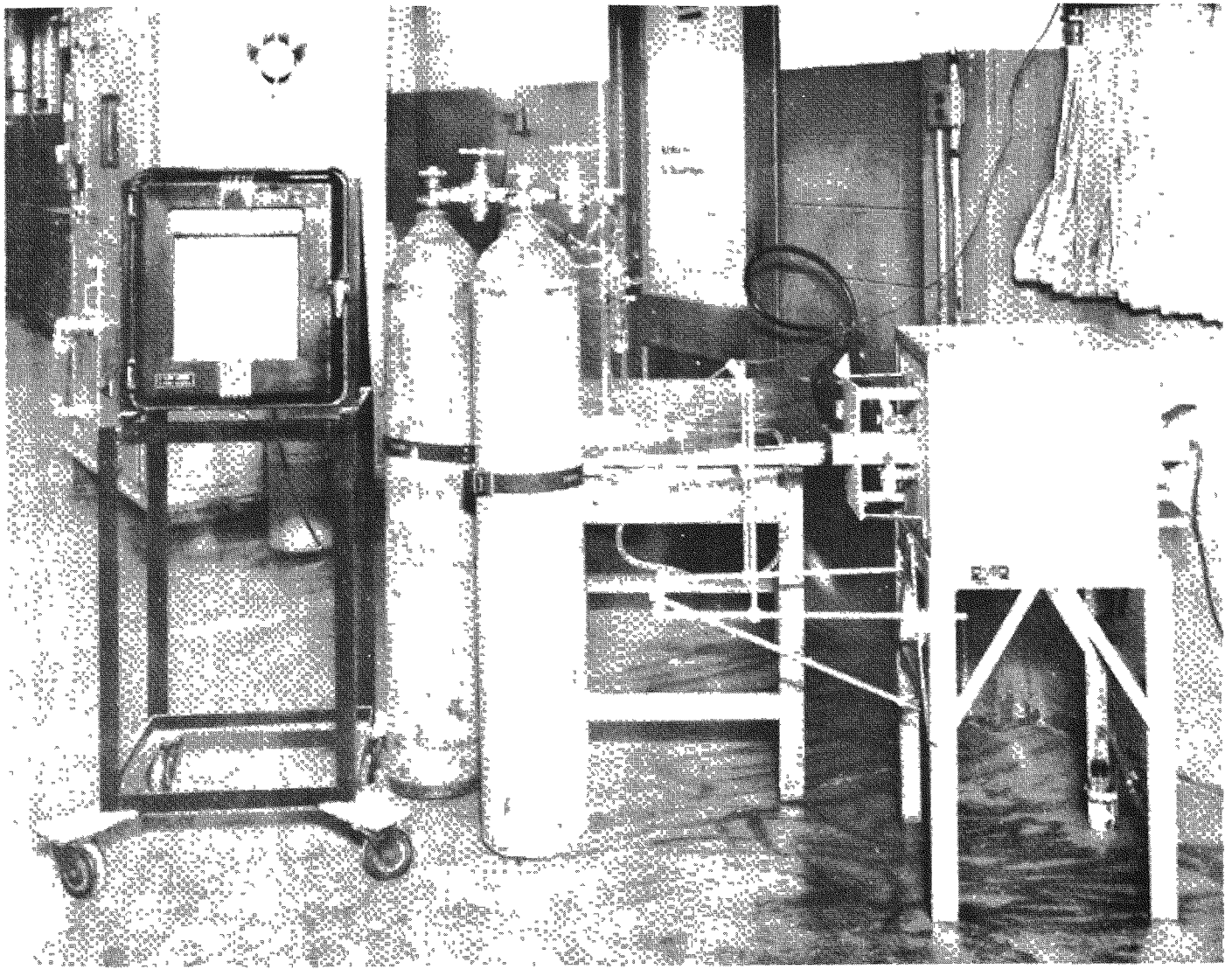

6-16 Thermal History Apparatus for SP-4

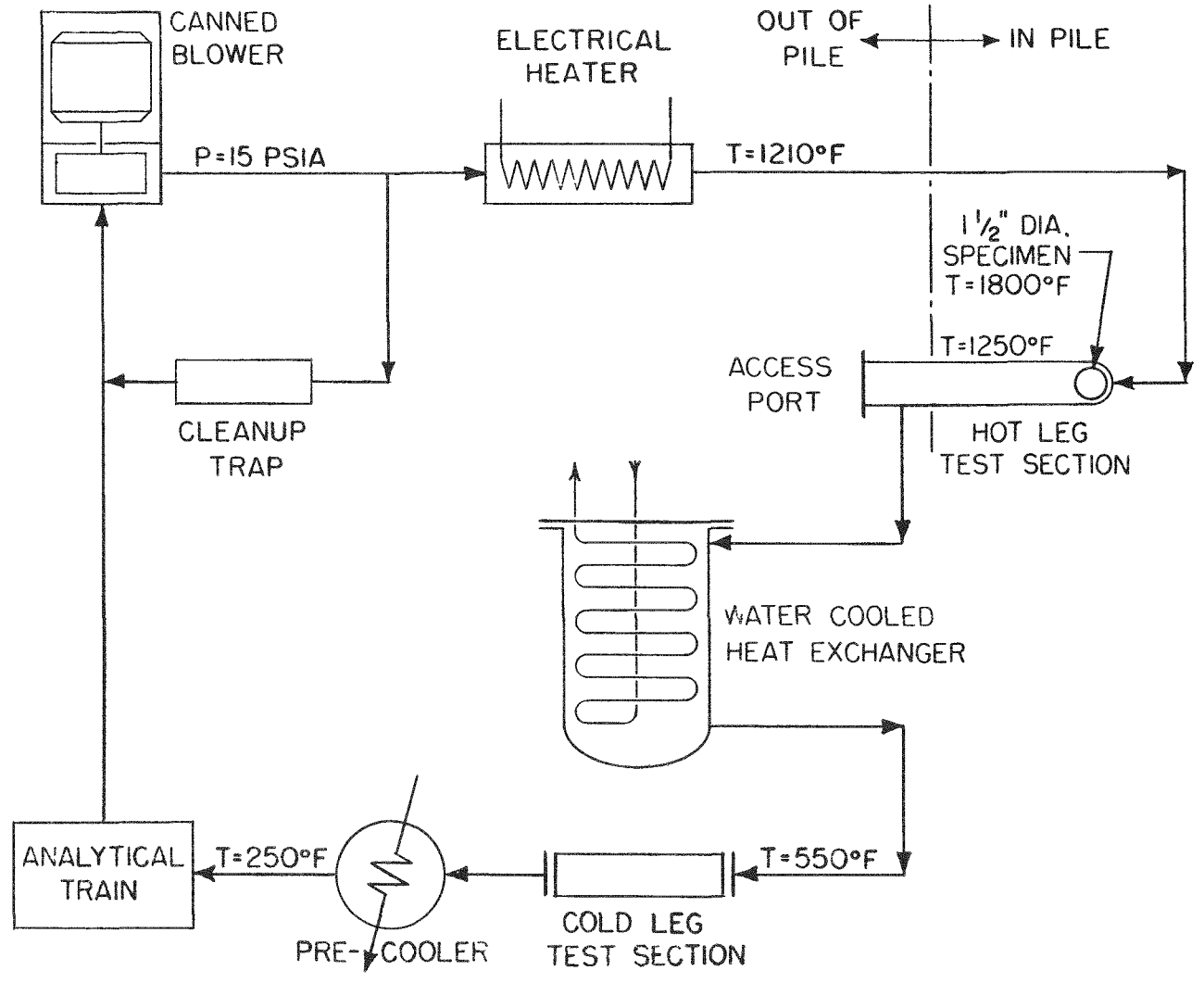

FIG. 6-17 PBR IN-PILE LOOP

7.0 Physical Characteristics

This section describes test data that has been obtained during Phase I on the specimens described in Section 4.0 using the test apparatus described in Section 6.0. Table 7-1 lists these tests and indicates the status of the test program in terms of completed and planned test for the various fuel element types under consideration. Table 7-1 shows all tests performed prior to and during Phase I. Completed tests are indicated by the symbol + and test planned or in progress by the symbol 0. Section 7.0 is concerned only with test data pertinent to the physical characteristics of the test specimen, both before and after irradiation. Fission product release data are given in Section 8.0. All the data reported here were obtained by Battelle Memorial Institute.

TABLE 7-1

Status of PBR Fuel Element Testing

Fuel Element Type	Impact	Compression	Abrasion	Radiograph	Metallography	Thermal Cycle	Self-Weld	Internal Pressure	Alpha Count	"Hot Oil" Permeability	High Temp. Permeability	Hot Air-"Popcorn"	Carburization	Neutron Activation	Furnace Capsule	Sweep Capsule	Static Capsule
FI-1	+	+	+	+										+		+	+
FI-6	+	0	0	0	0		0	0	+	+							
FA-1	+	+	+	+	+									+		+	0
FA-5														+			
FA-6	+	+	+	+	+	+	+	0	+	+	0			+		+	
FA-7	+													+			
FA-8	+	+	+	+	+	+	+	+	+	+	+			+			0
FA-9														+			
FA-10	+	+		+						+				+			0
FA-11	+								+	+							
FA-14	+	+			0									+			
FA-16	0								0	+	0			0	0		
FA-17										+							
FA-19	0	0			0												
FA-20	0	+	0	+	+	0		0	+	+	0			+	+		0
FL-1	+	+															
FL-2	+	+		+	+			0	+	+				+			
FX-1	+				0					+							
FX-2	+	+			+					+							
FX-3										+							
FP-1									+			+	+				
FP-2									+			+	+				
FP-3									+			+	+				
FP-4									+			+	+	+			

\+ test completed

0 test planned or in progress

7.1 Pre-Irradiation Test Data

Pre-irradiation tests are a graduated series of tests designed to screen for further testing the various fuel element concepts submitted for evaluation. Pre-irradiation tests also provide valuable data for comparison with physical property data obtained after irradiation. The test data obtained during Phase I are discussed here in terms of the type of fuel element but are tabulated, where appropriate, by the nature of the test so that comparisons can be made between the various test specimens. The contents of the summary data tables are as follows:

TABLE 7-2

Impact and Compression Test Data

Fuel Element Type	Coating	Impact Energy at Failure, ft. lbs.		Compressive Failure		Load Modulus Lb/in (c)
		Coating	Matrix	Load, lbs.	Deflection in.	
FA-6	SiC	1.33(a)		2070	0.040	48,700
	SiC	1.25(a)		1595	0.062	
	SiC	3.0		1162	0.05	
	SiC	1.9	3.6	1925	0.03	64,200
FA-8	SiC	0.5(a)		530	0.011	
		0.42(a)		837	0.036	
		1.0				
		0.6	1.3			
		0.5	0.9			
FI-6	ZrC	1.1				
FL-2	"	0.9	1.7	915	0.031	32,800
FX-2	"	0.8	13.0(b)	2995	0.127	24,500
FX-1	TiC	0.8	13.0(b)			
FA-11	PryoC	1.1				
FA-20	"	3.6	7.8	2577	0.097	44,300
FA-7	none	-	1.9			
FA-10	"	-	10.4	3750	0.057	76,900
FA-14	"	-	8.3	4550	0.089	58,600
FL-1	"	-	1.7	800	0.047	21,700

(a) Impacts made at one location. In all other tests specimen was rotated between impacts.
(b) Testing machine limit.
(c) Indicated by the slope of the best straight-line portion of the load deflection curve.

TABLE 7-3

Uranium Contamination of Surface Coatings

Fuel Element Type No.	Sample No.	Position	Net Counting Rate cpm, Normalized to Total Surface	Surface Uranium, ppm of Total U in Sphere
FA-6	17E	1	134	6.3
	19E	1	120	5.6
	"	2	174	8.2
	"	3	237	11.1
	"	4	237	11.1
	"	5	0	0
FA-8	E2	1	25,500	1140
	E3	1	40,500	1790
	E6	1	40,000	1770
	E7	1	122,000	5400
	E8	1	58,000	2570
	E9	1	31,000	1390
	E10	1	60,000	2700
	E11	1	58,000	2570
	E12	1	140,000	6250
FA-11	336	1	250	44
FA-20	330	1	390	70
	314	1	120	21
FL-2	1	1	11.9	3.4
	"	2	9.8	2.7
	2	1	30.1	8.4
	"	2	0.0	0.0
	3	1	41.3	11.4
	"	2	40.6	11.1
	6	1	31.5	8.6
	"	2	23.1	6.3

TABLE 7-4

"Hot Oil" Permeability

Full Element Type	Number of Specimens Tested	Number of Leaking Specimens
FI-6	1	1
FA-6	23	12
FA-8	17	10
FA-11	3	2
FA-17	2	0
FA-20	6	0
FL-2	4	4
FX-1	2	2
FX-2	2	2
FX-3	1	0

TABLE 7-5

Uranium Contamination in Metal Coated UO_2 Particles

Specimen Type No.	Batch No.	Leached	Uranium Contamination mg of U/gram of powder
FP-2 (nickel coating)	1	no	47
	2	no	7.4
	2	yes	6.6
FP-3 (nickel chromium coating)	1	no	21
	2	no	2.4
	2	yes	3.0
FP-4 (Niobium coating)	1	no	33
	1	no	18
	1	yes	18

Silicon Carbide Coatings

Type FA-6: Impact and compression results are given in Table 7-2. The impact strength when the ball was rotated between impacts was generally about twice that when all the impacts were on the same spot. One specimen had a coating impact strength of 1.33 ft.-lbs. when 15 impacts (by a 1 pound weight increased at one inch intervals) were made on the same spot. The same test applied to a duplicate specimen resulted in impact failure of 1.25 ft.-lbs. after 14 impacts. When the ball was rotated, a condition more typical of the environment in the PBR, impact strengths of 3.0 and 1.9 ft.-lbs. were measured. Loading requirements of a large scale PBR require a 20 foot free fall which is equivalent to an impact load of about 2.2 ft.-lbs. On the basis of these preliminary tests, the FA-6 type fuel element should meet the PBR impact requirements with very little further development. A typical impact failure, a chipping of the coating, is shown in Figure 7-1.

Compressive strengths of 2070 and 1595 pounds were measured on two FA-6 specimens. Although these strengths are far in excess of the required 500 pound strength, it should be recognized that post-irradiation compressive data is more meaningful since the greatest static load occurs on the fully irradiated fuel elements at the bottom of the reactor.

Two spheres were tested for self welding under a 50 pound load at 2000°F for 100 hours. Microscopic examination at 60x showed some fracturing of the SiC grains in the region of contact but no evidence of a self welding tendency. The contact region, shown in Figure 7-2, was lighter in color and about 1/32 of an inch in diameter, which indicates a local pressure of 65,000 psi. A hot oil permeability test showed that no leaks developed in this region.

Abrasion testing of two specimens showed weight losses of 0.002 grams and 0.0046 grams per ball after tumbling with other FA-6 balls for a hour in the abrasion testing apparatus described in Section 6.1. Both specimens showed no visual change in surface appearance and showed no leakage when subjected to the hot oil permeability test.

Uranium contamination in the surface of two FA-6 spheres is reported in Table 7-3. In one specimen surface contamination was measured at five random locations and was found to vary from 0 to 11 ppm of the total uranium in the sphere. A second specimen was measured in one location

and showed a contamination of 6 ppm. Each measurement location covered one-seventh of the total sphere. Data are converted to a per sphere basis by multiplying the observed count rate by seven and are reported as the fraction of total surface uranium to the total uranium in the specimen. The reported surface uranium would be increased by about a factor of two if the uranium was assumed to be uniformly distributed throughout the surface coating and a corresponding correction factor was applied.

Hot oil permeability data are given in Table 7-4. About half of the FA-6 specimens obtained passed this test satisfactorily. Specimens showing leaks were returned for patching prior to further testing.

Type FA-8: Coating fracture by impact occurred at energies ranging between 0.42 and 1.0 foot pounds. As can be seen from Table 7-2, the overall impact resistance of FA-8 specimens was less than for any other of the specimens tested. Figure 7-1 shows that the impact failure was in the form of long cracks in the ball rather than chipping of the coating. Improvement of the matrix strength should, therefore, result in a higher impact strength for a specimen utilizing the FA-8 coating.

Compressive strength, shown in Table 7-2, is adequate for PBR purposes, although the measured strength was less than for any other specimen tested.

A self welding test where two specimens were held under a compressive load of 50 pounds for 100 hours at 2000°F showed no evidence of self welding or damage to the coating at the point of contact. The specimens were microscopically examined up to 100x and showed no leaks when tested in hot silicone oil.

Abrasion testing for one hour resulted in a weight loss for each of two specimens of 0.024 and 0.044. Inspection and hot silicone oil testing showed no evidence of damage to the coating.

No leakage was observed when a specimen was subjected to an internal pressure of helium of 250 psi. The objectives and procedure for this test have been discussed in detail in Section 6.1.

A high uranium surface contamination was measured in seven specimens. These measurements, given in Table 7-3, showed that between

0.1% and 0.6% of the total uranium in the sphere was at the surface of the coating.

Of the as-received FA-8 specimens, 10 out of 17 showed leaks when subjected to the hot oil permeability test. Those that leaked were returned to the manufacturer for patching.

Metal Carbide Coatings

Type FI-6 (ZrC coating): This specimen showed profuse bubbling uniformly distributed over the surface when subjected to the hot oil permeability test. The coating was visibly damaged under an impact energy of 1.1 foot pounds, but no bubbles in excess of those previously observed evolved at the damaged area.

Type FL-2 (ZrC coating): Of four specimens of this type tested in hot silicone oil, all showed coarse bubbling at the fuel plug outline and fine bubbling uniformly distributed over the surface. Impact strength was measured at 0.9 and 1.7 foot-lbs. for the coating and matrix respectively. Compressive strength was 915 psi. Surface uranium was determined by alpha count to range up to 11 ppm of total uranium content.

Type FX-2 (ZrC coating): Both of the specimens tested in hot silicone oil showed immediate coarse bubbling from up to 10 identifiable locations. The coating failed by flaking away from the surface at an impact energy of 0.8 foot-pounds, but no fracture of the matrix was observed up to 13 foot-pounds, the limit of the apparatus. Compressive strength was 2,995 pounds.

Type FX-1 (TiC coating): Bubbles immediately evolved from all areas of the surfaces of each of two spheres tested in hot silicone oil. An impact energy of 0.8 foot-pounds was measured for the coating and 13 foot-pounds, the limits of the apparatus, for the matrix. Like FX-2, the coating failed by flaking from the sphere when impacted.

Carbonaceous Coatings

Type FA-11: Of three specimens received all shpwed leaks when subjected to the hot silicone oil test. After reprocessing by the vendor, one ot the three no longer showed leaks. An impact strength of 1.1 foot

pounds was measured for the coating. Failure was by flaking-off of the coating at the point of impact. Surface uranium, as determined by an alpha count, was 44 ppm of the total uranium in the specimen.

Type FA-17: Two specimens showed no evidence of leakage when immersed in hot silicone oil.

Type FA-20: Of six specimens tested in hot silicone oil, none showed evidence of leakage. Surface uranium was measured by alpha count to be 70 ppm of the total uranium in the sphere. The coating fractured under an impact energy of 3.6 foot pounds, which was the highest coating impact strength measured for all of the specimens tested to date. The matrix failed at an impact energy of 7.8 foot pounds. Compressive load was 2577 pounds.

Coated Particles

Type FP-1 (Nickel coated particles): Photomicrographs showing the reaction of Type FP-1 fuel particles with a AGOT graphite are given in Figure 7-3. Figure 7-3 a shows the extent of the reaction after the fuel particle-graphite system was baked at 1700°F for 4 hours. The fuel particles have maintained their integrity (gray, roughly circular areas) but the nickel coating was agglomerated leaving most of the particles without coatings. When the system was heated at 2500°F for 168 hours, Figure 7-3b, most of the particles lost their shapes and interaction between the UO_2, nickel and graphite was evident. Heating to 3000°F for 6 hours resulted in complete loss in the identity of the particles and severe interaction between UO_2, nickel and graphite. These studies were made on the first batch of particles received from the manufacturer. Similar results were obtained when the particles were reacted with Texas 55 coke at 1700° for 4 hours.

An alpha count to measure uranium contamination in the coating was made on samples from each of the two batches received. These data, reported in Table 7-4, show that the uranium contamination in the second batch was about seven times less than in the first. The sample from the second batch was leached with 2N nitric acid for 30 seconds, washed with water and then counted again. Since the leaching did not reduce the alpha count significantly the contamination is undoubtedly evenly distributed throughout the coatings.

A high degree of porosity was indicated since these samples were completely disrupted by oxidation of the UO_2 core when heated in 1200°F air. After one hour of heating the weight of samples from the first batch increased by 52.4 per cent. The weight gain for the second batch was considerably lower, 12.7 per cent. Although considerable improvement in coating contamination and porosity of the second batch was determined, carburization studies on this batch were not felt justified. The chemical composition of both batches was the same and there was no reason to expect that the reaction of the metal coating with carbon would differ in these two batches.

Type FP-2 (Nickel-Chromium coated particles): The reaction of FP-2 particles with AGOT graphite and Texas 55 coke was similar to that for FP-1. Figures 7-4a and 7-4b are photomicrographs for samples baked with AGOT graphite at 1700°F for 4 hours and samples baked at 2500°F for 168 hours, respectively. At 1700°F the fuel particles retained their shapes and some semblance of their coatings. A slight amount of melting and agglomeration occurred in the coating material forming a two-phase reaction product. A similar result was observed with a Texas coke matrix. At 2500°F most UO_2 particles lost their shapes and some appeared to dissolve in the coating. The coating formed agglomerations. Samples were further heated to 3000°F for 6 hours and a 3 or 4 phase reaction product was formed, with the UO_2 particles completely losing their identity. These carburization studies were made with the first batch of particles.

The data given in Table 7-5 show that uranium contamination was less than for the nickel coated particles, FP-1. The second batch of FP-2 particles had a uranium contamination which was about one-eighth of that for the first batch. Leaching with nitric acid showed that the contamination was spread throughout the coating and not concentrated at the surface. Weight gain after one hour of heating in air was 62.5 and 26.9 percent for the first and second batches, respectively.

Type FP-3 (Niobium coated particles): Figures 7-5a and 7-5b are photomicrographs showing the reaction of niobium coated UO_2 particles with AGOT graphite at temperatures of 1700°F for 4 hours and 2500°F for 168 hours, respectively. At 1700°F the fuel particles retained their shapes and the niobium coating was reduced to a series of non-adherent, small gray particles between larger particles of UO_2. When particles were baked with Texas 55 coke at 1700°F the result was the same. The sample

examined after the 2500°F exposure was similar to the 1700°F exposure except the particles and the coating were more porous. After a 6 hour bake at 3000°F the UO_2 particles lost their integrity entirely.

Only one batch of FP-4 particles was received. Counting of as-received and leached specimens showed that uranium contamination was uniformly distributed throughout the coating.

Type FP-4 (Alumina coated particles): Test results on this type of coated particle are given in Section 5.1.

7.2 Post-Irradiation Tests

Two capsules were irradiated in the Battelle Research Reactor during the past period. The primary purpose of Sweep Capsule SP-3 was to obtain fission product release data from coated specimens under high level irradiation in addition to determining the effects of irradiation on certain properties of the specimens. The irradiation and post-irradiation examination of Capsule SP-3 was completed during the past period. Fission product release data is given in Section 8.3. The objective of Static Capsule SP-4 was to determine the effect of irradiation at 2000°F on the stability of four types of UO_2 fuel particles in graphite and on certain properties of surface coated specimens. The irradiation of SP-4 was started during the past period and will continue to December 1959, so that no results from SP-4 are included in this report.

7.2.1 Capsule SP-3

Capsule SP-3 contained two each of the FA-6 and FA-8 types of specimens. Both types were coated with SiC and the FA-6 had a 0.15 in unfueled graphite shell between the fueled graphite core and the external SiC coating. The method of mounting the spheres and other capsule design features are described in Section 6.2.

The capsule was inserted in the BRR core position CP-45 on May 6 and was removed from the BRR on August 3. During this period, several intentional low power runs were made to permit fission product release data to be obtained as described in Section 8.3. The capsule was irradiated at the full BRR power level of 2 MW for 61 days (1460 hours) of the total calendar time of 83 days. During one 31 hour period (June 17-18) the BRR operated at a power level of 2.5 MW when the estimated specimen surface temperatures rose to 1850°F for FA-6 and 2300°F for FA-8. The average operating conditions during the irradiation are summarized in Table 7-6.

TABLE 7-6

Summary of Capsule SP-3 Operating Conditions

Specimen	Measured Block Temp. °F	Calc. Spec. Surface Temp. °F	Calc. Spec. Center Temp. °F	Calc. Ht. Gen. Rate KW/Ball	Total Exposure KWH/Ball Calc.	Dosim.
FA-6 (18E)	1000	1300	1600	1.7	2500	2400
FA-6 (20E)	1000	1300	1600	1.7	2500	1950
FA-8 (E4)	1200	1600	1900	2.2	3200	2400
FA-8 (E5)	1200	1600	1900	2.2	3200	2600

Specimen power level is calculated from the measured graphite block temperature, the pool water temperature, and the effective thermal resistance properties of the capsule. The specimen temperatures are then calculated, using a value of a thermal conductivity of 20 BTU/hr - ft - °F. The total exposures based both on the estimated power levels and on the results of measurements on the dosimeter wires are compared in Table 7-6. The dosimetry values have a higher degree of accuracy than the values calculated from the thermal conditions.

Post-irradiation examination of the specimens was conducted in the Battelle Hot Cell Facility during the week of August 10. The examination consisted of visual inspection, macrography, metallography, weights, dimensions, hot-oil tests, impact tests and compression tests. Results are described below.

Visual Examination: Visual examination of both FA-6 specimens (18E and 20E) revealed numerous surface cracks. Figure 7-6 is a view of the inner capsule which contained the two FA-6 specimens just after it was opened in the Hot Cell. A portion of the graphite support and a thermocouple lead can be seen. Specimen 18E is seen to have an equatorial crack which was the most prominent crack in this specimen. The prominent crack in 20E was about 30° above the equatorial plane. There was visible evidence that the prominent cracks penetrated the graphite matrix. In addition to the major cracks, there were numerous hairline cracks intersecting the major cracks, usually at right angles. Figure 7-7 is a 4X photograph of the prominent crack in FA-6 (18E). Small shiny areas along the major cracks can be noted. These areas appeared to be inter-layer chipping of the SiC-Si coating.

The two FA-8 specimens (E4 and E5) appeared in good condition. There was no visible evidence of cracks or any other flaws. Typical surface condition of the irradiated FA-8 specimens is shown in Figure 7-8 which is a 4X photograph of specimen FA-8(E5) after impact testing described below.

Hot Oil Tests: All four specimens were subjected to the hot oil test. The two FA-8 specimens were tested immediately after visual examination to preclude any accidental damage to the coating during weighing and measuring. The cracked FA-6 specimens were tested after weighing.

Specimen FA-8 (E-5) exhibited no leakage during the 17 min. immersion in 375°F silicone oil. After specimen FA-8 (E4) had been immersed for 52 sec, a single stream of bubbles from only one location was observed. The bubble rate could be defined as "steady-slow". The test was interrupted after 3 min. and in two subsequent tests the bubble stream did not appear. Both of the cracked FA-6 specimens emitted several streams of bubbles from the cracks which could be defined as "steady-rapid".

Weight and Dimension Measurements

A summary of weight and dimensional changes is given in Table 7-7.

TABLE 7-7

Weight and Dimension Changes in Capsule SP-3 Specimens

Specimen	Pre-irrad Wt. gms.	Weight Change, % After irrad.	Weight Change, % After 1st hot oil test	Weight Change, % After 2nd hot oil test	Change in dia. after irrad., %
FA-6 (18E)	59.995	-0.1	+2.4	-	-0.3
FA-6 (20E)	56.164	0.0	+0.6	-	0.0
FA-8 (E4)	64.526	-	-0.3	0.0	+0.01
FA-8 (E5)	59.746	-	-0.1	-	+0.08

Hot oil tests on unirradiated specimens had shown a tendency for leaking specimens to gain weight during the test due to absorption of oil. This is confirmed by the weight gains of the cracked FA-6 specimens after hot oil testing. It is not clear whether a greater weight loss for FA-8 (E4) would have been observed prior to hot oil testing. Dimensional changes are small and are considered insignificant since no accurately machined flats were put on the coated spheres.

Impact Tests: Since the FA-6 (20E) specimen was visibly cracked, it was subjected to a 1 ft. free fall impact test rather than the normal impact test. On impact, the specimen fractured into four approximately equal segments and a few chips. This load was equivalent to a 1.5 in.-lb. impact, well below the pre-irradiation values of 24 to 36 in.-lb., indicating that the presence of the cracks seriously weakened the specimen.

The FA-8 (E5) specimen was first subjected to a 1 ft. free fall test and a subsequent hot oil test showed no damage to the coating as evidenced by a lack of bubble streams. This specimen was then transferred to the standard impact test machine (see Section 6.1) for further testing. The test was started by dropping a 1 lb. weight from a 1 inch height onto the specimen and increasing the height of fall in 1 inch increments. After each impact, the specimen was given a 3 min. hot oil test to detect the point of coating failure. A different point on the sphere was impacted each time. At 9 in.-lb., a bubble stream appeared. At 12 in.-lb. the first visible crack appeared. Figure 7-8 shows the crack developed by the 15 in.-lb. impact. Testing was continued up to 24 in.-lb., the limit of the apparatus, where the specimen was badly cracked, but still in one piece.

A comparison of the effect of irradiation on impact strength of uncoated and coated spheres is shown in Figure 7-9. The level of impact strength is lower for the coated specimens since the coatings tend to crack first at lower loads. However, where radiation hardening of the graphite matrix tends to slightly reduce the impact strength of uncoated spheres, the impact strength of coated spheres tends to be increased.

Compression Tests: Specimen FA-8 (E4) was compression tested while immersed in hot oil in an attempt to determine whether there was any coating failure prior to matrix failure. The specimen failed at a compressive load of 1697 lbs. where the deflection was 0.0172 in. The slope of the straight line portion of the load-deflection curve was 146,000 lbs./in. compared with values of 50,000 - 80,000 lbs./in. for unirradiated specimens. There was no evidence of bubbling prior to the failure of the graphite matrix.

The effect of irradiation on the compressive strength of both coated and uncoated specimens is shown in Figure 7-10. It is seen that the effect of radiation hardening increases the compressive strength of both the coated and uncoated specimens.

The FA-6(18E) specimen was not subjected to the compression test so that it could be sectioned in an attempt to learn more about the nature of the cracks in this specimen.

Metallographic Examination: The FA-6(18E) specimen was first mounted in plastic so that it could be gripped while being sectioned. However, an unanticipated radiation hardening of the plastic occurred, causing the specimen and mount to drop from the jig as the plastic was being cut. This drop fractured the specimen. From visual examination of the pieces it appeared that the major cracks penetrated through the shell into the core of the specimen. One of the pieces was remounted, polished and etched for metallographic examination. The following observations were made.

1. The SiC-Si coated showed no evidence of radiation damage to either the SiC grains or the SiC matrix. Figure 7-11 shows a comparison of the coating before and after irradiation. Since the photographs were of two different specimens, the greater SiC-Si thickness in the post-irradiation photograph is due to variation in the as-fabricated coating thickness of the two specimens.

2. There was no evidence of any separation of the coating from the matrix, as can be noted in Figure 7-11.

3. There was no evidence of any separation of the unfueled shell as shown in Figure 7-12. This photograph is a 4X enlargement of one of the pieces of FA-6(20E) as it appeared directly after the impact failure.

4. There was no evidence of any radiation induced flaws in the graphite matrix as shown in Figure 7-13. The whitish areas in this picture are the fuel particles.

A portion of specimen FA8(E4), which had been cracked in the compression test, was mounted, polished and etched for metallographic examination. Unfortunately, grinding and polishing of this piece did not reveal

the SiC-Si coating, so that no information on the condition of the coating or coating-graphite bond is available at this writing. Typical views of the fueled matrix are shown in Figure 7-14. This lower density graphite matrix is somewhat more porous than the graphite in the FA-6 specimen. The fracturing of some fuel particles had been noted in some pre-irradiation examination of this type. However, cracks similar to the one in a graphite grain in Figure 7-14 had not been detected prior to irradiation.

7.2.2 Capsule SP-4

One specimen of each of 6 types were loaded into static capsule SP-4. The distinguishing features of each of the six types are listed below.

1. Type FI-1: 1μ UO_2, by infiltration
2. Type FA-2: 67μ UO_2, by admixture
3. Type FA-1: 100μ UO_2, by admixture
4. Type FA-10: 400μ UO_2, by admixture
5. Type FA-20: Same as FA-1 except graphitized and PyC coated
6. Type FA-8: SiC-Si coated

The objective of this experiment was to determine the effect of irradiation on the stability of UO_2 in the first four graphite specimens above. The target temperature was 1900°F which would result in central temperatures in the range of 2000° F to 2100°F. Since shrinkage occurs under high temperature irradiation of uranium-graphite, two types of coated specimens were included (items 5 and 6). Also, the effect of the degree of graphitization on matrix shrinkage can be assessed by comparing items 2 and 5.

The design of capsule SP-4 is described in Section 6.3. The capsule was inserted in the BRR on August 25. Typical operating conditions are listed in Table 7-8.

TABLE 7-8

Operating Conditions for Capsule SP-4

Specimen	Measured Graphite Block Temp. °F	Ht. Gen. Rate, KW	Calculated Surface Temp.	Central Temp., °F
FA-1	1290	1.95	1620	1780 (a)
FA-8	1410	2.24	1770	1830
FI-1	1400	2.37	1760	1850
FA-2	1410	2.27	1770	1910
FA-20	1250	1.96	1560	1770
FA-10	1300	1.75	1630	1730

(a) Measured temperature. One thermocouple is imbedded in the center of this specimen only. All other central temperatures are calculated.

As can be noted, the target temperature of 1900°F surface temperature was not achieved. Several factors were investigated in an attempt to explain or improve the situation. Since no auxiliary electrical heaters were included, the target temperature was to have been achieved by proper selection of the thickness and material of the various thermal barriers with respect to the anticipated flux levels. One factor was uncovered when laboratory measurements of the thermal conductivity of the Inconel-X used for the inner capsule showed that the literature value used in design was 20% low. An attempt was made to increase the neutron flux by rearranging fuel elements in the BRR core. However, there was no significant increase. Several plans were studied to apply an external thermal barrier to the capsule to increase the temperature. However, the close tolerance required at the capsule-barrier interface appeared impractical to achieve with remote handling devices under 23 ft. of pool water.

No further attempts were made to increase temperatures. The capsule will continue irradiation at the conditions listed in Table 7-8 until the end of December 1959 at which time the expected exposure will be 4500 to 5500 KWH per sphere.

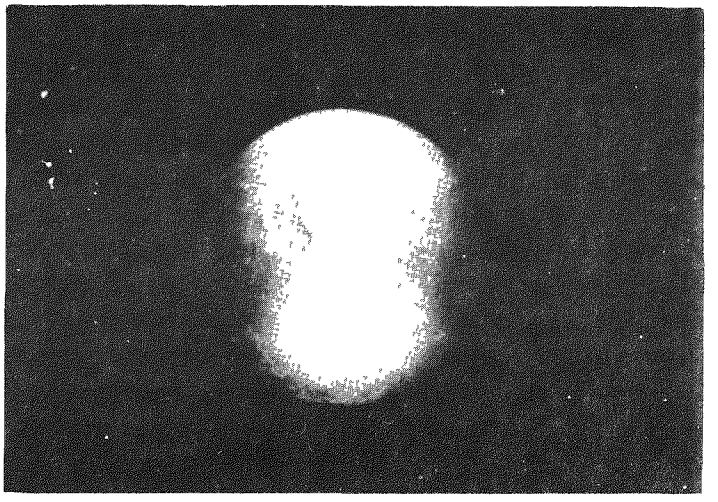

(a) FA-6

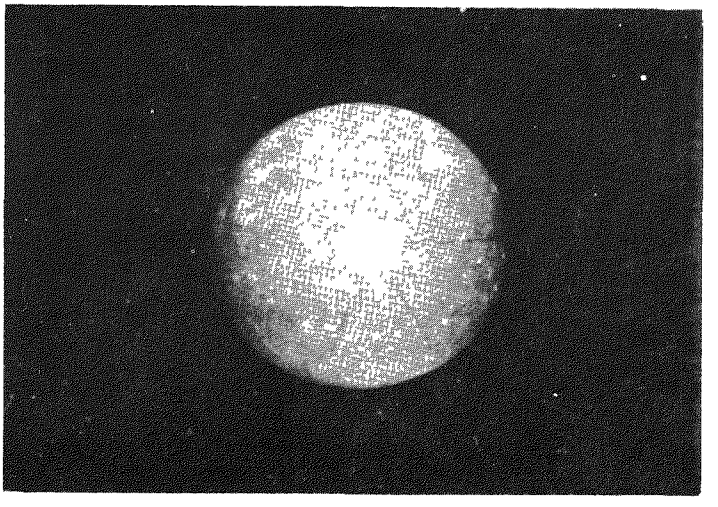

(b) FA-8

Figure 7-1 Typical Impact Fractures for Type FA-6 and FA-8 Test Specimens

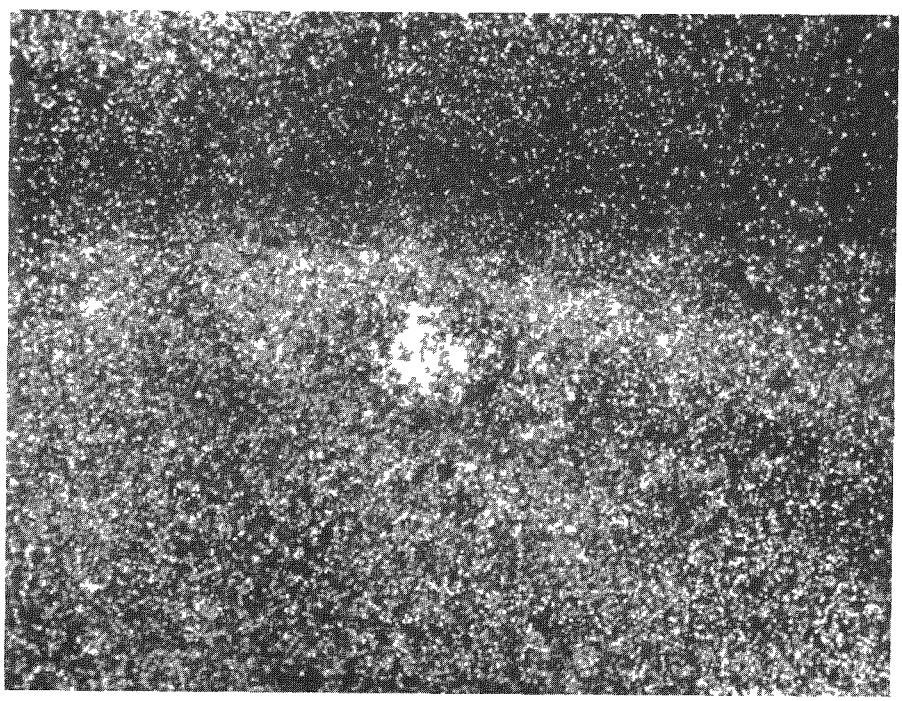

Figure 7-2 Surface of FA-6 Specimens After Self-Welding Test (10X)

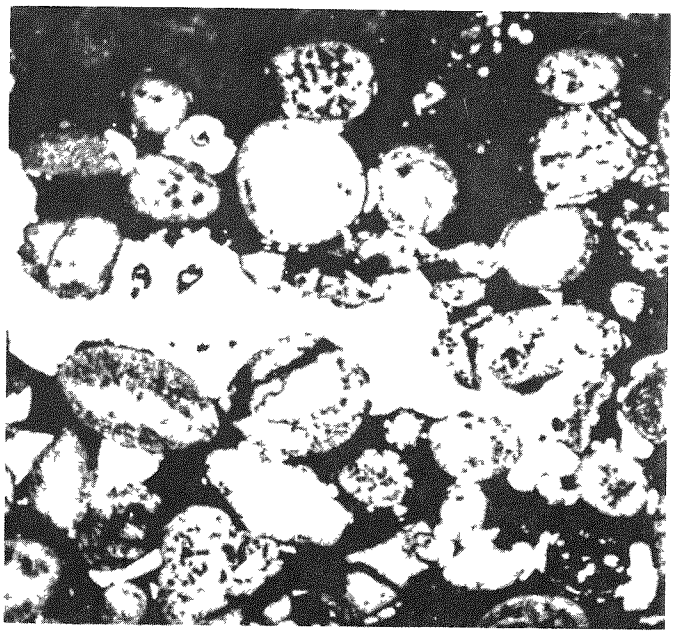

(a) heated at 1700°F for 4 hours (100X)

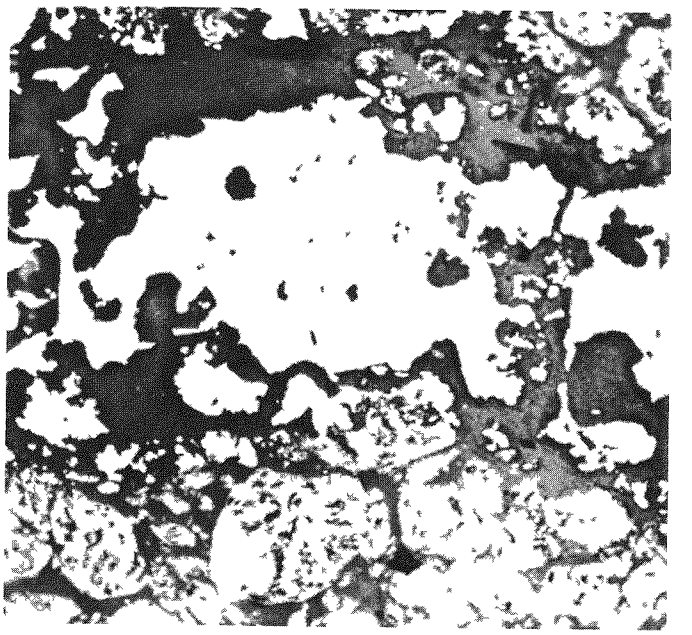

(b) heated at 2500°F for 4 hours (100X)

Figure 7-3 Nickel-Coated UO_2 Particles After Reaction at 1700°F and 2500°F with AGOT Grade Graphite in Helium

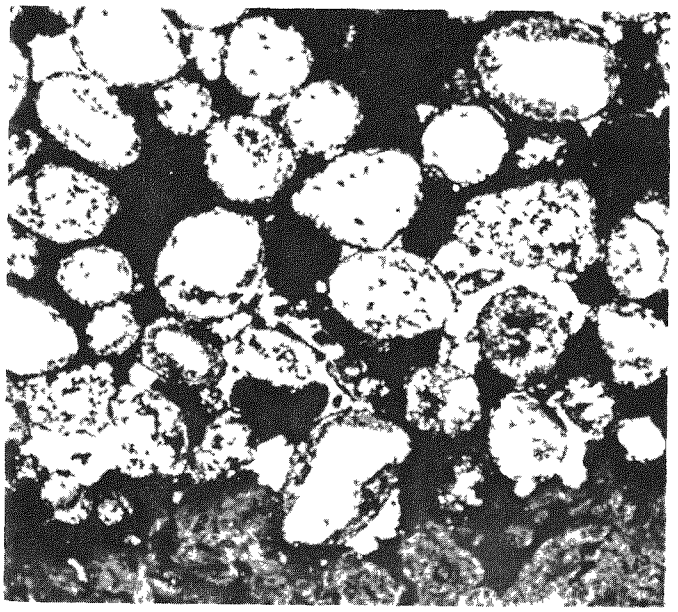

(a) heated at 1700°F for 4 hours (100X)

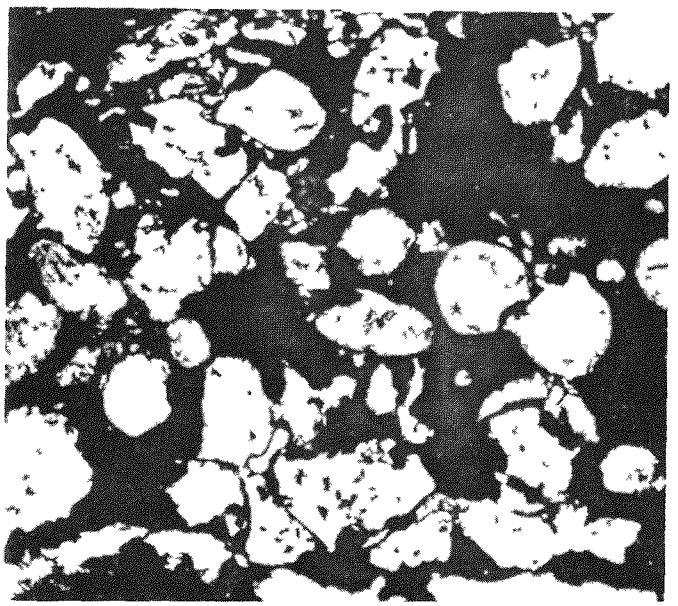

(b) heated at 2500°F for 4 hours (100X)

Figure 7-4 Nickel-Chromium Coated UO_2 Particles After Reaction at 1700°F and 2500°F with AGOT Grade Graphite in Helium

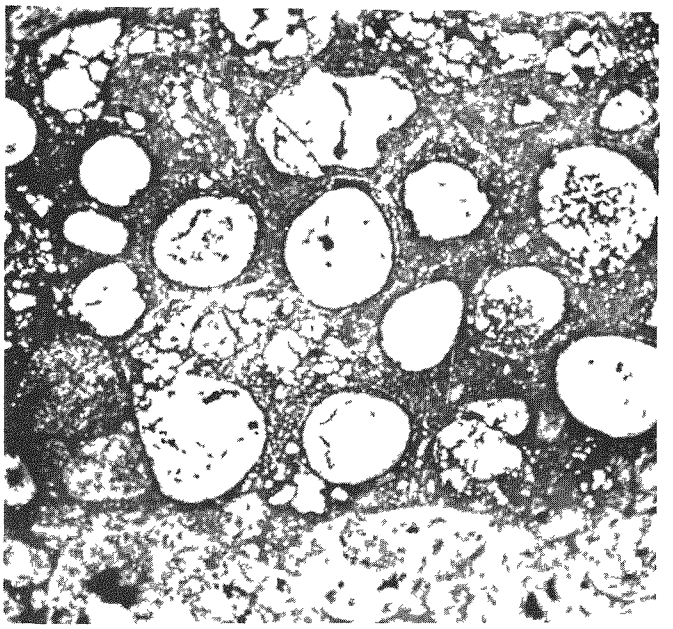

(a) heated at 1700°F for 4 hours (100X)

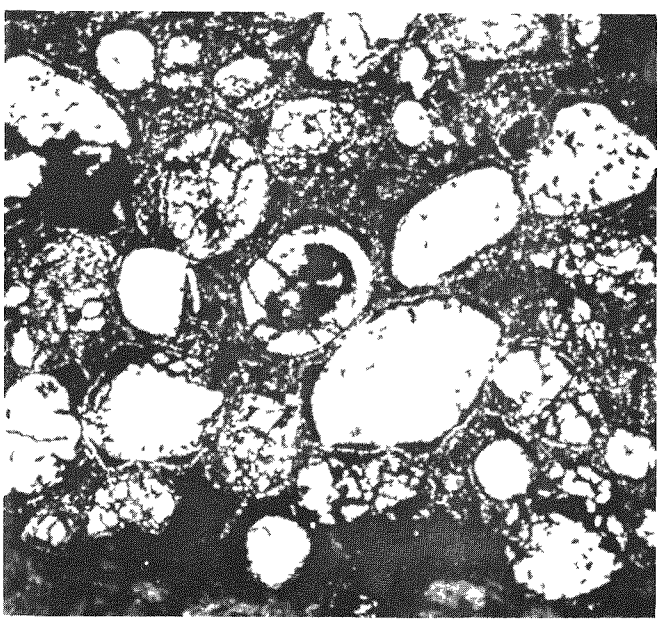

(b) heated at 2500°F for 4 hours (100X)

Figure 7-5 Niobium-Coated UO_2 Particles After Reaction at 1700°F and 2500°F with AGOT Grade Graphite in Helium

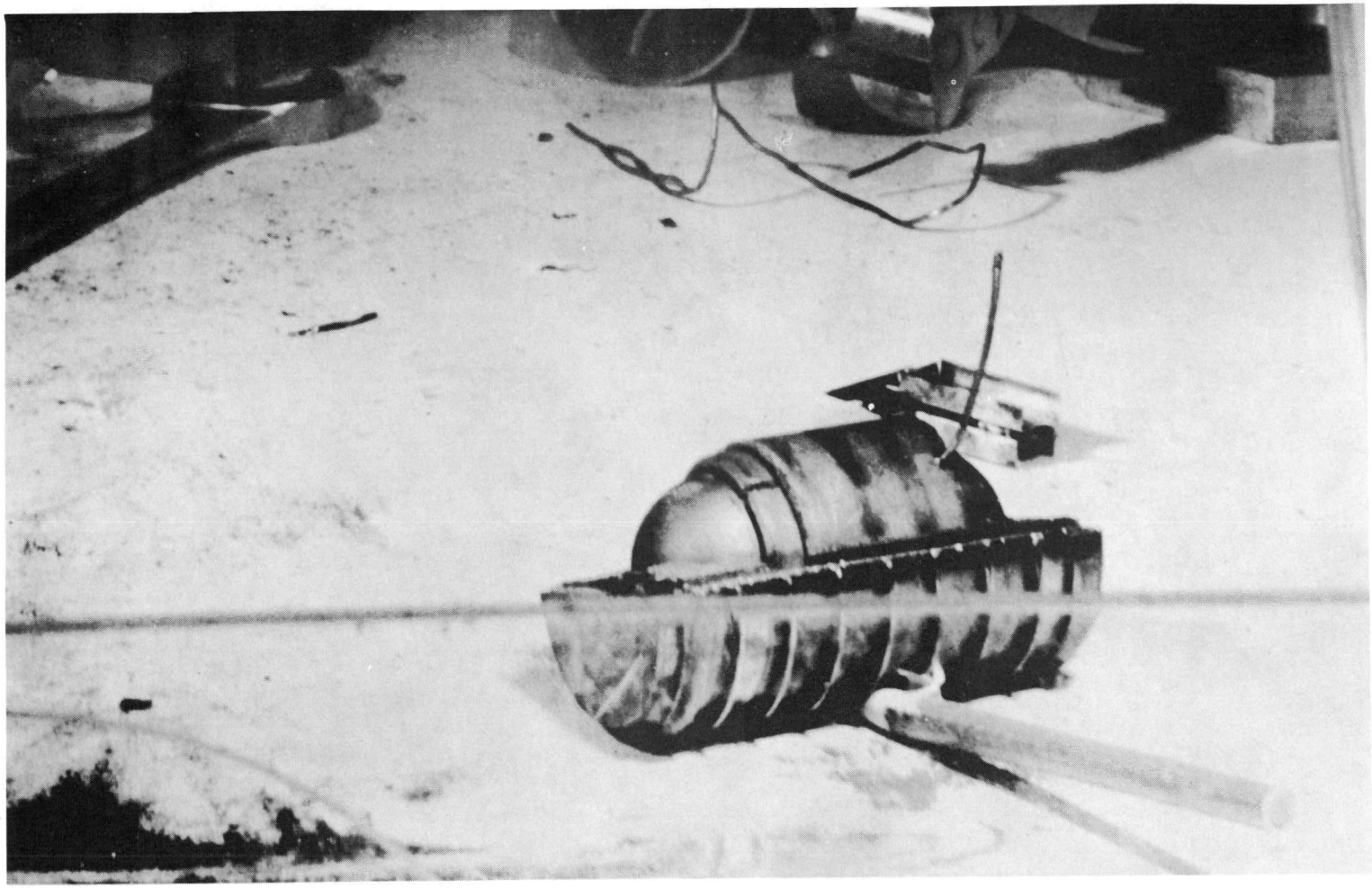

FIG. 7-6 View of FA-6 Specimens After Opening Capsule SP-3 In Hot Cell.

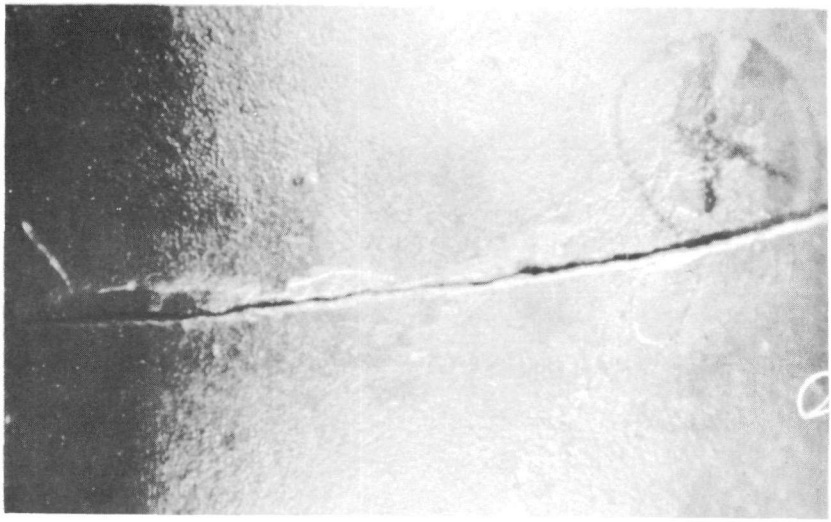

FIG. 7-7 Typical View (4X) of Major Crack in FA-6 (18E) Specimen After Irradiation in Capsule SP-3.

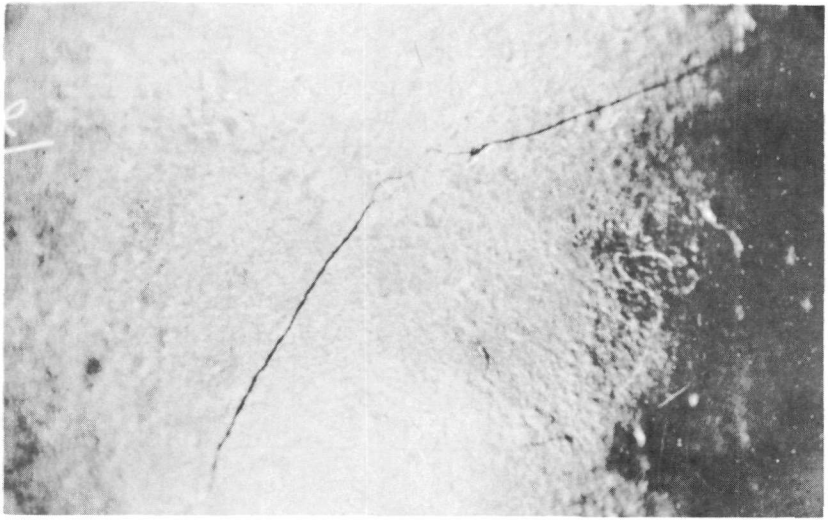

FIG. 7-8 Irradiation Specimen FA-8 (E5) After 15 in lb Impact.

IMPACT TESTS ON PBR FUEL ELEMENTS

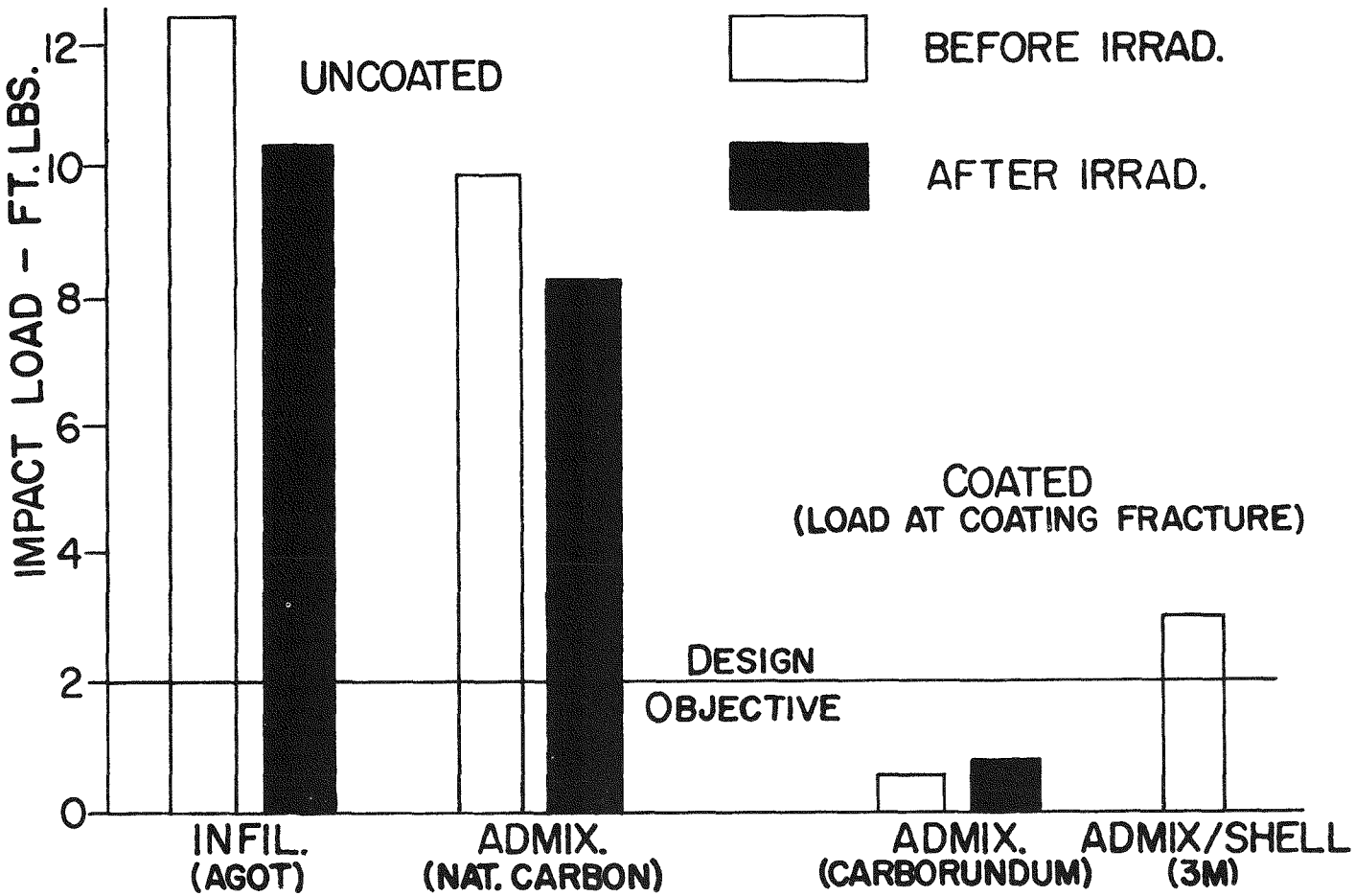

FIG. 7-9

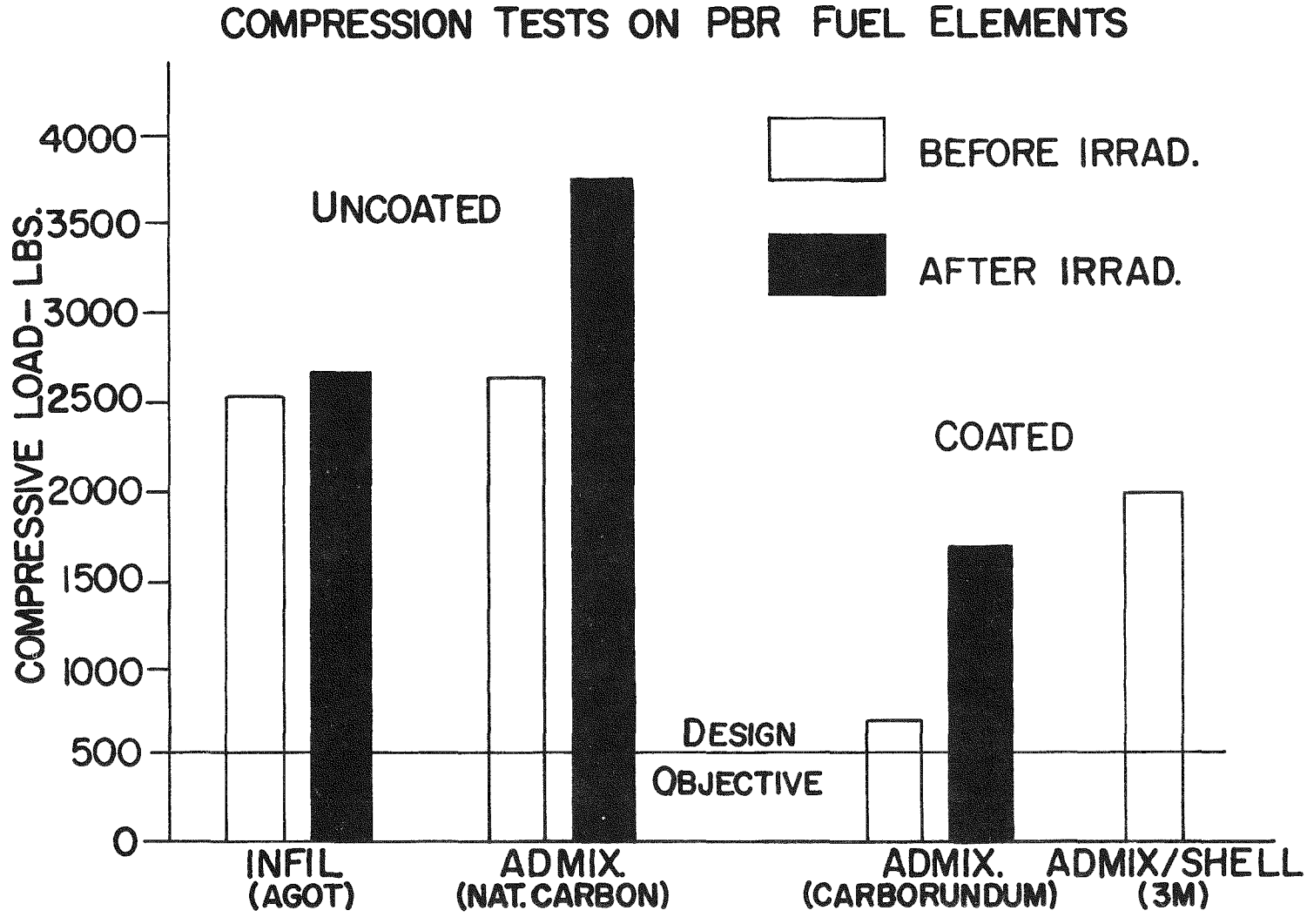
COMPRESSION TESTS ON PBR FUEL ELEMENTS
COMPRESSIVE LOAD - LBS.
4000
3500
3000
2500
2000
1500
1000
500
0
BEFORE IRRAD.
AFTER IRRAD.
UNCOATED
COATED
DESIGN
OBJECTIVE
INFIL
(AGOT)
ADMIX.
(NAT. CARBON)
ADMIX.
(CARBORUNDUM)
ADMIX/SHELL
(3M)

FIG. 7-10

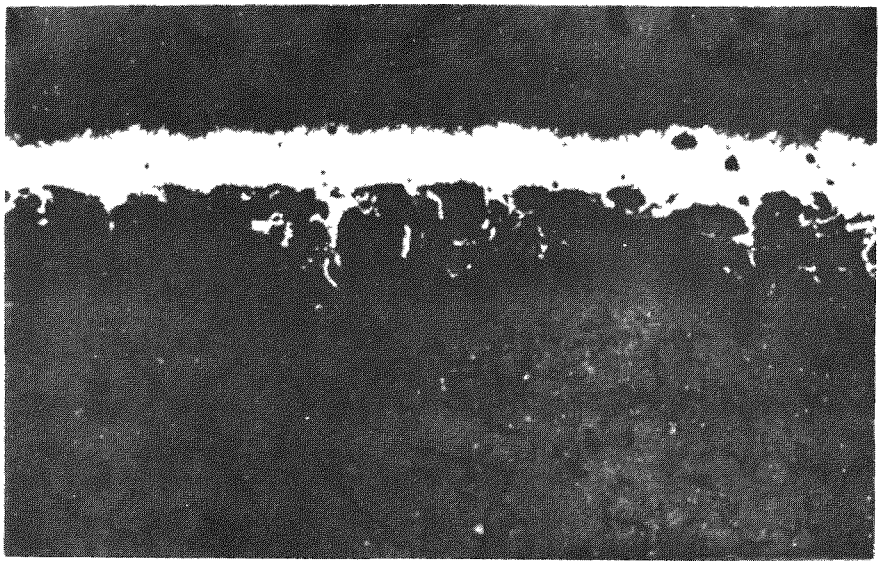

(a) Before Irradiation (100X)

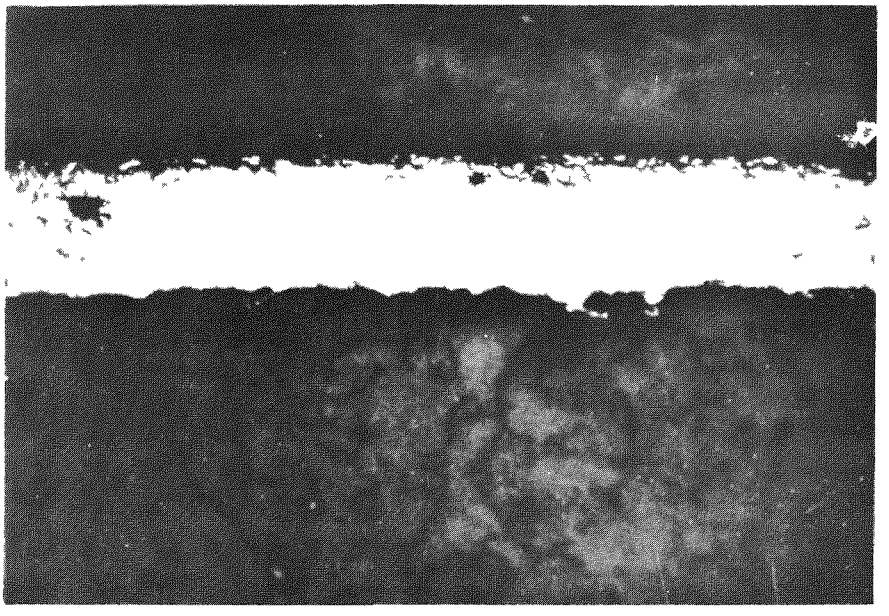

(b) After Irradiation (100X)

FIG. 7-11 Comparison of SiC-Si Coating on FA-6 Specimens Before and After Irradiation.

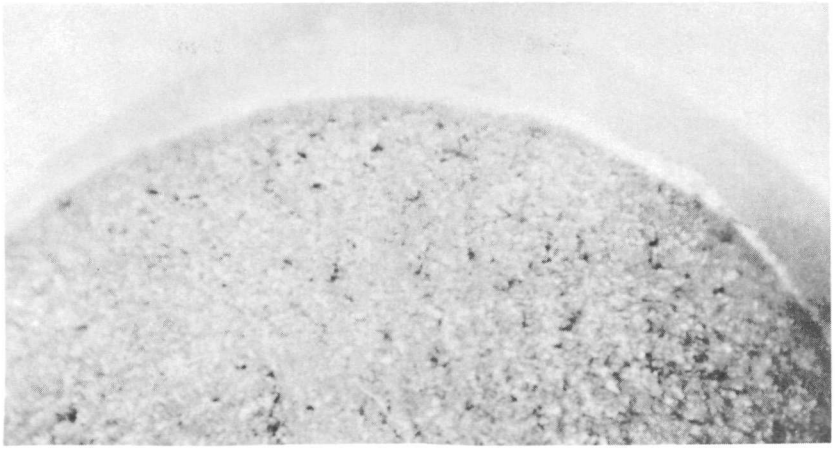

FIG 7-12 Piece of Irradiated Specimen FA-6(20E) at 4X Showing Adherence of SiC-Si Coating and Graphite Shell to Fuel Graphite Core.

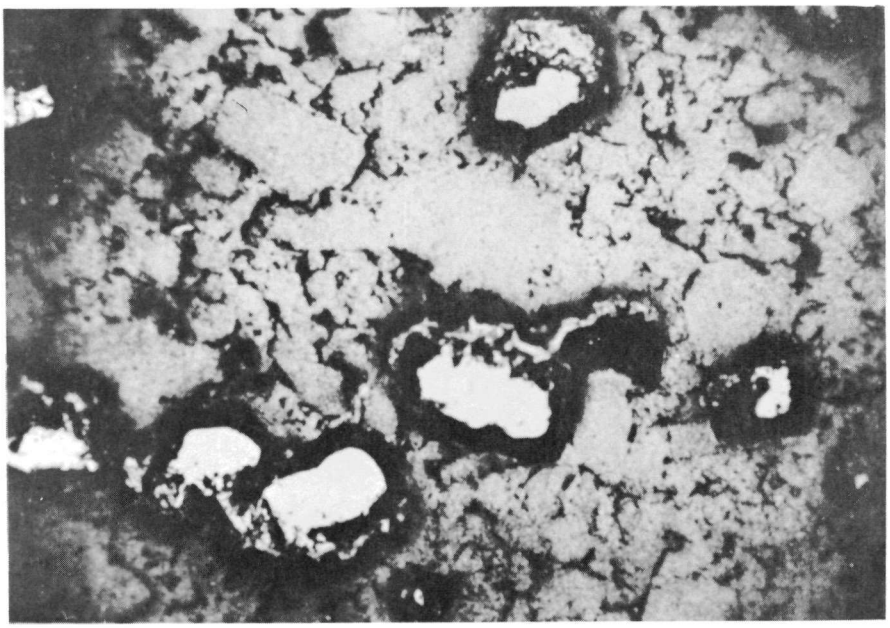

FIG 7-13 Uranium Carbide Particles in Graphite Matrix of Specimen FA-6(18E) After Irradiation (100X).

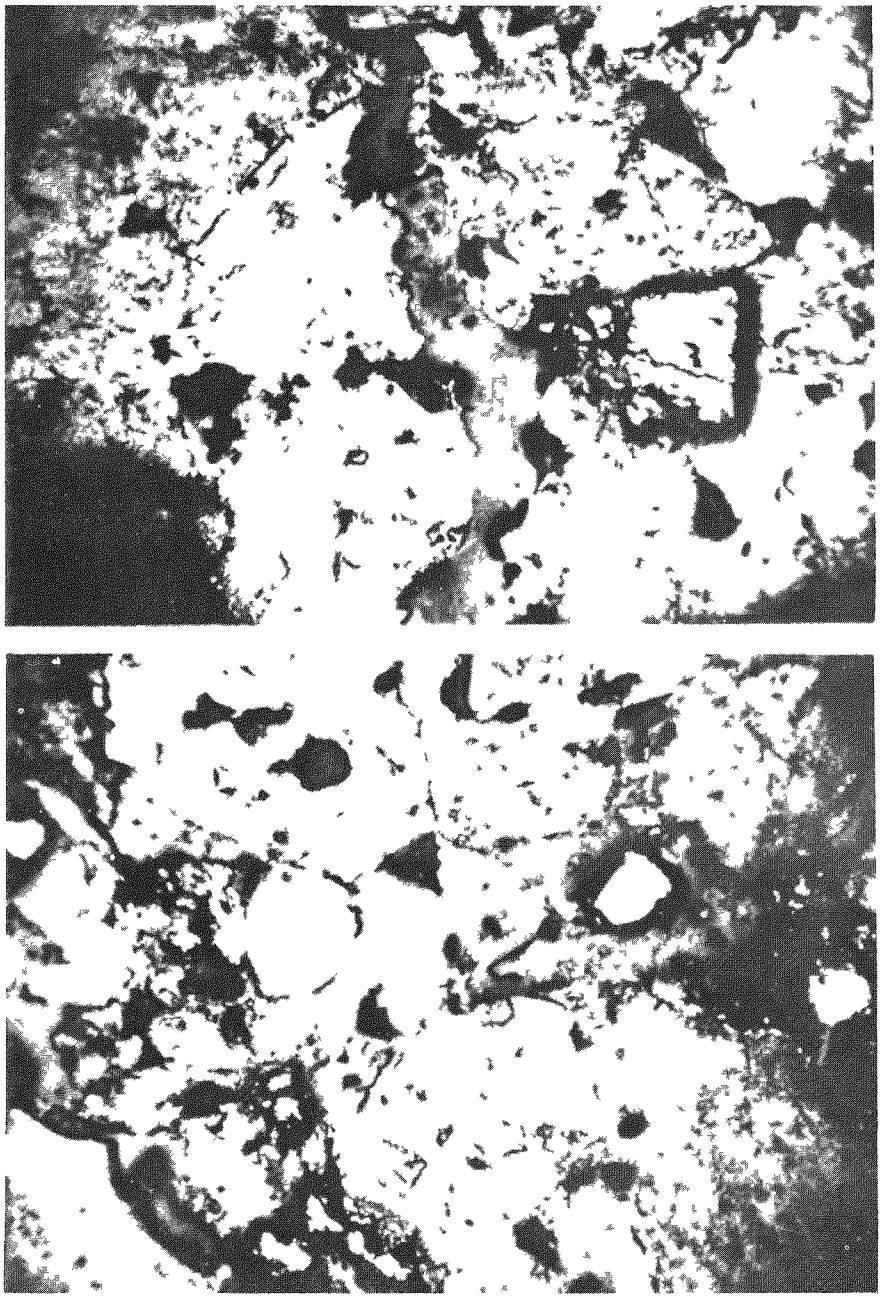

FIG. 7-14 Two Views of Uranium Carbide in Graphite Matrix of Specimen FA-8 (E4) After Irradiation (100X).

8.0 Fission Product Retention Test Results

This section summarizes the fission product retention test results obtained from the three types of tests performed during the past period. A summary of all experiments performed is shown in Table 8-1.

TABLE 8-1

Summary of Fission Product Retention Tests in Phase I

	Neutron Activation	Furnace Capsule	Sweep Capsule
A. Uncoated Spheres			
1. UO_2 Fueled	FA-1 (278)		
	" (282)		
	" (283)		
2. ThO_2/UO_2 Fueled	FA-14 (373)		
B. Coated Spheres			
1. SiC Coated	FA-6 (1)[(a)]		FA-6(18E)
			" (20E)
	FA-8 (4)[(a)]		FA-8(E4)
			" (E5)
2. SiC Coated & Defected	FA-8(4)		
	FA-8 (7)		
3. PyroC Coated	FA-20 (310)	FA-20 (310)	
	FA-11 (298)		
4. ZrC Coated	FL-2 (1)		
C. Coated Particles	Bare UO_2		
	Al_2O_3 Coated		

(a) Neutron Activation performed prior to Phase I.

8.1 Neutron Activation

The first series of runs were made with the basic admixtured and uncoated specimens of the FA-1 type, fueled with UO_2. Three identical specimens were used. Results for the three FA-1 specimens and the uncoated FA-14 specimens (fueled with ThO_2/UO_2) are given in Table 8-2.

TABLE 8-4

Neutron Activation Tests in Pyrolytic Carbon Coated Specimens

Specimen	Test Temp, °F	Test Time, Min	% Xe 133 Released
FA-11 (298)	1500	220	0.07
	1500	110	0.08
FA-20 (310)	1500	200	0.03
	1500	158	0.06

Data for both specimens is plotted in Figures 8-2 and 8-3. The straight line relationship between fraction released and time is to be expected for a coated sphere where a single mode of diffusion (i.e. through the coating) is controlling. Diffusion coefficients for these coatings have been calculated as shown in Section 8.4.

A single test was run on a lumped type of fuel element coated with ZrC (Type FL-2). At 1500°F, 0.03% of the Xe 133 was released during the 30 min test period indicating that the combined effect of lumping plus the ZrC coating gave about the same degree of fission product retention as the PyroC coating.

Other neutron activation tests, on alumina coated fuel particles, are described in Section 5.1.

8.2 Furnace Capsule

During the past period, Furnace Capsule SPF-1 was operated containing pyrolytic carbon coated specimen FA-20 (310) which was the same one used in the neutron activation test.

Capsule irradiation started on October 14 and nine gas samples were taken from the off-gas train during the remainder of the month. Data from the nine samples is given in Table 8-5. During the period from October 14 to October 19, when the first five samples were taken, several reactor scrams and small but significant power changes occurred, complicating the estimate of fission product production rate (B') due to growth and decay of the precursors. The effective flux in the specimen

was 3×10^{10} nv at the normal 2 MW BRR power level, as determined from the external cobalt dosimeter wire on the capsule. The BRR was shut down from Oct. 19 to Oct. 21. The remaining operation, during which time samples 6-9 were taken, was stable except that the effective flux was down to 4×10^{9} nv due to an unanticipated shift in the position of the capsule. The accuracy of the leakage rate values (R) are probably better than the accuracy in estimating the B' values, particularly for the first 5 samples. The relative accuracy of the R values, which depend on gamma spectroscopy techniques, is probably Kr 85m, Xe 135 > Kr 87 > Xe 133, Kr 88. During the entire operating time, the electrical heater maintained a constant specimen temperature of 1500°F.

TABLE 8-5

Results from Furnace Capsule SPF-1 Containing Type FA-20

		Leak Rate/Production Rate (R/B')				
Sample No.	Date	Kr 85m	Kr 87	Kr 88	Xe 133	Xe 135
1	10/14	.036	.012	.0047	.145	.024
2	10/15	.054	.014	.0038	.017	.019
3	10/16	.016	.012	.0022	.040	.016
4	10/18	.033	(1)	(1)	.026	.028
5	10/19	.086	.013	.0046	.039	.063
6	10/23	.015	.011	.0058	.055	.0088
7	19/26	.017	.016	.0042	.037	.0090
8	10/28	.016	.012	.0031	.040	.0084
9	10/30	.016	.012	.0028	.033	.0098

(1) Decay between sample collection and analysis prevented analysis.

8.3 Sweep Capsule

One sweep capsule, designated SP-3, was operated during the past period. It contained two each of the FA-6 and FA-8 SiC coated specimens. The operating conditions and results of the post-irradiation examinations have been described in Section 7.2.1.

Full power irradiation of Capsule SP-3 was initiated in the BRR on May 6. On May 8, the first attempts were made to sample the off-gas from the capsule. The level of activity in the line leading from the FA-8 specimens was too high to permit safe sampling of the gas from this capsule. A sample was obtained from the FA-6 specimens, however.

After the concentration gradient in the coating becomes constant with time, ϕ in eq. 8-4 becomes unity. That is, as $T = Dt/h^2$ becomes larger with increasing time, the second term in eq. (8-4) approaches zero.

The equation for fission product decay during diffusion through the coating is:

$$\frac{\partial C}{\partial t} = D\frac{\partial^2 C}{\partial x^2} - \lambda C \qquad (8\text{-}5)$$

The solution to eq. 8-5 at the steady state condition where $\partial c/\partial t = 0$ and the following boundary conditions:

$$\frac{\partial C}{\partial t} = \frac{B}{V} + \frac{AD}{V}\frac{\partial C}{\partial x} - \lambda C, \quad at\ x = 0$$

$$C(h, t) = C(x, 0) = 0$$

is given in eq. 8-6.

$$C' = \frac{B a \sinh (h-x)\sqrt{\lambda/D}}{V(3\sqrt{\lambda/D}\cosh h\sqrt{\lambda/D} + a\lambda \sinh h\sqrt{\lambda/D})} \qquad (8\text{-}6)$$

The fractional release rate at steady state conditions is then

$$\frac{R}{B} = \frac{3}{a\sqrt{\lambda/D}\sinh(h\sqrt{\lambda/D}) + 3\cosh(h\sqrt{\lambda/D})} \qquad (8\text{-}7)$$

The concentration M in the non-decaying case and the production rate B in the decaying case are both taken to represent quantities which are available for diffusion through the coating. Until a better understanding of the diffusion of fission products through the graphite matrix is obtained, only the fission products recoiling from the admixtured fuel particles are assumed to be available for diffusion. For fuel particles in the range of 100 to 150μ, the recoil fraction is 0.11. Thus, the relationship between M or B and the total concentration (M') or total production rate (B') is:

$$M/M' = B/B' = 0.11 \qquad (8\text{-}8)$$

The diffusion coefficients for the two types of pyrolytic carbon coatings can be calculated from the neutron activation data in Table 8-3 by the use of eq. 8-3. As a first approximation, a value of $\phi = 1$ is used. The values of R/M' are obtained from the slopes of the lines at the end of the second run at 1500°F for the FA-20 specimen in Fig. 8-3 and the FA-11 specimen in Fig. 8-2. Coating thicknesses of .0051 cm for FA-20 and .0127 cm for FA-11 are used. Results are shown in Table 8-7.

TABLE 8-7

Diffusion Coefficients for Pyrolytic Carbon Coatings Based on Neutron Activation Tests at 1500°F.

Specimen	Testing time, min	R/M' min^{-1}	R/M min^{-1}	D cm^2/sec
FA-20(310)	358	5×10^{-6}	4.5×10^{-5}	2.4×10^{-9}
FA-11(298)	330	9×10^{-6}	8.2×10^{-5}	1.1×10^{-8}

Trying these values of D in eq. 8-4, where $T = Dt/h^2$, gives values of ϕ within 1% of the initially assumed value of $\phi = 1$ thus requiring no further iteration. The lower value of D for the FA-20 specimen is possibly due to the higher bake temperature that this coating received.

The in-pile release data obtained from Capsule SPF-1 for specimen FA-20(310) can also be used to calculate diffusion coefficients for Xe and Kr through the pyrolytic carbon coating. Eq. 8-7, which allows for isotope decay during diffusion, can be used to solve for D. Data from samples 6 through 9 in Table 8-5 are used since these last four samples were taken during a period of stable operation which permitted a more accurate estimate of the isotope production rates (B'). Results are shown in Table 8-8.

TABLE 8-8

Diffusion Coefficients for Pyrolytic Carbon Coating (FA-20) Based on Furnace Capsule Data at 1500°F.

D, cm^2/sec.

Sample No.	Kr 85m	Kr 87	Kr 88	Xe 133	Xe 135
6	2.3×10^{-8}	5.4×10^{-8}	1.3×10^{-8}	4.9×10^{-9}	6.0×10^{-9}
7	2.6×10^{-8}	8.2×10^{-8}	9.3×10^{-9}	2.5×10^{-9}	6.2×10^{-9}
8	2.5×10^{-8}	5.9×10^{-8}	6.9×10^{-9}	2.8×10^{-9}	5.7×10^{-9}
9	2.5×10^{-8}	5.9×10^{-8}	6.2×10^{-9}	2.1×10^{-9}	6.8×10^{-9}
Avg.	2.5×10^{-8}	6.4×10^{-8}	8.9×10^{-9}	3.1×10^{-9}	6.2×10^{-9}

A general trend of larger diffusion coefficients for Kr isotopes compared with the Xe isotopes can be noted. This tends to confirm similar evidence on uncoated uranium-graphite specimens reported in NYO 2373 and reflects the smaller molecular weight of krypton. Since small differences in molecular weight between isotopes of the same species should have little effect on the diffusion coefficients for the isotopes, the variation noted between the various krypton isotopes was not expected. It is interesting to note that values of $D = 2.4 \times 10^{-9}$ for Xe 133 based on Neutron Activation data of the FA-20 specimen is in rather good agreement with the Xe 133 values from Furnace Capsule data shown in Table 8-8.

It is interesting to speculate on the effect that decay during diffusion will have on the retention of the much shorter lived isotopes. This can be done by the use of eq. 8-7. Using the average values of $D = 3.3 \times 10^{-8}$ for Kr and 4.6×10^{-9} for Xe and assuming these values to apply to all species of each isotope, values of R/B' for several of the important gaseous fission products can be postulated. The results are shown in Table 8-9.

TABLE 8-9

Postulated Leakage Factors (R/B') for Certain Short Lived Volatile Fission Products

Basis: $D = 3.3 \times 10^{-8}$ cm^2/sec for Kr
$D = 4.6 \times 10^{-9}$ cm^2/sec for Xe
Pyrolytic Carbon Coating Thickness = .002"

Isotope	Half-Life	R/B'
Kr 89	3.18m	2.0×10^{-4}
Kr 90	33s	7.5×10^{-6}
Kr 91	9.8s	1.4×10^{-7}
Kr 92	3s	1.9×10^{-10}
Kr 93	2s	8.0×10^{-13}
Kr 94	1.4s	2.5×10^{-13}
Xe 137	3.9m	7.3×10^{-6}
Xe 138	17m	1.3×10^{-4}
Xe 139	41s	1.1×10^{-8}
Xe 140	16s	2.0×10^{-11}
Xe 141	1.7s	10^{-26}
Xe 143	1s	10^{-32}
Xe 144	1s	10^{-32}

The trend towards insignificant leakage rates seen in Table 8-9 is important since the shorter lived isotopes, particularly the xenons, decay into non volatile daughter products such as Cs, Ba, La and Ce which would cause maintenance problems in the primary loop. Since no data was available for iodine and bromine, they were not included in Table 8-9. However, it is expected that the effective diffusion coefficients for I and Br in graphite would be several orders of magnitude lower than for Xe or Kr because of their chemical affinity for carbon. Also the present model will have to be extended to allow for those chains which include two volatile isotopes, such as I-Xe and Br-Kr.

Nomenclature for Section 8.0

R = Rate of release from the coating, atoms/sec

B = Recoil production rate, atoms/sec

B' = Total production rate in sphere, atoms/sec

M = Recoil atoms in the sphere, atoms

M' = Total atoms in the sphere, atoms

C = Concentration of atoms in the coating, atoms/cm^3

h = Thickness of coating, cm

x = Coordinate in the coating, cm

D = Diffusion coefficient, cm^2/sec

t = time, min

A = Surface area of the sphere, cm^2

V = Volume of the sphere, cm^3

a = Radius of the sphere, cm

λ = Decay constant sec^{-1}

T = Dt/h^2

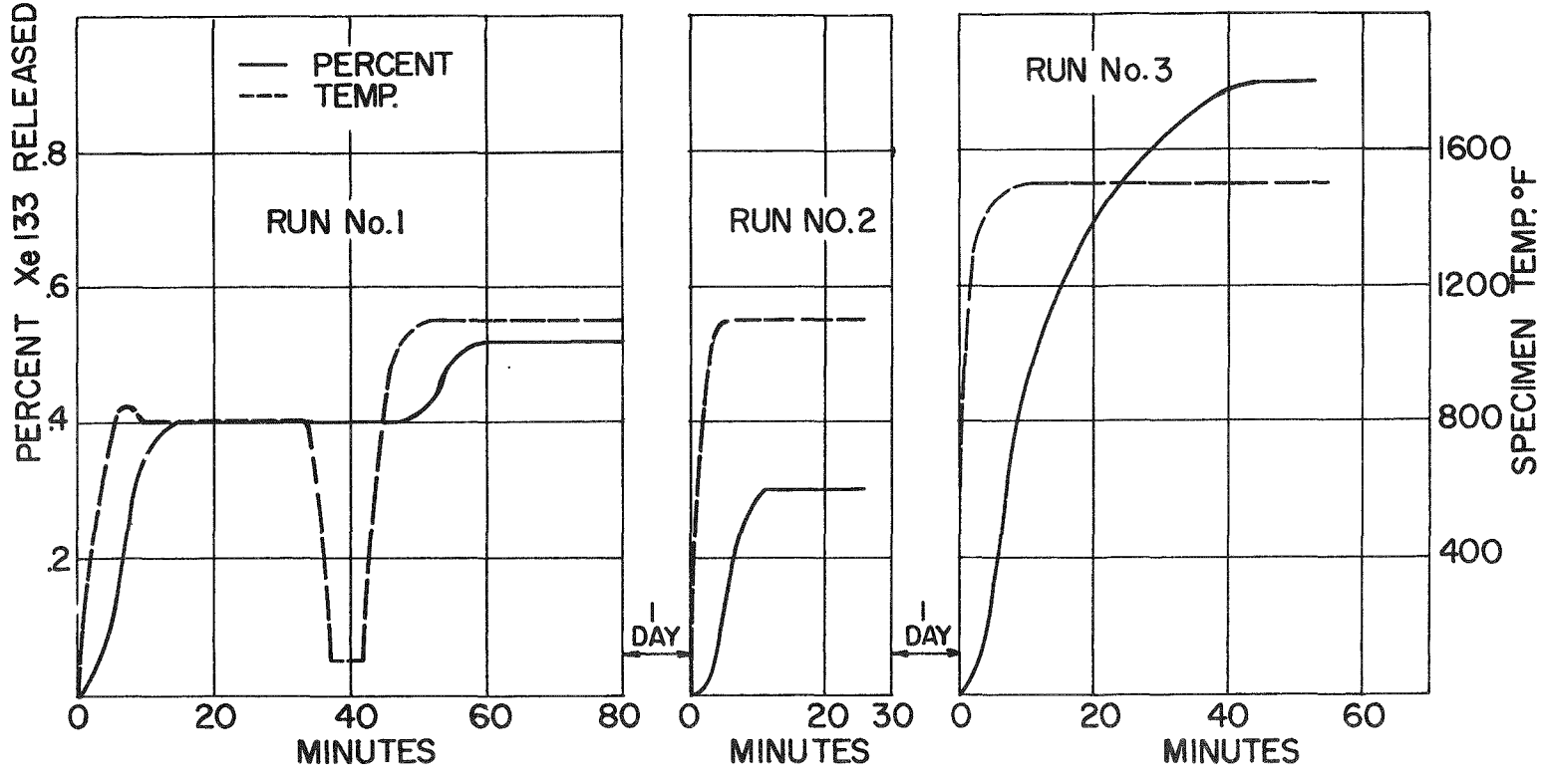

FIG. 8-1 NEUTRON ACTIVATION DATA FOR SPECIMEN FA-1(283)

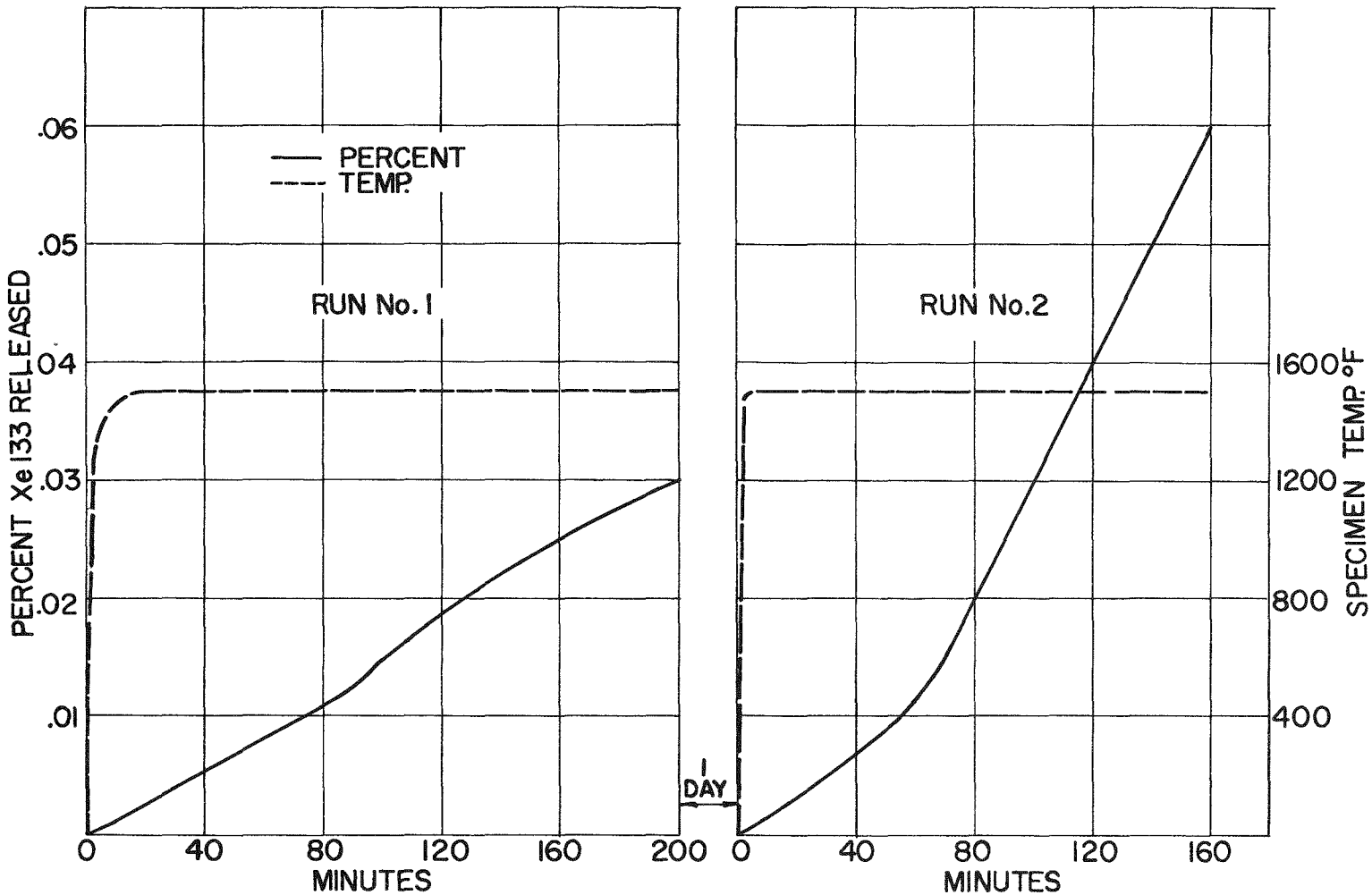

FIG. 8-2 NEUTRON ACTIVATION DATA FOR SPECIMEN FA-20(310)

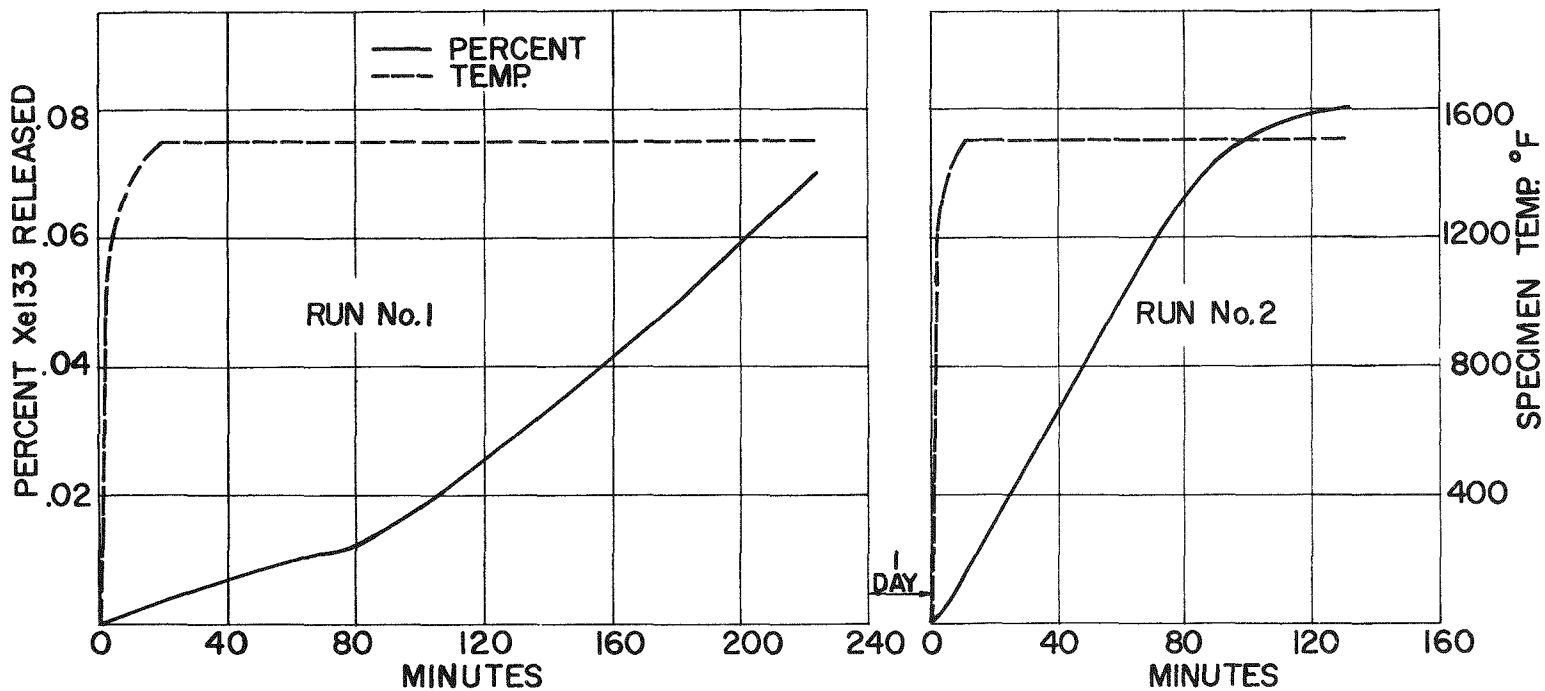

FIG.8-3 NEUTRON ACTIVATION DATA FOR SPECIMEN FA-11(298)

9.0 Conclusions

Phase I of the PBR Fuel Element Development Program has shown that there are several types of high temperature ceramic fuel elements that show promise of having a satisfactory degree of fission product retention. These are silicon carbide and pyrolytic carbon surface coatings and alumina coated fuel particles.

Two elements having silicon carbide coatings with an excess silicon phase (types FA-6 and FA-8) showed no detectable fission product leakage in Neutron Activation tests. One, type FA-6, showed leakage factors of 10^{-6} to 10^{-8} during the early phase of a high level irradiation at 1500°F. The other, a type FA-8, had a high activity release during this irradiation which was attributed to uranium contamination of the coating. Post-irradiation examination of these elements showed that the subsequent increase in leakage rate from the FA-6 specimen was caused by failure of the graphite matrix, which in turn caused cracking of the coating (see Figure 7-7). The matrix failure was attributed to incipient flaws in the graphite prior to irradiation (see Figure 4-1) which developed into major cracks due to the internal temperature gradients under irradiation which were not high enough to overstress sound graphite (see Figure 3-3). Significantly, no visible irradiation effects were noted within the SiC-Si coating (Figure 7-11) and no coating separation from the matrix was detected. Later versions of the FA-6 specimen have shown an absence of incipient cracks. No failures occurred in the FA-8 specimens except for a pinhole in one of the specimen coatings. Impact and compressive strength actually improved due to radiation hardening of the graphite matrix. The most feasible solution at this time to the problem of uranium reaction with the silicon in the coating is the use of an unfueled graphite shell between the fueled core and coating. Self-welding tests have been run on both of these types and there is no tendency of silicon carbide coated elements to self-weld at temperatures up to 2000°F.

In summary, the silicon carbide coating having an excess of free-phase silicon will receive major consideration because of its fission product retention ability at high temperature and the apparent lack of radiation damage to its physical properties.

Dense alumina coatings on fuel particles have also shown good fission product retention abilities in Neutron Activation tests up to 2450°F.

Graphites fueled with these coated particles cannot be fully graphitized since severe alumina-carbon reactions were noted at 3000°F. It should be noted, however, that the partially graphitized FA-1 specimens behaved well under irradiation as discussed in NYO 2373. Metal coated particles (Ni, Ni-Cr and Nb coatings) will not be given further consideration since the type of reaction with graphite destroys the potential value of the coating. Since a successful particle coating would reduce fission fragment damage to the graphite matrix and would relieve the problem of a broken fuel element, emphasis will continue on fabrication development of alumina coatings, and other types of ceramic fuel particle coatings will be investigated.

Carbonaceous coatings have shown some improvement in their ability to be tightly deposited on a graphite sphere, as evidenced by impact testing. Coatings which are leak-tight in the hot-oil test can be also produced. Uranium contamination is less severe than for a SiC-Si coating when deposited on fueled graphite. Some fission product leakage through the coating has been found in the FA-20 type. However, mathematical analysis of the data has shown that significant retention of the short-lived volatile isotopes may still be achieved, thus improving the prospects for decontamination and direct maintenance in a primary loop.

Of the other metal carbide surface coatings, the flame sprayed and fused ZrC and TiC coatings were found to be too porous to warrent further consideration. Another type of ZrC coating (FL-2) was found to have an apparent fine porosity from the hot-oil test, although the preliminary metallographic inspection of the coating did not clearly reveal the nature of this apparent porosity. Further information on this type of coating will be obtained.

As a result of the work described herein, the Phase II program will concentrate in three basic areas, namely ceramic-coated fuel particles, silicon carbide-silicon coatings, and pyrolytically deposited carbon coatings. Different types of ceramic coatings on fuel particles will be investigated. Evaluation of improved versions of silicon carbide-silicon coatings and pyrolytically deposited carbon coatings will be continued until an optimum type is established.